NASA TECHNICAL MEMORANDUM

NASA TM X-64727

A COMPARISON OF CMG STEERING LAWS FOR HIGH ENERGY ASTRONOMY OBSERVATORIES (HEAOs)

Program Development

July 17, 1972

NASA

George C. Marshall Space Flight Center
Marshall Space Flight Center, Alabama

MSFC - Form 3190 (Rev June 1971)

TECHNICAL REPORT STANDARD TITLE PAGE

1. REPORT NO.	2. GOVERNMENT ACCESSION NO.	3. RECIPIENT'S CATALOG NO.
TM X-64727		

4. TITLE AND SUBTITLE	5. REPORT DATE
A comparison of CMG Steering Laws for High Energy Astronomy Observatories (HEAOs)	July 17, 1972
	6. PERFORMING ORGANIZATION CODE PD-DO-ES
7. AUTHOR(S) Billy G. Davis	8. PERFORMING ORGANIZATION REPORT #
9. PERFORMING ORGANIZATION NAME AND ADDRESS	10. WORK UNIT NO.
George C. Marshall Space Flight Center Marshall Space Flight Center, Alabama 35812	11. CONTRACT OR GRANT NO.
12. SPONSORING AGENCY NAME AND ADDRESS	13. TYPE OF REPORT & PERIOD COVERED
National Aeronautics and Space Administration Washington, D.C. 20546	Technical Memorandum
	14. SPONSORING AGENCY CODE

15. SUPPLEMENTARY NOTES

Prepared by the Navigation and Control Systems Branch, Electronics and Control Division, Preliminary Design Office, Program Development

16. ABSTRACT

This report contains a comparison of six selected control moment gyro (CMG) steering laws for use on the HEAO spacecraft. Basic equations are developed to project the momentum and torque of four skewed, single gimbal CMGs into vehicle coordinates. In response to the spacecraft attitude error signal, six algorithms (steering laws) are derived for controlling the CMG gimbal movements. HEAO performance data were obtained using each steering law and compared on the basis of such factors as accuracy, complexity, singularities, gyro hang-up and failure adaption. Moreover, each law was simulated with and without a magnetic momentum management system. With magnetics, momentum is continuously dumped against the earth's magnetic field and the gimbal angles stay small, thus permitting linear operation of the steering law. The performance of any steering law was enhanced by the magnetic system and all performed equally well. Without magnetics, the gimbal angles get large and there are significant differences in steering law performances due to cross coupling and nonlinearities. The performance of the pseudo inverse law was consistently better than the other laws and is recommended for HEAO.

17. KEY WORDS		18. DISTRIBUTION STATEMENT
HEAO Spacecraft	Momentum Desaturation	STAR ANNOUNCEMENT
Attitude Control	Gravity Torque	
CMGs	Magnetic Control	
CMG Control Laws	Euler Equations	ERICH E. GOERNER Director, Preliminary Design Office

19. SECURITY CLASSIF. (of this report)	20. SECURITY CLASSIF. (of this page)	21. NO. OF PAGES	22. PRICE
Unclassified	Unclassified	138	NTIS

TABLE OF CONTENTS

LIST OF ILLUSTRATIONS

LIST OF ILLUSTRATIONS (Continued)

LIST OF ILLUSTRATIONS (Continued)

LIST OF ILLUSTRATIONS (Concluded)

LIST OF TABLES

DEFINITION OF SYMBOLS

Symbol	Definition
$\bar{\ }$	superscript bar denotes a vector
$\sim$	superscript tilde denotes a vector in matrix notation
$\cdot$	superscript dot denotes the time derivative
$*$	superscript asterisk denotes the transpose of a matrix
-1	superscript minus one denotes the inverse of a matrix
A_{rs}	matrix transformation from s to r coordinates
a_{ij}	elements of the matrix A
X, Y, Z	coordinate reference axes (subscripts for identification)
i, j, k	unit vectors (subscripts for identification) along X, Y, Z
X_v , Y_v , Z_v	vehicle coordinates (structure)
X_r , Y_r , Z_r	spacecraft reference coordinates (control)
X_c , Y_c , Z_c	CMG constant coordinates (c = 1, 2, 3, 4)
X_n , Y_n , Z_n	CMG null coordinates (n = 1, 2, 3, 4)
CMG	control moment gyro
DG	double gimbal
SG	single gimbal
RCS	reaction control system
t	time

DEFINITION OF SYMBOLS (Continued)

Symbol	Definition
T	torque
ω	angular rate
I	inertia
H	momentum
α_c	CMG gimbal angle ($c = 1, 2, 3, 4$)
h_c	CMG momentum ($c = 1, 2, 3, 4$)
k_c	CMG torque axis ($c = 1, 2, 3, 4$)
β	CMG skew angle
T_c	commanded torque
γ	angle between commanded and CMG torque vectors
A_{cn}	transformation from CMG null to constant coordinates
A_{nr}	transformation from reference to CMG null coordinates
G_{cr}	transformation from reference to CMG constant coordinates
C	cosine
S	sine
C	CMG torque matrix (C_{ij} elements)
K	constants (subscripts for identification)
A_i	CMG torque matrix with the ith column deleted

DEFINITION OF SYMBOLS (Concluded)

Symbol	Definition
a_i	gimbal solution corresponding to A_i
B_i	augmented inverse of A_i
Δ	determinate of a matrix
ghu	gyro hang-up

A COMPARISON OF CMG STEERING LAWS FOR HIGH ENERGY ASTRONOMY OBSERVATORIES (HEAOs)

SECTION I. INTRODUCTION

During the past year and one-half, the Preliminary Design Office, Program Development at Marshall Space Flight Center (MSFC) has conducted rather extensive Phase A studies of spacecraft designed to detect and observe high energy radiation sources. These spacecraft have been designated as high energy astronomy observatories (HEAOs). Missions A and B are supposed to scan the entire celestial sphere over an extended time period and, then, point to selected radiation sources [1]. Mission C has been designated only to point to selected targets. All HEAO configurations utilize solar panels to receive power and, hence, must be solar oriented within certain power and thermal constraints. HEAO-C, however, has more demanding pointing specifications than HEAO-A or -B. Due to the limitations of fuel weight and inherent limitations in pointing performance of an all thruster reaction control system (RCS), control moment gyros (CMGs) have been baselined for HEAO-C. An RCS will be used for momentum management of the CMGs, but electromagnets offer more growth potential and allow continuous CMG momentum dump without interrupting vehicle pointing (Appendix A). This report contains a description of the CMG system which has been selected during preliminary studies for HEAO. More specifically, the orientation of the CMGs relative to the HEAO reference axes have been selected to provide a near spherical momentum envelope with all CMGs operational and also provide complete vehicle control, even with one CMG failed.

Four single gimbal (SG) CMGs are arranged in a skewed configuration about the sun pointing vehicle axis. To provide effective vehicle control torques, the CMGs must be gimbaled in response to an attitude error signal. As will be shown, the gimbal commands are not necessarily unique but depend upon the assumptions made to obtain a solution to the CMG torque equations. Whatever the solution, it is referred to as the CMG "steering law." Several condidate steering laws are derived and evaluated according to their effectiveness in producing the control torque required by the attitude error signal.

The candidate steering laws are the constant gain, MSFC maximum contribution, pseudo inverse, Bendix three gimbal inverse, General Electric (G. E.) transpose with torque feedback, and the Teledyne Brown Engineering Company (BECO) H-distribution. Each steering law was utilized in conjunction with the Euler equations for HEAO (Appendix B) with the four skewed SG CMGs in a digital simulation (Appendix C) to obtain the corresponding vehicle pointing performance. Each steering law was then evaluated on the basis of complexity in implementation, accuracy of pointing performance, avoidance of mathematical singularities, possible CMG gimbal angle positions which prevent the desired torque from being produced (gyro hang-up), adaptation to a CMG failure, and performance after a failure. Based on accumulated study results, the pseudo inverse CMG steering law is recommended for HEAO.

SECTION II. CMG CONFIGURATION SELECTION

A. Introduction to CMG Control

The path of an orbiting vehicle is predetermined by its orbital parameters, essentially that of a free-falling ballistic trajectory in its orbit. The basic objective of the spacecraft attitude control system is not to change its orbital path but to maintain a prescribed attitude (orientation) as a function of time relative to inertial space irrespective of the flight path. The principle of conservation of angular momentum led to the "momentum exchange" idea, whereby in the absence of externally applied torques, if one part of a closed system increased its momentum by a specified amount, the remainder of the system lost an equal amount of momentum. An example is a flywheel supported by a frame hard-mounted to the spacecraft with a momentum given by

$$I_f W_f = H_f \quad , \tag{1}$$

where I_f is the flywheel inertia, W_f is the wheel angular velocity, and H_f is the flywheel momentum. By decreasing the flywheel speed, a torque is generated about the flywheel spin axis which counter rotates the spacecraft. The angular momentum stored in the flywheel decreases in proportion to the change in flywheel velocity while the spacecraft momentum, H_v, increases.

Since the flywheel support frame is hard-mounted to the spacecraft, the torque applied to the spacecraft is given by

$$\bar{T} = -\frac{d\bar{H}}{dt} = -I_f \dot{\bar{W}}_f \quad . \tag{2}$$

After the flywheel momentum has been decreased by a prescribed amount, ΔW_f, the total momentum of the flywheel and spacecraft must remain constant assuming that no external torques act on the spacecraft. The change in spacecraft velocity, ΔW_v, due to an arbitrary change in flywheel momentum is

$$\Delta W_v = -\frac{I_f \Delta W_f}{I_v} \tag{3}$$

where I_v is the vehicle moment of inertia about the axis aligned with the flywheel spin vector.

Consider a constant-speed flywheel that is mounted on a gimbal relative to the spacecraft. By rotating about the gimbal axis, the spin axis of the flywheel and the direction of its momentum are changed relative to the vehicle. Although the flywheel momentum remains constant, a gimbal rate $\dot{\alpha}$ produces the torque

$$\bar{T} = -(\dot{\bar{\alpha}} \times \bar{H}_f) \tag{4}$$

which is perpendicular to both the gimbal axis and flywheel momentum vector.

After the flywheel momentum has been rotated by a prescribed small amount, $\Delta\alpha$, the corresponding change in the spacecraft velocity required to conserve angular momentum can be approximated by

$$\Delta W \approx -\frac{\Delta\alpha\, I_f\, W_f}{I_v} \quad . \tag{5}$$

In the first example, the flywheel momentum value was varied, whereas, in the second example the orientation of the flywheel momentum vector relative to the vehicle was varied to obtain a torque. For either case, the vehicle is reoriented relative to inertial space so that momentum is conserved assuming no external disturbances. The first method is called reaction wheel control, while the second is called gyro control. Generally, the gyro rotor has constant speed of rotation and is referred to as a control moment gyro. If only one gimbal is used to reorient the momentum, the CMG is referred to as a SG CMG, whereas, if two gimbals are used, the CMG is referred to as a double gimbal (DG) CMG. Since the vehicle requires three degrees of freedom to maintain a prescribed orientation relative to inertial space, the attitude control system must have actuators that provide effective control torque about three independent axes. Hence, a momentum exchange system must provide at least three degrees of freedom for control purposes. Conceivably, one variable speed reaction wheel mounted on two gimbals could provide three-axis control for the spacecraft. If SG CMGs are utilized for momentum exchange, then at least three units are required for three-axis spacecraft control. In addition, the three units must be mounted relative to each other such that three independent degrees of freedom are obtained.

B. Single Gimbal CMG

The characteristics of a SG CMG are illustrated in Figure 1. The flywheel turns at a constant speed producing momentum directed along the Y_c-axis. The flywheel momentum is rotated in the Y_c-Z_c plane by gimbaling about the X_c-axis, thereby producing a torque along the Z_c-axis. The torque produced obeys the vector cross product law, equation (4). Therefore, at any instant of time, the torque produced must be perpendicular to both the gimbal axis and the momentum axis. For example, assume that it is desired to generate a vehicle torque which lies in the X_c-Y_c plane. Then the desired torque cannot be generated by the SG CMG shown. For any desired torque, only the projection of that torque onto the Z_c-axis can be generated. From this simplified example, it is apparent that at least three SG CMGs must be utilized to obtain effective three-axis vehicle control. Moreover, the three CMG torque axes, $Z_c (c = 1, 2, 3)$, must span a three-dimensional vector space. When the torque axes of a SG CMG system are coplanar, a control torque perpendicular to that plane cannot be produced. Such a condition is referred to as gyro hang-up (ghu).

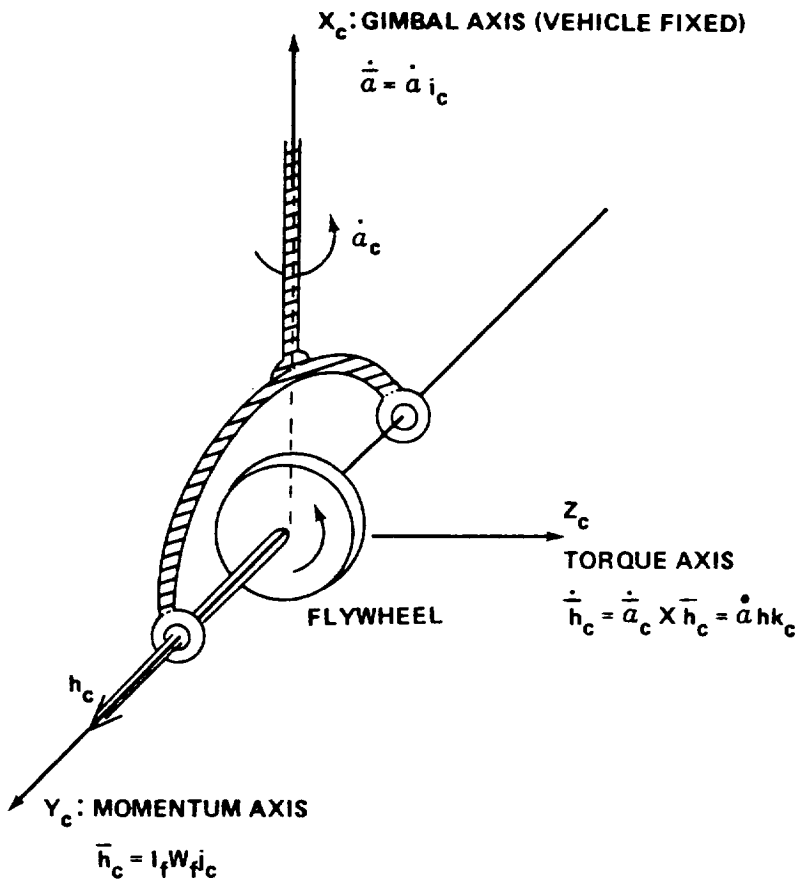

Figure 1. Single gimbal CMG.

The first general problem area is the selection of a momentum exchange system that is appropriately sized to counteract the environmental disturbance torques and, in addition, satisfy all specified vehicle maneuvering requirements.

The selected system must provide the following:

- Sufficient reliability/redundancy over the mission duration.
- Sufficient torque to counteract disturbances.
- Adequate momentum storage.
- Adequate maneuver rates.

- Spacecraft stability.
- Desired response characteristics.
- Adequate degrees of freedom.

As general design criteria, the CMGs should provide enough momentum to counteract all environmental disturbances over a one-orbit period before desaturation is required. In addition to cyclic disturbances, gravity gradient torque almost always produces a secular momentum component which eventually saturates the CMGs. That is, the CMG system produces all the momentum it can in a given direction until no more can be produced. The mounting of the CMGs relative to the vehicle reference axes determines the shape of the maximum momentum envelope within which the CMG system can provide momentum. In general, the momentum envelope is shaped proportional to the vehicle moment of inertia values, especially for an inertially oriented spacecraft that does not maneuver very often. However, when the spacecraft is reoriented, stored CMG momentum is transferred from one axis to another. Therefore, the momentum envelope should be spherical for spacecraft such as HEAO-C where many maneuvers are made, or for HEAO-A where the spacecraft spins to scan the celestial sphere. Moreover, the CMG mounting arrangement must permit the CMG torque vectors to span a three-dimensional space to obtain the degrees of freedom required to control the spacecraft. When four SG CMGs are used, as dictated by reliability considerations for example, the most independency between CMGs [2] can be obtained by arranging the CMGs symmetrically about a vehicle axis as shown in Figure 2. The four SG CMGs are shown at a zero momentum state (null position) and the CMG gimbal axes subtend an angle β (skew angle) relative to the body reference axis X_r. The skew angle can be used to shape the momentum envelope. The mounting arrangement shown in Figure 2 is referred to as four skewed CMGs and has been recommended for use on the HEAO spacecraft [3].

Based on previous study results [4, 5], CMGs offer several advantages over reaction wheels especially from a power and weight viewpoint. Moreover, based on hardware availability [6, 7], there are several SG CMGs that are sized appropriately for the HEAO-C spacecraft, from both a torque and momentum viewpoint. For these reasons, SG CMGs have been baselined for HEAO-C. To provide continued operation capability when one CMG fails, at least four CMGs must be utilized. However, more than four may be dictated by reliability considerations to achieve the required two-year lifetime. The CMG system selected by Bendix for the HEAO-A [6] seems to satisfy the

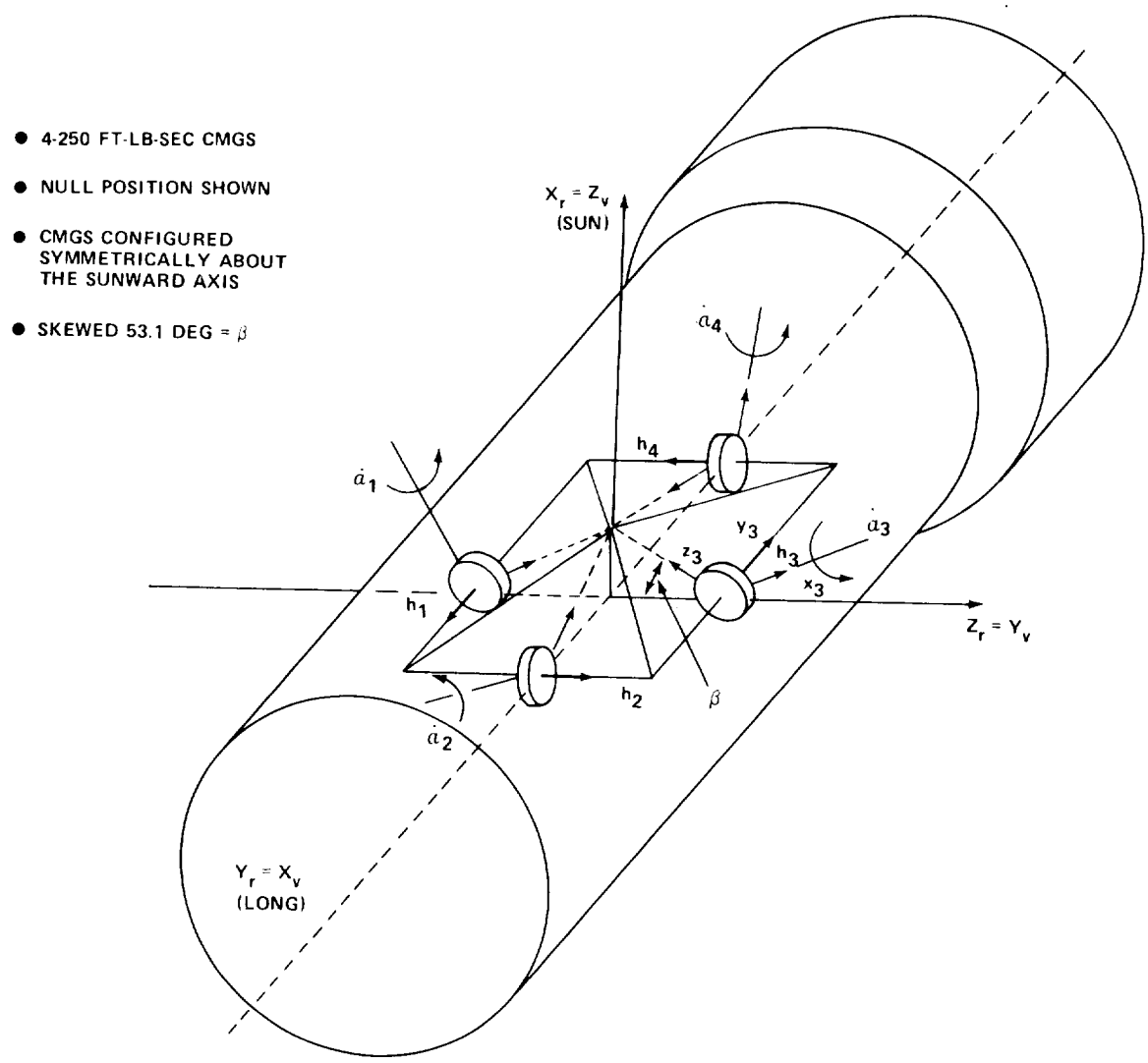

Figure 2. CMG mounting arrangement relative to HEAO reference axes.

HEAO-C requirements and, for commonality between the HEAO-A and -C spacecrafts, it has been baselined as the HEAO-C momentum exchange system. Figure 3 illustrates the CMG arrangement relative to vehicle reference axes. Each CMG momentum vector is restricted to a plane that is skewed relative to the vehicle Y_r-Z_r plane by the angle β ; the four planes form a pyramid whose apex is aligned with the vehicle X_r- axis; and each gimbal axis, X_c , is perpendicular to its associated plane as shown. The configuration is symmetrically skewed about the X_r vehicle axis so that none of the gimbal

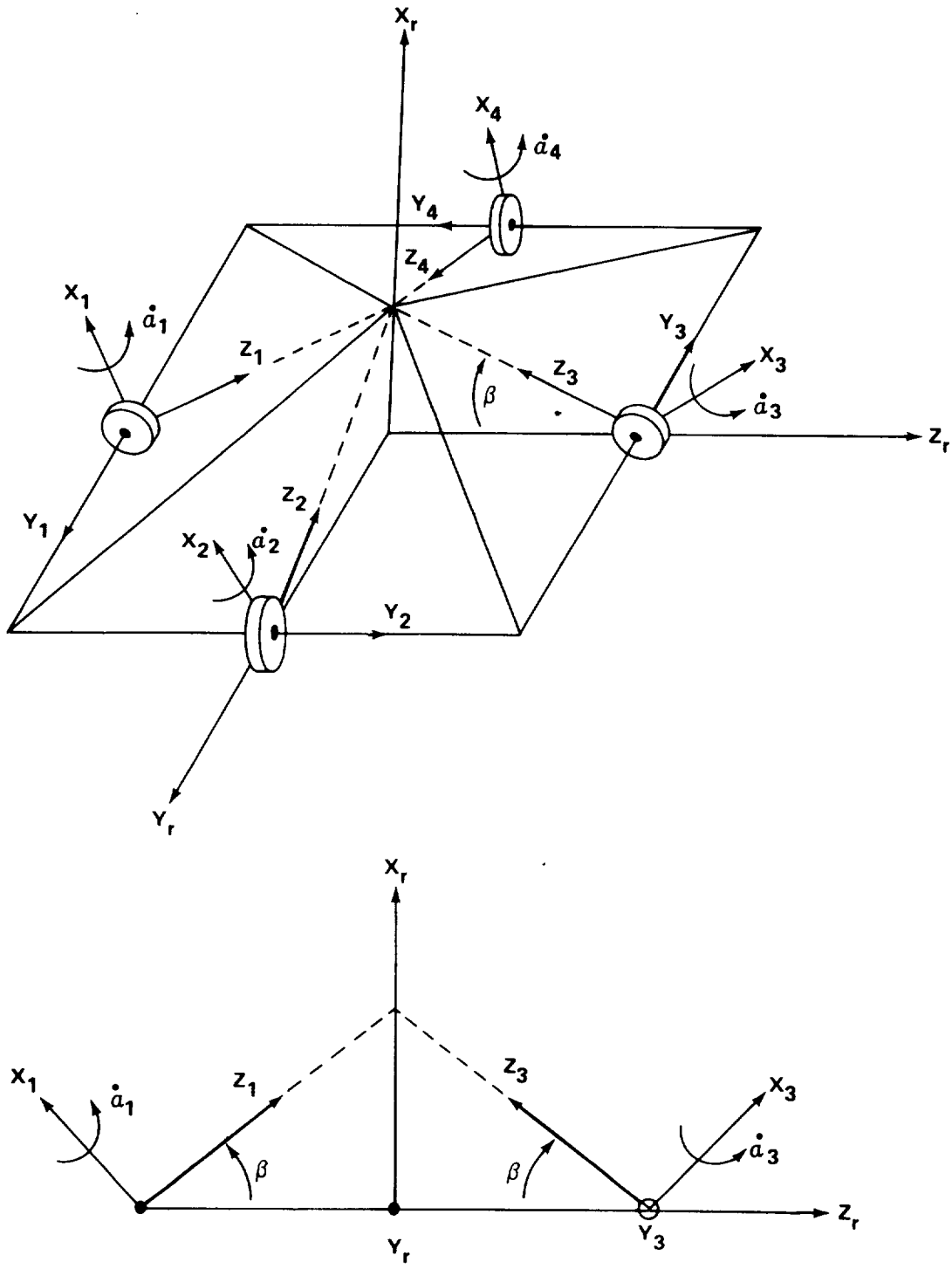

Figure 3. CMG coordinates relative to reference axes.

axes are parallel and none are parallel to a vehicle axis. As a result, each CMG can contribute momentum along each axis of the vehicle. If one CMG fails, the remaining three CMGs provide the three degrees of freedom required for attitude control.

Once the CMG configuration has been selected, the second general problem area is closure of the attitude control loop through the momentum exchange system by gimbaling the CMGs in response to the attitude error signals. The logic and error signals which are used to drive the CMG gimbals are defined as the CMG steering law. The steering law must be selected such that the CMG torque produced closely approximates the desired vehicle control torque that is needed to maintain the vehicle's specified orientation. The first task that must be done prior to deriving a CMG steering law is to relate the CMG momentum and torque to the vehicle control axis. The momentum of each CMG must be projected into body control axes and summed to obtain the total CMG system momentum. In carrying out the required operations, several coordinate systems must be defined.

C. CMG Reference Systems

For any single gimbaled CMG, a coordinate system in which the CMG momentum is always constant along one axis (Fig. 4) is defined as follows:

i_c unit vector along the gimbal axis X_c

j_c unit vector along the momentum axis Y_c

k_c unit vector along the torque axis Z_c

The CMG coordinate system moves as the gimbal is varied with respect to the spacecraft body axis. Therefore, the momentum is always aligned with the Y_c-axis and the gimbal rate vector with the X_c-axis. The torque produced by the cth CMG obeys the vector cross product law and always is aligned with the Z_c-axis. In the CMG constant momentum system, the gimbal rate $\dot{\alpha}_c$, momentum h_c, and the torque $\dot{h}_c$ can be written in vector form as follows:

$$\dot{\bar{\alpha}}_c = \dot{\alpha}_c \, \iota_c \quad , \tag{6}$$

$$\bar{h}_c = h_c \, j_c \quad , \tag{7}$$

and

$$\dot{\bar{h}}_c = \dot{\bar{\alpha}} \times \bar{h}_c = \dot{\alpha}_c \, h_c \, (\dot{\iota}_c \times j_c) = \dot{\alpha}_c \, h_c \, k_c \quad . \tag{8}$$

A second CMG system is defined by setting the CMG gimbal angle to zero or to a position which nulls out the total momentum of all CMGs. Such a reference, illustrated in Figure 5 by X_n, Y_n, Z_n, is defined as the CMG null coordinate system. When the gimbal angle is zero, the CMG null system is identical to the CMG constant momentum system. The CMG null system is related to the constant momentum system by the rotation α about the gimbal axis which is constant in either system. The subscript n denotes the null coordinate system for a particular CMG. The vector matrix form the transformation between the two systems is written as:

$$\tilde{X}_c = A_{cn} \tilde{X}_n \quad , \tag{9}$$

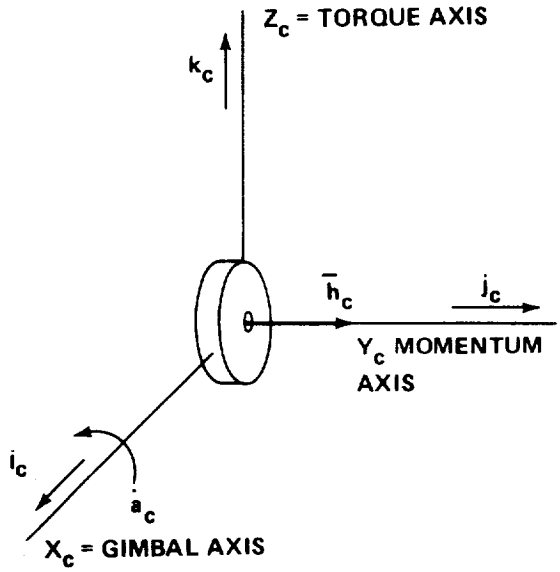

Figure 4. CMG coordinate system.

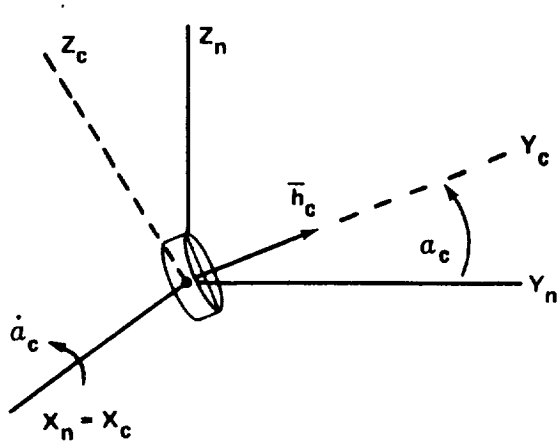

Figure 5. CMG null coordinate.

where

$$\tilde{X}_c = \begin{Bmatrix} X_c \\ Y_c \\ Z_c \end{Bmatrix}, \quad \tilde{X}_n = \begin{Bmatrix} X_n \\ Y_n \\ Z_n \end{Bmatrix}, \text{ and } A_{cn} = \begin{bmatrix} 1 & 0 & 0 \\ 0 & C\alpha_c & S\alpha_c \\ 0 & -S\alpha_c & C\alpha_c \end{bmatrix}.$$

The manner in which the two CMG reference systems have been defined permits the matrix A_{cn} to hold for any single-degree-of-freedom CMG. However, the mounting of each CMG is unique.

Each CMG has its own null coordinate system uniquely defined relative to the spacecraft body axis by its mounting arrangement. For each CMG, a matrix transformation A_{nr} must be derived to relate the spacecraft reference axis to the CMG null coordinates. The relation may be written as

$$\tilde{X}_n = A_{nr} \tilde{X}_r \quad , \tag{10}$$

where the subscript r denotes the body axis reference frame. The relation between body and CMG constant momentum systems is obtained by

$$\tilde{X}_c = A_{cn} \tilde{X}_n = (A_{cn} A_{nr}) \tilde{X}_r = G_{cr} \tilde{X}_r \quad , \tag{11}$$

where

$$G_{cr} = \begin{bmatrix} g_{11}^c & g_{12}^c & g_{13}^c \\ g_{21}^c & g_{22}^c & g_{23}^c \\ g_{31}^c & g_{32}^c & g_{33}^c \end{bmatrix} .$$

The elements of G_{cr} are obtained by matrix multiplication of A_{cn} and A_{nr} and must be derived for each CMG. The letter c would take on the number assigned to a specific CMG. Since the transformations in this case are orthogonal, the inverse is identical to the transpose, which is denoted by an asterisk superscript; hence,

$$\tilde{X}_r = G^*_{cr} \tilde{X}_c \quad . \tag{12}$$

Use of transformation (11) yields the following equations for the cth CMG gimbal rate, momentum, and torque in body axes:

$$\dot{\bar{\alpha}}_c = \dot{\alpha}_c \ (g^c_{11} i_r + g^c_{12} j_r + g^c_{13} k_r) \quad , \tag{13}$$

$$h_c = \bar{h}_c \ (g^c_{21} i_r + g^c_{22} j_r + g^c_{23} k_r) \quad , \tag{14}$$

and

$$\dot{\bar{h}}_c = \dot{\alpha}_c h_c \ (g^c_{31} i_r + g^c_{32} j_r + g^c_{33} k_r) \quad . \tag{15}$$

The equations for total momentum and torque from m CMGs is obtained by summing the vector components:

$$\bar{H} \ (CMG) = \sum_{c=1}^{m} \bar{h}_c = h_x i_r + h_y j_r + h_z k_r \tag{16}$$

and

$$\dot{\bar{H}} \ (CMG) = \sum_{c=1}^{m} \dot{\bar{h}}_c = \dot{h}_x i_r + \dot{h}_y j_r + \dot{h}_z k_r \quad . \tag{17}$$

Due to environmental forces acting on an orbiting spacecraft, the CMG momentum vectors will deviate considerably from their null positions. For most orbits in which the spacecraft is inertially oriented, momentum tends to accumulate in some direction due to biased environmental forces. Under these conditions the CMG momentum becomes concentrated in this direction until no further momentum can be obtained from the CMG system. This condition is referred to as CMG saturation. To desaturate the CMGs, a torque must be applied to the vehicle such that the CMGs are driven back either to their null position or some bias level by trying to counteract the applied torque.

D. Four-Skewed CMG Configuration

To develop a CMG steering law, the transformations, equation (11), must be derived for each CMG which relates its torque and momentum to spacecraft reference axes. The four-skewed CMG configuration, baselined for HEAO-C, is illustrated in Figure 3. Each CMG is shown at its null position and the geometry between the CMG null and spacecraft reference coordinates is illustrated. At the null position the momentum of CMG number 1 and number 3, as well as that of CMG number 2 and number 4, cancel. The transformations are carried out by first rotating negatively about each Y_n axis by the angle β which aligns the transformed X_n' axis with X_r reference axis. The next rotation is about the once transformed $X_n' = X_r$ axis until the coordinates are aligned as follows: 0 about X_1', 270 degrees about X_2', 180 degrees about X_3', and 90 degrees about X_4'. The results are summarized as follows in the form of equation (10) for each CMG.

$$\tilde{X}_1 = \begin{bmatrix} C\beta & 0 & -S\beta \\ 0 & 1 & 0 \\ S\beta & 0 & C\beta \end{bmatrix} \tilde{X}_r \quad , \quad n = 1 \tag{18}$$

$$\tilde{X}_2 = \begin{bmatrix} C\beta & S\beta & 0 \\ 0 & 0 & 1 \\ S\beta & -C\beta & 0 \end{bmatrix} \tilde{X}_r \quad , \quad n = 2 \tag{19}$$

$$\tilde{X}_3 = \begin{bmatrix} C\beta & 0 & S\beta \\ 0 & -1 & 0 \\ S\beta & 0 & -C\beta \end{bmatrix} \tilde{X}_r \quad , \quad n = 3 \tag{20}$$

$$\tilde{X}_4 = \begin{bmatrix} C\beta & -S\beta & 0 \\ 0 & 0 & -1 \\ S\beta & C\beta & 0 \end{bmatrix} \tilde{X}_r \quad , \quad n = 4 \tag{21}$$

As given by equation (9), the transformation between spacecraft reference and CMG constant momentum coordinates is

$$\tilde{X}_c = \begin{bmatrix} 1 & 0 & 0 \\ 0 & C\alpha_c & S\alpha_c \\ 0 & -S\alpha_c & C\alpha_c \end{bmatrix} \tilde{X}_n \quad , \quad n = 1, 2, 3, 4 \quad . \tag{22}$$

Equation (11) is obtained by substituting equations (18), (19), (20), and (21) into equation (22) and carrying out the matrix multiplications with $c = n$.

For four-skewed CMGs, the transformations between body and CMG constant momentum axes are summarized below.

CMG Number 1

$$\tilde{X}_1 = G_{1r} \tilde{X}_r \, , \quad G_{1r} = \begin{bmatrix} C\beta & 0 & -S\beta \\ S\beta S\alpha_1 & C\alpha_1 & C\beta S\alpha_1 \\ S\beta C\alpha_1 & -S\alpha_1 & C\beta C\alpha_1 \end{bmatrix} \tag{23}$$

CMG Number 2

$$\tilde{X}_2 = G_{2r}\tilde{X}_r, \quad G_{2r} = \begin{bmatrix} C\beta & S\beta & 0 \\ S\beta S\alpha_2 & -C\beta S\alpha_2 & C\alpha_2 \\ S\beta C\alpha_2 & -C\beta C\alpha_2 & -S\alpha_2 \end{bmatrix} \tag{24}$$

CMG Number 3

$$\tilde{X}_3 = G_{3r}\tilde{X}_r, \quad G_{3r} = \begin{bmatrix} C\beta & 0 & S\beta \\ S\beta S\alpha_3 & -C\alpha_3 & -C\beta S\alpha_3 \\ S\beta C\alpha_3 & S\alpha_3 & -C\beta C\alpha_3 \end{bmatrix} \tag{25}$$

CMG Number 4

$$\tilde{X}_4 = G_{4r}\tilde{X}_r, \quad G_{4r} = \begin{bmatrix} C\beta & -S\beta & 0 \\ S\beta S\alpha_4 & C\beta S\alpha_4 & -C\alpha_4 \\ S\beta C\alpha_4 & C\beta C\alpha_4 & S\alpha_4 \end{bmatrix} \tag{26}$$

Utilizing body to CMG transformations, the momentum for each CMG can be written in body coordinates [equation (14)] as

$$\left.\begin{aligned} \bar{h}_1 &= h_1 j_1 = h_1 (S\beta S\alpha_1 i_r + C\alpha_1 j_r + C\beta S\alpha_1 k_r) \\ \bar{h}_2 &= h_2 j_2 = h_2 (S\beta S\alpha_2 i_r - C\beta S\alpha_2 j_r + C\alpha_2 k_r) \\ \bar{h}_3 &= h_3 j_3 = h_3 (S\beta S\alpha_3 i_r - C\alpha_3 j_r - C\beta S\alpha_3 k_r) \\ \bar{h}_4 &= h_4 j_4 = h_4 (S\beta S\alpha_4 i_r + C\beta S\alpha_4 j_r - C\alpha_4 k_r) \end{aligned}\right\} \tag{27}$$

The total CMG momentum is the vector sum of all CMG momentum vectors [equation (16)]; thus,

$$\bar{H} = \sum_{c=1}^{4} \bar{h}_c = h_x i_r + h_y j_r + h_a k_r \quad , \tag{28}$$

where

$$h_x = S\beta \, (h_1 S\alpha_1 + h_2 S\alpha_2 + h_3 S\alpha_3 + h_4 S\alpha_4) \quad ,$$

$$h_y = h_1 C\alpha_1 - h_3 C\alpha_3 + C\beta \, (h_4 S\alpha_4 - h_2 S\alpha_2) \quad ,$$

and

$$h_z = h_2 C\alpha_2 - h_4 C\alpha_4 + C\beta \, (h_1 S\alpha_1 - h_3 S\alpha_3) \quad .$$

As previously stated, the CMG momentum in reference coordinates will be used as the basis for momentum management to prevent CMG saturation and to make the CMGs operate about their null positions. The components of equation (28) are zero when the gimbal angles are zero. However, there are other combinations of gimbal angles which also produce a null momentum condition.

Using equations (23) through (26), the individual CMG torques [equations (8) and (15)] are obtained in reference coordinates as follows:

$$\left.\begin{aligned}
\dot{\bar{h}}_1 &= \dot{\alpha}_1 h_1 \, (S\beta C\alpha_1 \, i_r - S\alpha_1 \, j_r + C\beta C\alpha_1, \, k_r) \\
\dot{\bar{h}}_2 &= \dot{\alpha}_2 h_2 \, (S\beta C\alpha_2 \, i_r - C\beta C\alpha_2 \, j_r - S\alpha_2 \, k_r) \\
\dot{\bar{h}}_3 &= \dot{\alpha}_3 h_3 \, (S\beta C\alpha_3 \, i_r + S\alpha_3 \, j_r - C\beta C\alpha_3 \, k_r) \\
\dot{\bar{h}}_4 &= \dot{\alpha}_4 h_4 \, (S\beta C\alpha_4 \, i_r + C\beta C\alpha_4 \, j_r + S\alpha_4 \, k_r)
\end{aligned}\right\} \tag{29}$$

The total CMG torque, equation (17), is obtained by summing the contributions from each CMG:

$$\dot{\bar{H}} = \sum_{c=1}^{4} \dot{\bar{h}}_c = \dot{h}_x i_r + \dot{h}_y j_r + \dot{h}_z k_r \quad , \tag{30}$$

where

$$\dot{h}_x = S\beta \left(\dot{\alpha}_1 h_1 C\alpha_1 + \dot{\alpha}_2 h_2 C\alpha_2 + \dot{\alpha}_3 h_3 C\alpha_3 + \dot{\alpha}_4 h_4 C\alpha_4\right) .$$

$$\dot{h}_y = -\dot{\alpha}_1 h_1 S\alpha_1 - \dot{\alpha}_2 h_2 C\beta\, C\alpha_2 + \dot{\alpha}_3 h_3 S\alpha_3 + \dot{\alpha}_4 h_4 C\beta C\alpha_4 \quad ,$$

and

$$\dot{h}_z = \dot{\alpha}_1 h_1 C\beta C\alpha_1 - \dot{\alpha}_2 h_2 S\alpha_2 - \dot{\alpha}_3 h_3 C\beta C\alpha_3 + \dot{\alpha}_4 h_4 S\alpha_4 \quad .$$

Equation (30) can be arranged in the vector matrix form

$$\begin{bmatrix} \dot{h}_x \\ \dot{h}_y \\ \dot{h}_z \end{bmatrix} = \begin{bmatrix} h_1 S\beta C\alpha_1 & h_2 S\beta C\alpha_2 & h_3 S\beta C\alpha_3 & h_4 S\beta C\alpha_4 \\ -h_1 S\alpha_1 & -h_2 C\beta C\alpha_2 & h_3 S\alpha_3 & h_4 C\beta C\alpha_4 \\ h_1 C\beta C\alpha_1 & -h_2 S\alpha_2 & -h_3 C\beta C\alpha_3 & h_4 S\alpha_4 \end{bmatrix} \begin{bmatrix} \dot{\alpha}_1 \\ \dot{\alpha}_2 \\ \dot{\alpha}_3 \\ \dot{\alpha}_4 \end{bmatrix} . \tag{31}$$

In compacted notation, equation (31) is written as

$$\dot{\tilde{H}} = C\, \dot{\tilde{\alpha}} \quad , \tag{32}$$

where C is a 3 by 4 matrix denoted as the CMG torque matrix and $\dot{\tilde{H}}$ and $\dot{\tilde{\alpha}}$ are column vectors. Notice that the columns of C are vectors directed along each CMG torque axis, Z_c. Since there are four torque vectors, the columns are linearly dependent. In the foregoing sections, the momentum and torque potentials for the baseline four-skewed CMG configuration have been developed relative to the spacecraft reference axes. The next steps are to select a skew angle and to examine several candidate steering laws.

E. Skew Angle and Momentum Capacity

The foregoing equations have been derived without selecting a specific value for the CMG skew angle β, which has been assumed to be equal for all CMGs. Several factors enter into the selection of β: (1) momentum capacity per axis and total momentum envelope, (2) control torque capability around the null position, (3) alignment of each gimbal axis to provide the independent degrees of freedom required for three-axis control. When one CMG has failed, the remaining three CMGs must be able to control the vehicle without degrading performance. With this in mind, a skew angle of 45 degrees would provide the greatest angular distance between gimbal rate vectors and between reference and gimbal axes. The CMG system would, therefore, provide the best operational capability with one CMG out. If the skew angle were 90 degrees, control torques could be attained about each reference axis but the X_r axis would have twice the momentum storage capacity as the other two axes. Moreover, with one CMG out, severe cross coupling would result on the X_r axis by trying to command only a Y_r or Z_r torque. For example, if h_1 were out, with β equal 90 degrees, only CMG Number 3 could produce a Y_r axis torque, but that torque could not be produced without also torquing the X_r and Z_r axes.

The skew angle could be selected to give equal torque capability per axis near the CMG null position. By setting the gimbal rates to some predetermined upper limit (depending on the CMG torque motor characteristics) and setting the sign to give maximum torque per axis, equation (31) at the null position reduces to the following equations:

$$\left.\begin{aligned} \dot{h}_x\,(\max) &= 4h\,S\beta\,\dot{\alpha}_1 \\ \dot{h}_y\,(\max) &= 2h\,C\beta\,\dot{\alpha}_1 \\ \dot{h}_z\,(\max) &= 2h\,C\beta\,\dot{\alpha}_1 \end{aligned}\right\} . \qquad (33)$$

Equating maximum torque components produces

$$\tan(\beta) = 0.5 \quad . \tag{34}$$

A skew angle of 26.6 degrees, therefore, provides equal torque per axis capability near the CMG null position. However, the momentum envelope is not symmetric and, as the gimbal angles vary, the torque capability per axis does not stay equal. Since the gimbal angles may become rather large if momentum is dumped infrequently, equal torque per axis at the CMG null does not appear to be a good criterion for selecting the skew angle.

A more logical approach is to select the skew angle so that the CMG momentum envelope is spherical, that is, equal momentum capacity per axis. By setting the gimbal angles to values which produce maximum momentum per reference axis, equation (28) reduces to the following equations:

$$\left.\begin{aligned} h_x\,(\max) &= 4h\,S\beta \\ h_y\,(\max) &= 2h\,(1 + C\beta) \\ h_z\,(\max) &= 2h\,(1 + C\beta) \end{aligned}\right\} \quad . \tag{35}$$

Equating maximum momentum components produces

$$2\,S\beta = 1 + C\beta \quad . \tag{36}$$

By squaring each side and eliminating $S^2\beta$ by trigonometric identity, the following quadratic equation is obtained:

$$5\,C^2\beta + 2\,C\beta - 3 = 0 \quad . \tag{37}$$

The solution of equation (37) gives a skew angle of 180 or 53.1 degrees. However, 180 degrees is a false solution since the X_r axis momentum would be zero. Table 1 gives the maximum momentum capability per axis for several

TABLE 1. MAXIMUM MOMENTUM CAPABILITY FOR FOUR-SKEWED CMGs (ft-lb-sec)

	β = 0 deg		β = 28.1 deg		β = 45 deg		β = 53.1 deg		β = 90 deg	
h/CMG	h_x	h_y h_z	h_x	h_y h_z	h_x	h_y h_z	h_x	h_y h_z	h_x	h_y h_z
25	0	100	47	94	71	85	80	80	100	50
50	0	200	94	188	141	171	160	160	200	100
100	0	400	188	376	283	966	320	320	400	200
250	0	1000	470	940	707	854	800	800	1000	500
500	0	2000	940	1880	1414	1707	1600	1600	2000	1000

skew angles and CMG momentum values. With a skew angle of 53.1 degrees and a unit CMG momentum of 250 ft-lb-sec, each axis has a CMG momentum potential of 800 ft-lb-sec for control purposes. A skew angle of 28.1 degrees gives twice as much momentum on the Y_r and Z_r axes as on the X_r axis, whereas 45 degrees gives 150 ft-lb-sec less on the X_r axis as compared to the transverse axis. Based on the foregoing analysis, a skew angle of either 45 or 53.1 degrees is recommended for HEAO-C.

An analog computer program has been developed[1] to determine the maximum momentum surface that a particular set of four single-degree-of-freedom, skewed CMGs can generate. The CMGs are mounted so that their momentum vectors always lie in the planes of the faces of a pyramid, as shown in Figure 3. As each CMG is gimbaled, its momentum vector will rotate in the plane. No gimbal position or rate limits are placed on the CMGs, and it is assumed that they have equal momentum. The angle of inclination of the faces of the pyramid (β) may be varied from 0 to 90 degrees.

There is always some total momentum vector $\bar{H}$ which is the vector sum of the individual CMG momentum vectors. If the four CMGs were caused to rotate in a random fashion, the locus of the tip of the total momentum vector

1. W. J. Weiler, PD-DO-ES, MSFC, contributed the material on CMG momentum envelopes.

would describe a solid. The boundary of this solid is the desired maximum momentum surface, or momentum envelope. This envelope is a function of the physical system and is independent of the control law used to command the CMGs. However, a control law is a necessary part of the scheme used to generate plots of the momentum envelope with the maximum contribution steering law presently being utilized. The accuracy of this control law determines the conformance of the representation to the actual envelope.

The program commands a total momentum vector of greater magnitude than the system can produce. This commanded vector remains fixed in length and follows a prescribed pattern in direction. It begins pointing up the +X-axis. It then increments through a fixed angle in the X_r-Y_r plane toward the Y_r-axis and then revolves about the X_r-axis. It continues incrementing and rotating until it reaches the $-X_r$-axis. The control law causes the individual CMGs to rotate making the total actual momentum vector follow the commanded total momentum vector. The rectangular components of the actual total momentum vector are plotted by an X-Y plotter to obtain various views of the locus of its tip. Ideally, the actual vector would follow the commanded vector exactly in direction, and would maintain the greatest length possible in every direction. Actually, due to sensitivity points and singularity points of the control law, there is some deviation in parallelism of the actual vector to that commanded in some regions, especially when the commanded vector becomes nearly parallel with one of the CMG gimbal axes. In this case the other CMGs must provide all the momentum in that direction and also cancel out the CMG whose momentum is perpendicular to that direction.

One or more CMGs may be failed by setting its momentum to zero. No modification to the control law is required when the CMGs are failed. Figures 6 and 7 show profiles of the momentum envelopes for $\beta = 53.1$ degrees with all CMGs operational and with one CMG failed. The figures are scaled in terms of normalized momentum where one major graph division represents one H, the momentum of one CMG. Much distortion of the surface is observed when a CMG is failed. The white areas centered about the gimbal axis should be interpreted as depressions in the surface, not as holes extending through the solid. The absence of contours in the regions is mainly due to deviation of the actual vector from the commanded because of control law sensitivity points. Depressions do exist there and have been verified by digital computer simulations.

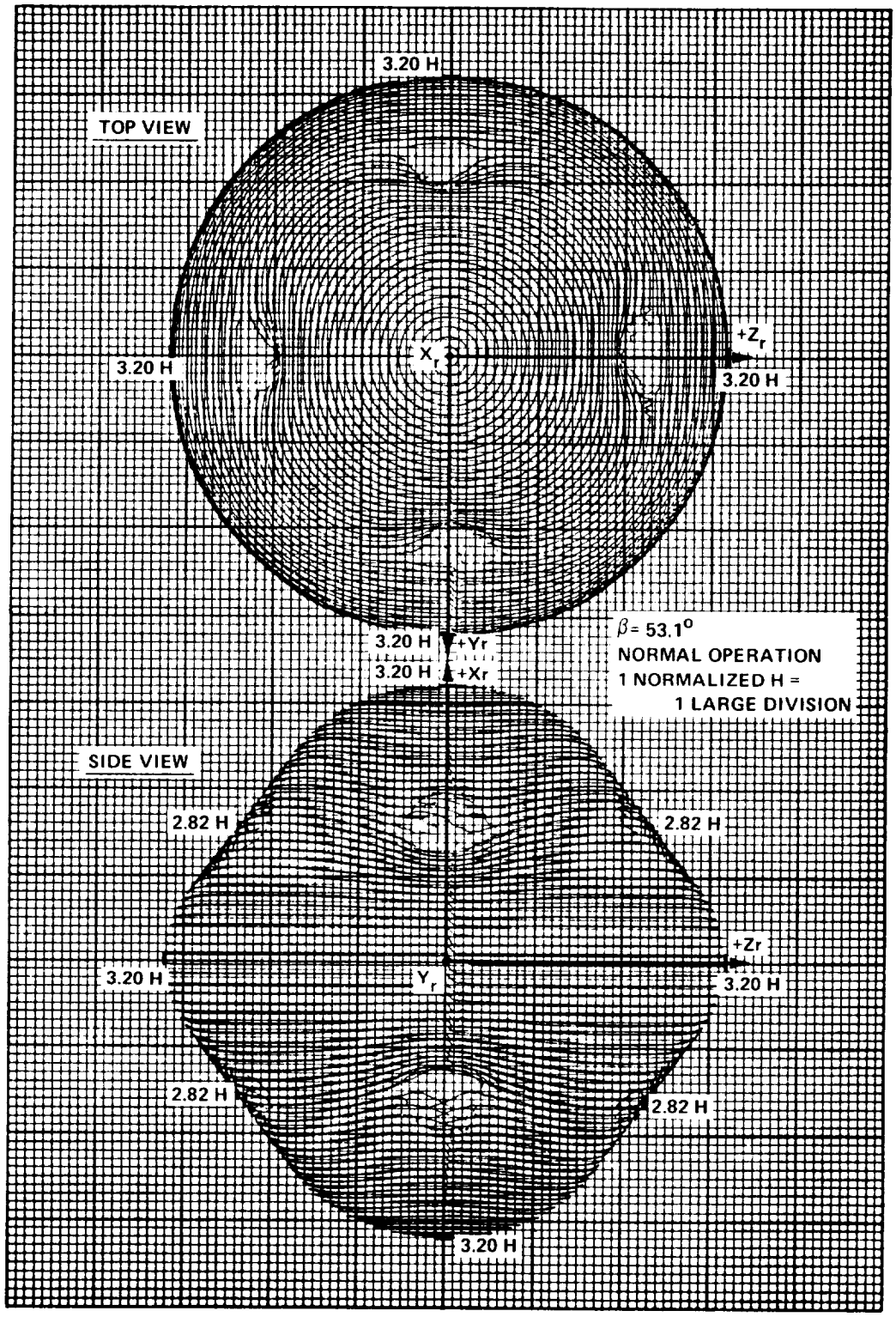

Figure 6. Four-skewed CMG maximum momentum envelope.

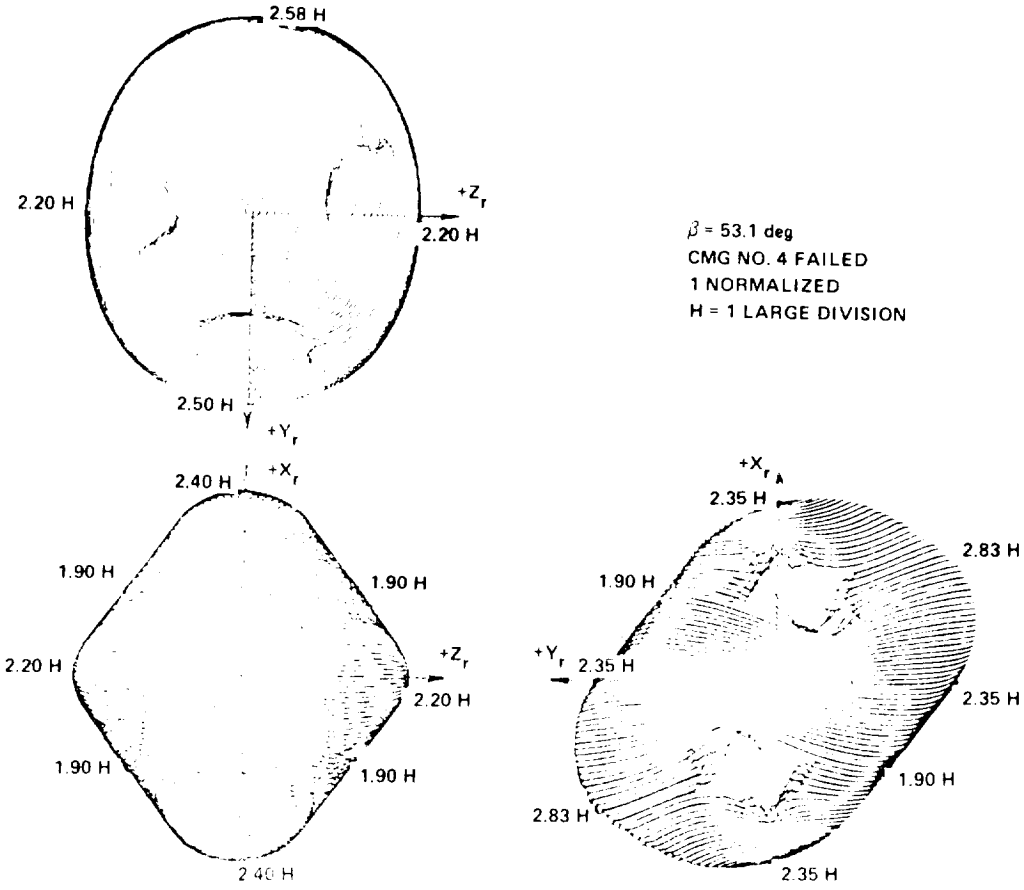

Figure 7. Maximum momentum envelope with CMG number 4 failed.

When the vehicle is rotated, as in a normal 90 degree maneuver, momentum is interchanged between vehicle axes. Simulations indicate that environmental torques cause CMG momentum to accumulate in a bias direction. These torques depend upon orbital and attitude hold conditions. By the proper maneuver, the accumulated momentum can be transferred to any other axis. Since HEAO has to maneuver often, the phenomenon of momentum transfer by maneuvering makes a near-spherical CMG momentum profile highly desirable. A skew angle β of 53.1 degrees will produce the near-spherical momentum envelope shown in Figure 6; therefore, it has been recommended for HEAO. There are slight indentures at each CMG gimbal axis because a CMG cannot contribute any momentum along its gimbal axes. At the indentures, $|H|$ is about 675 ft-lb-sec for 4-250 ft-lb-sec CMGs. With one CMG failed, $|H|$ at the indenture is about 368 ft-lb-sec for three 250 ft-lb-sec CMGs. It should be noted that doubling the $|H|$ per CMG would also double the size of the momentum envelope.

SECTION III. CMG STEERING LAWS

A. Introduction

When the CMG gimbal angles are moved, a corresponding change occurs in the momentum relative to the body axes. By definition, torque is the time rate of change of angular momentum. Therefore, the spacecraft is acted upon by a torque when the CMG gimbal angles are changing. In general, a spacecraft control law is derived as a linear combination of sensor outputs such as rate gyros, sun sensors, star trackers, etc., which have been weighted by a constant gain on each output. The gains are selected to give the desired vehicle response and stability characteristics. Ideal control would be obtained if the torque called for by the vehicle control law could be produced by the CMGs. The control law is typically derived with respect to the spacecraft reference axes and may be written in the following general vector form:

$$\bar{T}_c = T_{cx}\, i_r + T_{cy}\, j_r + T_{cz}\, k_r \quad . \tag{38}$$

The basic objective is the derivation of a CMG gimbal control law providing some approximation of the torque specified by the spacecraft control law.

The standard approach is to equate the total change in CMG angular momentum $\dot{\bar{H}}$, equation (32), to the desired torque $\bar{T}_c$. The vector components are equated with a negative sign and arranged in the following vector matrix form:

$$\begin{bmatrix} T_{cx} \\ T_{cy} \\ T_{cz} \end{bmatrix} = \begin{bmatrix} & & \\ & 3 \times n & \\ & \text{Matrix} & \\ & & \end{bmatrix} \begin{bmatrix} \dot{\alpha}_1 \\ \dot{\alpha}_2 \\ \cdot \\ \cdot \\ \cdot \\ \dot{\alpha}_n \end{bmatrix} \quad . \tag{39}$$

The 3 by n matrix must be inverted to obtain a general solution for the CMG gimbal rate commands. Several problems are obvious: (1) With four or more CMGs, the linear system is underdetermined, meaning that when the equations are consistent there is an infinite number of solutions (there are only three equations but n unknowns); (2) For some gimbal angles, the system is known to be inconsistent and not all sets of gimbal angles producing inconsistency have been determined (for some gimbal angle combinations no solution exists); (3) These considerations and the algebra involved make a general solution almost impossible without resorting to a digital computer.

A second approach is to restrict the range of the CMG gimbals and assume small deviations from the CMG null positions. In such a case, small angle approximations are used, $\sin \alpha = \alpha$ and $\cos \alpha = 1$, and the equations are linearized. The gimbal rates are solved so that cross coupling between axes is eliminated. The resultant solution, however, is valid only for small CMG angular excursions from the null positions. At this point in the CMG control system design, each individual designer will have or devise his own method for selecting a CMG steering law. Several candidate steering laws were derived and compared on the basis of their effectiveness in producing the desired actuator response as well as their complexity in implementing each scheme. Each steering law was derived for the four-skewed CMG momentum exchange system which has been baselined for HEAO-C.

For the four-skewed CMG configuration there are three equations (components of the CMG torque vector) and four unknowns (four CMG gimbal rates). To obtain an exact solution, a constraint equation or relation between the unknowns is needed. For each constraint or assumption that is made, a solution will be obtained for the gimbal rates. Whatever the solution, it is referred to as the CMG steering law. The following are several candidate steering laws that were considered:

1. Constant gain.
2. Maximum contribution.
3. Psuedo inverse.
4. The Bendix summation of three-gimbal inverses.
5. The BECO momentum vector distribution.
6. The G. E. transpose with torque feedback.

Because of the large quantity of data, simulation results for each steering law are included in Appendix C, including magnetic momentum management for the CMGs.

B. A Constant Gain

A constant gain steering law can be derived by assuming that each CMG will operate about its null position and that torque must be generated about any vehicle axis. The CMG torque in body axes is equated to the desired control torque to obtain the following variation of equation (39):

$$\left.\begin{aligned} -T_{cx} &= hS\beta(\dot{\alpha}_1 C\alpha_1 + \dot{\alpha}_2 C\alpha_2 + \dot{\alpha}_3 C\alpha_3 + \dot{\alpha}_4 C\alpha_4) \\ -T_{cy} &= h(-\dot{\alpha}_1 S\alpha_1 - \dot{\alpha}_2 C\beta\, C\alpha_2 + \dot{\alpha}_3 S\alpha_3 + \dot{\alpha}_4 C\beta\, C\alpha_4) \\ -T_{cz} &= h(\dot{\alpha}_1 C\beta\, C\alpha_1 - \dot{\alpha}_2 S\alpha_2 - \dot{\alpha}_3 C\beta\, C\alpha_3 + \dot{\alpha}_4 S\alpha_4) \end{aligned}\right\} . \qquad (40)$$

Assuming small gimbal angles, $C\alpha_i = 1$ and $S\alpha_i = 0$, equations (40) reduce to

$$\left.\begin{aligned} -T_{cx} &= hS\beta(\dot{\alpha}_1 + \dot{\alpha}_2 + \dot{\alpha}_3 + \dot{\alpha}_4) \\ -T_{cy} &= hC\beta(\dot{\alpha}_4 - \dot{\alpha}_2) \\ -T_{cz} &= hC\beta(\dot{\alpha}_1 - \dot{\alpha}_3) \end{aligned}\right\} . \qquad (41)$$

For either torque or momentum capability, CMGs number 2 and number 4 dominate the Y-axis, and CMGs number 1 and number 3 dominate the Z-axis. Any CMG can be used to produce torque on the X-axis. Since there are four unknowns in the gimbal rates but only three equations, the solution for gimbal rates as a function of desired control torques is not unique. Some criterion or constraint between the gimbal angles is needed for a unique solution.

Assume that only X-axis torque is wanted and that it must be produced without introducing torque on the transverse axis. By setting $\dot{\alpha}_3 = \dot{\alpha}_1$ and $\dot{\alpha}_4 = \dot{\alpha}_2$, both the Y and Z torque components are zero and, by setting $\dot{\alpha}_2 = \dot{\alpha}_1$, the X-axis torque attains a maximum value of

$$-T_{cx} = 4\, hS\beta\dot{\alpha}_1 \quad . \tag{42}$$

Solving equation (42) for the gimbal rates produces

$$\dot{\alpha}_{xi} = -\frac{T_{cx}}{4\, hS\beta} \quad , \quad i = 1,\ 2,\ 3,\ 4 \quad , \tag{43}$$

where the subscript x represents the X-axis solution.

Similarily, the Y-axis torque is maximized and the transverse torques are zeroed by setting $\dot{\alpha}_2 = -\dot{\alpha}_1$ and $\dot{\alpha}_1 = \dot{\alpha}_3 = 0$. The Y-axis torque component is

$$-T_{cy} = hC\beta(2\,\dot{\alpha}_4) \quad . \tag{44}$$

The corresponding gimbal rate solutions are

$$\dot{\alpha}_{y1} = \dot{\alpha}_{y3} = 0 \quad ; \quad \dot{\alpha}_{y2} = -\dot{\alpha}_{y4} = T_{cy}/2\, hC\beta \quad . \tag{45}$$

The Z-axis torque is maximized by setting $\dot{\alpha}_3 = -\dot{\alpha}_1$ and $\dot{\alpha}_2 = \dot{\alpha}_4 = 0$. Using these values, both the X and Y torque components are zero and

$$-T_{cz} = hC\beta(2\,\dot{\alpha}_1) \quad . \tag{46}$$

The gimbal rate solutions are

$$\left.\begin{aligned} \dot{\alpha}_{z1} &= -\dot{\alpha}_{z3} = -T_{cz}/2\ hC\beta \\ \dot{\alpha}_{z2} &= \dot{\alpha}_{z4} = 0 \end{aligned}\right\} \quad . \tag{47}$$

The constant gain steering law is obtained by summing up equations (43), (45), and (47) as follows:

$$\left.\begin{aligned} \dot{\alpha}_1 &= \dot{\alpha}_{x1} + \dot{\alpha}_{y1} + \dot{\alpha}_{z1} = -T_{cx}/4\ hS\beta - T_{cz}/2\ hC\beta \\ \dot{\alpha}_2 &= \dot{\alpha}_{x2} + \dot{\alpha}_{y2} + \dot{\alpha}_{z2} = -T_{cx}/4\ hS\beta + T_{cy}/2\ hC\beta \\ \dot{\alpha}_3 &= \dot{\alpha}_{x3} + \dot{\alpha}_{y3} + \dot{\alpha}_{z3} = -T_{cx}/4\ hS\beta + T_{cz}/2\ hC\beta \\ \dot{\alpha}_4 &= \dot{\alpha}_{x4} + \dot{\alpha}_{y4} + \dot{\alpha}_{z4} = -T_{cx}/4\ hS\beta - T_{cy}/2\ hC\beta \end{aligned}\right\} \quad . \tag{48}$$

By defining constants

$$\left.\begin{aligned} K_A &= -\frac{1}{4\ hS\beta} \\ K_B &= -\frac{1}{2\ hC\beta} \end{aligned}\right\} \quad , \tag{49}$$

equations (48) can be written as

$$\left.\begin{aligned} \dot{\alpha}_1 &= K_A\ T_{cx} + K_B\ T_{cz} \\ \dot{\alpha}_2 &= K_A\ T_{cx} - K_B\ T_{cy} \end{aligned}\right\} \tag{50}$$

$$\left.\begin{aligned} \dot{\alpha}_3 &= K_A T_{cx} - K_B T_{cz} \\ \dot{\alpha}_4 &= K_A T_{cx} + K_B T_{cy} \end{aligned}\right\} \qquad (50)\ (\text{Cont'd})$$

Equations (50) illustrate the constant gain CMG steering law that was first used in the HEAO-C CMG performance simulation studies. At a later date, the maximum contribution steering law was derived, which reduces to the same constant gain steering law by assuming small gimbal angles and linearizing. For a skew angle of 53.1 degrees and 250 ft-lb-sec CMGs, the gain constants are

$$\left.\begin{aligned} K_A &= -0.00125047 \\ K_B &= -0.00333111 \end{aligned}\right\} \qquad (51)$$

The constant gain steering law is most simple to implement and could easily be simulated on an analog computer. However, it is valid only for small gimbal angles. In the digital simulations, excellent performance was obtained if the gimbal angles were less than ±45 degrees. For many cases, satisfactory performance was obtained with gimbal angles up to ±80 degrees. Control was lost if the angles exceeded ±90 degrees. With continuous momentum dump using magnetic coils, for example, the gimbal angles stay small and the constant gain steering law meets all HEAO-C requirements. However, with periodic momentum dump using RCS thrusters, less than half the available momentum can be used before the gimbal angles exceed their linear operating range. For the baseline HEAO-C configuration with four 250 ft-lb-sec CMGs, momentum would have to be dumped each one-half orbit under worst-case environmental torque conditions. As an alternative, a more general type constant gain steering law with periodic gain switching could be defined to permit better utilization of the total momentum capacity. The latter approach was not pursued during this study.

With one CMG failed, the CMG null position must be redefined and a constant gain steering law derived which is valid about the new null position. The dump frequency would have to be increased to about four times per orbit, assuming worst-case environmental effects. Hence, for each CMG failure, a contingency steering law must be defined with a new CMG null position.

With continuous momentum dump with electromagnets, any CMG can be failed and a new null automatically found without reprogramming. However, vehicle maneuverability is restricted by the linear operating range of the steering law. So even with continuous momentum dump, the constant gain steering law should be redefined for each failure mode.

Assume that CMG number 3 has failed. With the failed CMG eliminated, the momentum becomes

$$\left.\begin{aligned} h_x &= hS\beta(S\alpha_1 + S\alpha_2 + S\alpha_4) \\ h_y &= h(C\alpha_1 - C\beta S\alpha_2 + C\beta S\alpha_4) \\ h_z &= h(C\beta S\alpha_1 + C\alpha_2 - C\alpha_4) \end{aligned}\right\} \quad . \qquad (52)$$

One new null position can be found by setting $\alpha_1 = 0$ and solving for α_2 and α_4. With $\alpha_1 = 0$ the X-axis equation gives $\alpha_2 = -\alpha_4$, which also produces zero in the Z-axis. The Y-axis momentum set to zero gives

$$0 = h(1 - C\beta S\alpha_2 + C\beta S\alpha_4) \quad . \qquad (53)$$

With $\alpha_2 = -\alpha_4$, equation (56) reduces to

$$S\alpha_2 = \frac{1}{2\,C\beta} \quad . \qquad (54)$$

With $\beta = 53.1$ degrees, the solution for a new null position is

$$\left.\begin{aligned} \alpha_1 &= 0 \text{ deg} \\ \alpha_2 &= 56.4 \text{ deg} \\ \alpha_4 &= -56.4 \text{ deg} \end{aligned}\right\} \quad . \qquad (55)$$

The CMG torque potential with CMG number 3 out is [equation (40) with $S\alpha_1 = 0$, $C\alpha_1 = 1$, $C\alpha_2 = C\alpha_4 = 0.5534$, $S\alpha_2 = 0.8329$, and $S\alpha_4 = -0.8329$]

$$\left.\begin{aligned} \dot{h}_x &= -T_{cx} = hS\beta(\dot{\alpha}_1 + 0.5534\,\dot{\alpha}_2 + 0.5534\,\dot{\alpha}_4) \\ \dot{h}_y &= -T_{cy} = hC\beta(0.5534)\ (\dot{\alpha}_4 - \dot{\alpha}_2) \\ \dot{h}_z &= -T_{cz} = h(C\beta\,\dot{\alpha}_1 - 0.8329\,\dot{\alpha}_2 - 0.8329\,\dot{\alpha}_4) \end{aligned}\right\} \quad . \tag{56}$$

Since there are three equations and three unknowns, an exact solution can be found, assuming the equations are consistent. In vector matrix form, equations (56) become

$$\begin{bmatrix} 1 & 0.5534 & 0.5534 \\ 0 & -1 & 1 \\ C\beta & -0.8329 & -0.8329 \end{bmatrix} \begin{Bmatrix} \dot{\alpha}_1 \\ \dot{\alpha}_2 \\ \dot{\alpha}_4 \end{Bmatrix} = \begin{Bmatrix} -T_{cx}/hS\beta \\ -T_{cy}/0.5534\ hC\beta \\ -T_{cz}/h \end{Bmatrix} . \tag{57}$$

The determinant of the matrix, Δ, for $\beta \doteq 53.1$ degrees is

$$\Delta = 2(0.8329 + 0.5534\,C\beta) = 2.3306 \quad . \tag{58}$$

Since the determinant is not zero, a solution is found by using Cramer's rule. With $h = 250$ ft-lb-sec, the constant gain steering law is given by the following equations:

$$\left.\begin{aligned} \dot{\alpha}_1 &= -0.003576\,T_{cx} - 0.0019\,T_{cz} \\ \dot{\alpha}_2 &= -0.001289\,T_{cx} + 0.00602\,T_{cy} + 0.001716\,T_{cz} \\ \dot{\alpha}_4 &= -0.001289\,T_{cx} - 0.00602\,T_{cy} + 0.001716\,T_{cz} \end{aligned}\right\} \quad . \tag{59}$$

Substituting the steering law, equation (59), into the CMG torque equations, equations (56), the CMG torque per unit command torque is

$$\left.\begin{aligned} \dot{h}_x/T_{cx} &= 1 \\ \dot{h}_y/T_{cy} &= 1 \\ \dot{h}_z/T_{cz} &= 1 \end{aligned}\right\} \quad . \tag{60}$$

Thus, with $h_3 = 0$, the gain through the CMG system on any axis is unity, and the steering law solution is verified. A similar procedure would be required to obtain a solution for any other CMG out.

C. The MSFC Maximum Contribution

A second and somewhat novel approach is to command each CMG separately based on its ability to contribute to the desired control torque. The criteria are to consider each CMG independently and to command its gimbal rate so that as much as possible of the desired control torque is produced. If no part of the control torque can be produced, the gimbal position is not moved. Since each CMG can produce a torque only about its torque axis as defined by k_c, the desired control torque $\bar{T}_c$ will be projected into the CMG constant momentum coordinates and used to command the gimbal rate. Using the transformation G_{cr}, the desired torque, as defined by the control law, in CMG coordinates is as follows:

$$\bar{T}_c = t_{cx}\, i_c + t_{cy}\, j_c + t_{cz}\, k_c \quad , \tag{61}$$

where

$$t_{cx} = g_{11}{}^{c} T_{cx} + g_{12}{}^{c} T_{cy} + g_{13}{}^{c} T_{cz} \quad ,$$

$$t_{cy} = g_{21}{}^{c} T_{cx} + g_{22}{}^{c} T_{cy} + g_{23}{}^{c} T_{cz} \quad ,$$

and

$$t_{cz} = g_{31}^{c} T_{cx} + g_{32}^{c} T_{cy} + g_{33}^{c} T_{cz} \quad .$$

Previously, the torque produced by the cth CMG was defined as

$$\dot{\bar{h}}_c = \dot{\alpha}_c h_c k_c \quad . \tag{62}$$

By equating elements of $\dot{\bar{h}}_c$ and $-\bar{T}_c$, the CMG gimbal rate command is obtained as

$$\dot{\alpha}_c = -t_{cz}/h_c = -(g_{31}^{c} T_{cx} + g_{32}^{c} T_{cy} + g_{33}^{c} T_{cz})/h_c \quad . \tag{63}$$

By defining the angle between $\bar{T}_c$ and k_c as γ, the vector scalar product is

$$\bar{T}_c \cdot k_c = g_{31}^{c} T_{cx} + g_{32}^{c} T_{cy} + g_{33}^{c} T_{cz} = T_c C\gamma \quad ; \tag{64}$$

therefore,

$$\dot{\alpha}_c = -T_c C\gamma/h_c \quad . \tag{65}$$

Note that equation (64) is the projection of the desired control torque on the k_c axis. That portion of $\bar{T}_c$ which is perpendicular to the CMG torque axis is given by

$$T_c S\gamma = T_c (1 - C^2\gamma)^{\frac{1}{2}} \tag{66}$$

and cannot be obtained by gimbaling the cth CMG at any time. Since $T_c C_\gamma$ contains basically magnitude information without polarity, the expanded scalar product form should be used for the CMG gimbal commands. Each CMG is commanded individually, regardless of its angular position, based on its ability to contribute to the desired torque vector. For a specified CMG system configuration, however, the transformation between body and CMG coordinates must be derived and evaluated at each time step.

If the components of G_{cr} from equations (23) through (26) are substituted into equation (63), with $c = 1, 2, 3, 4$, the following equations are obtained for the gimbal rate commands for four-skewed CMGs:

$$\left.\begin{aligned}
\dot{\alpha}_1 &= -(S\beta C\alpha_1 T_{cx} - S\alpha_1 T_{cy} + C\beta C\alpha_1 T_{cz}) / h_1 \\
\dot{\alpha}_2 &= -(S\beta C\alpha_2 T_{cx} - C\beta C\alpha_2 T_{cy} - S\alpha_2 T_{cz}) / h_2 \\
\dot{\alpha}_3 &= -(S\beta C\alpha_3 T_{cx} + S\alpha_3 T_{cy} - C\beta C\alpha_3 T_{cz}) / h_3 \\
\dot{\alpha}_4 &= -(S\beta C\alpha_4 T_{cx} + C\beta C\alpha_4 T_{cy} + S\alpha_4 T_{cz}) / h_4
\end{aligned}\right\} \quad . \tag{67}$$

Assuming equal momentum per CMG, the steering law can be arranged in the following vector matrix form:

$$\dot{\tilde{\alpha}} = A \tilde{T}_c / h \quad . \tag{68}$$

As previously shown by equation (32), the CMG torque with equal momentum per CMG is

$$\dot{\tilde{H}} = h C \dot{\tilde{\alpha}} \quad . \tag{69}$$

By comparing the elements of A and C, the matrix A equals the negative transpose of C ; that is,

$$A = -C^* \quad . \tag{70}$$

Hence, the CMG steering law shown in equation (67) is equivalent to a transpose type steering law. The important characteristics of this type steering law are no mathematical (computation or algorithmic) singularities, no matrices to invert, and easy implementation of the equations for the CMG gimbal rates. Its undesirable characteristic is that the control system gain through the CMGs is not constant. Control authority about each vehicle axis varies as the gimbal angles are moved from their null position since at each instant of time, each CMG is maximizing its contribution to the desired control torque.

Assuming small gimbal angles, the CMG torque per vehicle axis, equation (30), reduces to the following equations:

$$\left.\begin{aligned} \dot{h}_x &= h\, S\beta\, (\dot{\alpha}_1 + \dot{\alpha}_2 + \dot{\alpha}_3 + \dot{\alpha}_4) \\ \dot{h}_y &= h\, C\beta\, (-\dot{\alpha}_2 + \dot{\alpha}_4) \\ \dot{h}_z &= h\, C\beta\, (\dot{\alpha}_1 - \dot{\alpha}_3) \end{aligned}\right\} . \tag{71}$$

Substitution of equations (67) into equations (71) results in the following equations:

$$\left.\begin{aligned} \dot{h}_x &= -4\, S^2\beta\, T_{cx} \\ \dot{h}_y &= -2\, C^2\beta\, T_{cy} \\ \dot{h}_z &= -2\, C^2\beta\, T_{cz} \end{aligned}\right\} . \tag{72}$$

To obtain unit gain through the CMG system with the CMGs at their null position, either the desired torque components, T_c, or the steering law must be normalized by dividing by the appropriate sine and cosine function of the skew angle. If one chooses to normalize the steering law, those terms with T_{cx} are divided by $4S^2\beta$ and those terms with T_{cy} or T_{cz} are divided by $2C^2\beta$. The maximum contribution steering law ensues from the normalization of equations (67) as follows:

$$
\left.
\begin{aligned}
\dot{\alpha}_1 &= (-C\alpha_1/4h\ S\beta)\ T_{cx} + (S\alpha_1/2h\ C^2\beta)\ T_{cy} - (C\alpha_1/2h\ C\beta)\ T_{cz} \\
\dot{\alpha}_2 &= (-C\alpha_2/4h\ S\beta)\ T_{cx} + (C\alpha_2/2h\ C\beta)\ T_{cy} - (S\alpha_2/2h\ C^2\beta)\ T_{cz} \\
\dot{\alpha}_3 &= (-C\alpha_3/4h\ S\beta)\ T_{cx} - (S\alpha_3/2h\ C^2\beta)\ T_{cy} + (C\alpha_3/2h\ C\beta)\ T_{cz} \\
\dot{\alpha}_4 &= (-C\alpha_4/4h\ S\beta)\ T_{cx} - (C\alpha_4/2h\ C\beta)\ T_{cy} - (S\alpha_4/2h\ C^2\beta)\ T_{cz}
\end{aligned}
\right\} \cdot \quad (73)
$$

Once specified, the skew angle is constant. By making the following definitions,

$$
\left.
\begin{aligned}
K_a &= -1/4h\ S\beta \\
K_b &= -1/2h\ C\beta \\
K_c &= K_b/C\beta
\end{aligned}
\right\} , \quad (74)
$$

the maximum contribution steering law can be written as follows:

$$
\left.
\begin{aligned}
\dot{\alpha}_1 &= K_a\ C\alpha_1\ T_{cx} - K_c\ S\alpha_1\ T_{cy} + K_b\ C\alpha_1\ T_{cz} \\
\dot{\alpha}_2 &= K_a\ C\alpha_2\ T_{cx} - K_b\ C\alpha_2\ T_{cy} - K_c\ S\alpha_2\ T_{cz} \\
\dot{\alpha}_3 &= K_a\ C\alpha_3\ T_{cx} + K_c\ S\alpha_3\ T_{cy} - K_b\ C\alpha_3\ T_{cz} \\
\dot{\alpha}_4 &= K_a\ C\alpha_4\ T_{cx} + K_b\ C\alpha_4\ T_{cy} + K_c\ S\alpha_4\ T_{cz}
\end{aligned}
\right\} . \quad (75)
$$

The maximum contribution CMG steering law has been used extensively in the HEAO-C simulations with four-skewed CMGs. Very satisfactory pointing performance was obtained in the cases simulated. Although there are no computational singularities in the maximum contribution steering law, there are gimbal positions for which a component of the desired torque cannot be produced. This condition for the maximum contribution law is ghu. For

example, assuming CMG saturation in the X-axis direction with all gimbal angles at 90 degrees, no torque can be produced in the X-axis direction, $\dot{h}_x = 0$. Concurrently, the desired torque component T_{cx} cannot drive the CMG gimbals through the steering law; the coefficients of T_{cx} in equation (75) are zero. In general, however, ghu conditions are dependent on the CMG system configuration and are not necessarily associated with the ability to command through the steering law. Consider the ghu condition $\alpha_1 = 90$ degrees, $\alpha_2 = 0$ degrees, $\alpha_3 = -90$ degrees, and $\alpha_4 = 0$ degrees. The Z-axis CMG torque, $\dot{h}_z$, is zero but the CMGs are not saturated. Also the Z-axis command T_{cz} cannot be fed through the steering law. The implication is that for the transpose type steering law, ghu conditions also correspond to gimbal positions which prevent a commanded torque component from driving the CMG gimbal angle rates.

D. The Pseudo Inverse

By equating the desired control torque, $\bar{T}_c$, [equation (38)] to the CMG torque, $\dot{\bar{H}}$, [equation (30)] the vector-matrix equation, equation (32), becomes

$$-\tilde{T}_c = \dot{\tilde{H}} = C(h\tilde{\dot{\alpha}}) \tag{76}$$

where C has been normalized by factoring out $h = h_i$, $i = 1, 2, 3, 4$. The matrix C is a 3 by 4 whose inverse must be obtained to solve the gimbal angular rates as functions of the desired control torque. However, since there are four unknowns but only three equations, a general solution, if one exists, is not unique. One, therefore, must resort to a pseudo inverse.

Reference 8 gives the general conditions and theory for finding a pseudo inverse solution, one form of which can be given by

$$F = C^* (C\,C^*)^{-1} \tag{77}$$

provided that the matrix C is of rank three or, what is the same, that the instantaneous torque vectors are not coplanar. The steering law then becomes

$$(h \dot{\tilde{\alpha}}) = -C^* (C\, C^*)^{-1} \tilde{T}_c = -F \tilde{T}_c \quad , \tag{78}$$

where superscript asterisk represents the transpose of a matrix and minus one represents the general inverse of a matrix. For the baseline CMG configuration, the elements of C have been defined by equation (31) which must also be normalized by factoring out $h = h_i$, $i = 1, 2, 3, 4$. To obtain the inverse, the determinant of CC^* must be calculated. Those gimbal angle combinations which make the determinant go to zero and cause program divergence are denoted as singularities. For the pseudo inverse, singularities are synonymous with ghu conditions. However, other steering laws can have singularities without a corresponding ghu. Since mathematical manipulations required to obtain the pseudo inverse are too complicated to perform without a digital computer, the elements of equation (77) will be developed only to the extent required for calculations. Most digital subroutines for matrix inversion accept the elements of the matrix to be inverted and give as outputs the elements of the inverse matrix. Let

$$D = C\, C^* \tag{79}$$

and

$$E = D^{-1} \quad . \tag{80}$$

The normalized elements of C are obtained from equation (31) from which the elements of D are calculated as shown in the following:

$$
\left.
\begin{aligned}
D_{11} &= C_{11}^2 + C_{12}^2 + C_{13}^2 + C_{14}^2 \\
D_{12} &= C_{11} C_{21} + C_{12} C_{22} + C_{13} C_{23} + C_{14} C_{24} \\
D_{13} &= C_{11} C_{31} + C_{12} C_{32} + C_{13} C_{33} + C_{14} C_{34} \\
D_{21} &= D_{12} \\
D_{22} &= C_{21}^2 + C_{22}^2 + C_{23}^2 + C_{24}^2 \\
D_{23} &= C_{21} C_{31} + C_{22} C_{32} + C_{23} C_{33} + C_{24} C_{34} \\
D_{31} &= D_{13} \\
D_{32} &= D_{23} \\
D_{33} &= C_{31}^2 + C_{32}^2 + C_{33}^2 + C_{34}^2 \quad .
\end{aligned}
\right\} \quad . \qquad (81)
$$

As indicated above, the matrix D is skew symmetric.

The elements of D are inputs to a digital matrix inversion routine to obtain the elements of E as outputs. Multiplying the elements of E by C^* gives the elements of F, a 4 by 3 matrix, as shown below.

$$
\left.
\begin{aligned}
F_{11} &= C_{11} E_{11} + C_{21} E_{21} + C_{31} E_{31} \\
F_{12} &= C_{11} E_{12} + C_{21} E_{22} + C_{31} E_{32} \\
F_{13} &= C_{11} E_{13} + C_{21} E_{23} + C_{31} E_{33} \\
F_{21} &= C_{12} E_{11} + C_{22} E_{21} + C_{32} E_{31} \\
F_{22} &= C_{12} E_{12} + C_{22} E_{22} + C_{32} E_{32} \\
F_{23} &= C_{12} E_{13} + C_{22} E_{23} + C_{32} E_{33} \\
F_{31} &= C_{13} E_{11} + C_{23} E_{21} + C_{33} E_{31} \\
F_{32} &= C_{13} E_{12} + C_{23} E_{22} + C_{33} E_{32}
\end{aligned}
\right\} \quad . \qquad (82)
$$

$$
\left.
\begin{aligned}
F_{33} &= C_{13} E_{13} + C_{23} E_{23} + C_{33} E_{33} \\
F_{41} &= C_{14} E_{11} + C_{24} E_{21} + C_{34} E_{31} \\
F_{42} &= C_{14} E_{12} + C_{24} E_{22} + C_{34} E_{32} \\
F_{43} &= C_{14} E_{13} + C_{24} E_{23} + C_{34} E_{33}
\end{aligned}
\right\} . \qquad (82) \text{ (cont'd)}
$$

Utilizing the elements of the pseudo inverse matrix, the CMG steering law is obtained by expanding equation (78) as follows:

$$
\left.
\begin{aligned}
\dot{\alpha}_1 &= -(F_{11} T_{cx} + F_{12} T_{cy} + F_{13} T_{cz}) / h_1 \\
\dot{\alpha}_2 &= -(F_{21} T_{cx} + F_{22} T_{cy} + F_{23} T_{cz}) / h_2 \\
\dot{\alpha}_3 &= -(F_{31} T_{cx} + F_{32} T_{cy} + F_{33} T_{cz}) / h_3 \\
\dot{\alpha}_4 &= -(F_{41} T_{cx} + F_{42} T_{cy} + F_{43} T_{cz}) / h_4
\end{aligned}
\right\} . \qquad (83)
$$

As noted previously, the columns of C are CMG torque vectors for each CMG. It can be rigorously proven that when any three are colinear the determinant of $C C^*$ goes to zero, producing a singularity in the steering law. There is a large number of gimbal angle combinations that can produce singular conditions. However, in digital simulations, the only singular conditions which prevented proper operation of the steering law were those which also corresponded to CMG saturation.

In most cases when an internal singularity was approached, a small pointing error was observed. However, the system would recover and operate satisfactory until CMG saturation was reached. The cyclic nature of environmental torques prevented ghu at the singularities. But when constant torques were commanded, internal singularities could always be encountered with subsequent loss of control. Only about 50 to 60 percent of the momentum envelope is usable without any possible singularities. More research is needed to fully understand the singularity and ghu conditions associated with single gimbal CMGs and to develop possible avoidance schemes.

When a CMG fails, it is acceptable to set the failed gyro elements to zero. The failed CMG must be identified and the column corresponding to the failed CMG set to zero. The pseudo inverse routine need not be reprogrammed. With one CMG out, however, C reduces to a 3 by 3 matrix whose inverse can be obtained without resorting to the pseudo inverse procedure. The advantage of the pseudo inverse steering law is that most of the time the exact torque needed for attitude error correction can be obtained through the CMGs without any cross coupling. Possible disadvantages are the complexity of implementing the pseudo inverse matrix inversion routine and the requirement for detecting and compensating for CMG failures. An onboard digital computer would be required to implement the pseudo inverse steering law.

E. The Bendix Three-Gimbal Inverse

In the foregoing sections, the basic characteristic of the four-skewed CMG system is that there are more control variables, gimbal rates, than there are basic relations, torque equations, between the variables. As previously shown, the three components of the CMG torque vector provides three equations which can be arranged in the vector matrix form

$$\dot{\tilde{H}} = C(h\dot{\tilde{\alpha}}) \tag{84}$$

where C is a 3 by 4 torque matrix whose columns correspond to unit vectors directed along each individual CMG torque axis. From the basic definition of the CMG reference coordinate systems defined in equation (8), the individual CMG torque is

$$\dot{\bar{h}}_c = h_c \dot{\tilde{\alpha}}_c k_c \quad , \qquad c = 1, 2, 3, 4 \tag{85}$$

where k_c is a unit vector in the CMG coordinate system. The vector components of k_c in the vehicle reference coordinate system form the elements of the cth column of the C matrix. In vehicle coordinates, let k_c, c = 1, 2, 3, 4, be the column vector corresponding to the torque vector of the cth CMG, then equation (84) can be reqritten as

$$\dot{\tilde{H}} = [k_1\ k_2\ k_3\ k_4]\ (h\dot{\tilde{\alpha}}) \quad . \tag{86}$$

After replacing the CMG torque, $\dot{\tilde{H}}$, with the desired control torque components, $\tilde{T}_c$, the objective is to solve the torque equations for the CMG gimbal rates such that the CMG system generates the exact control torque. However, there are an infinite number of gimbal rate combinations which will satisfy the torque equations. By specifying some subsidiary condition between control variables, an equation between the variables can be obtained which can be utilized to eliminate one of the variables from the torque equations, hence, reducing the torque matrix to a 3 by 3 matrix which will have a unique inverse if the columns are linearily independent. The constraint equation must necessarily be based on some preconception of what comprises a desirable CMG system state or response characteristic.

In the absence of a universally accepted subsidiary condition between the CMGs, Bendix has proposed "the three-gimbal inverse" steering law [6] for use on HEAO. If there were only three CMGs, the torque matrix would reduce to a 3 by 3 matrix by deleting the column corresponding to the deleted CMG. In this case, a unique solution exists for the three gimbal angles, assuming that the determinant of the 3 by 3 matrix is not zero. In the Bendix scheme, the CMGs are grouped into sets of three and the desired control torque is apportioned to each set. Each set of three CMGs is required to deliver its apportioned part of the desired control torque. Then, the corresponding CMG gimbal rate commands are obtained by inverting each 3 by 3 matrix and summing the results from each set. For the four-skewed CMG configuration there are four possible sets of three CMGs which result in the following equations:

$$\left.\begin{aligned}
\dot{\tilde{H}} &= [k_2\ k_3\ k_4]\ (h_i\ \dot{\tilde{\alpha}}_i) \quad , \quad i = 2,\ 3,\ 4 \\
\dot{\tilde{H}} &= [k_1\ k_3\ k_4]\ (h_i\ \dot{\tilde{\alpha}}_i) \quad , \quad i = 1,\ 3,\ 4 \\
\dot{\tilde{H}} &= [k_1\ k_2\ k_4]\ (h_i\ \dot{\tilde{\alpha}}_i) \quad , \quad i = 1,\ 2,\ 4 \\
\dot{\tilde{H}} &= [k_1\ k_2\ k_3]\ (h_i\ \dot{\tilde{\alpha}}_i) \quad , \quad i = 1,\ 2,\ 3
\end{aligned}\right\} \quad . \tag{87}$$

In each equation, let A_c, $c = 1, 2, 3, 4$, be the torque matrix corresponding to the set of three CMGs with the cth CMG deleted from the 3 by 4 torque

matrix C. The inverse of each A_c exists if the determinant of A_c is not zero. Let A_c^{-1} denote the inverse of A_c and $\dot{\tilde{a}}_c$ denote the corresponding solution for the three gimbal rates based on the cth set of three CMGs. The gimbal rate solutions for the four CMG sets are

$$\left.\begin{aligned}
\dot{\tilde{a}}_1 &= (A_1^{-1}\,\dot{\tilde{H}})/h \quad , \quad \text{CMG no. 1 out} \\
\dot{\tilde{a}}_2 &= (A_2^{-1}\,\dot{\tilde{H}})/h \quad , \quad \text{CMG no. 2 out} \\
\dot{\tilde{a}}_3 &= (A_3^{-1}\,\dot{\tilde{H}})/h \quad , \quad \text{CMG no. 3 out} \\
\dot{\tilde{a}}_4 &= (A_4^{-1}\,\dot{\tilde{H}})/h \quad , \quad \text{CMG no. 4 out}
\end{aligned}\right\} \quad . \qquad (88)$$

Although it is not necessary to prorate the desired torque equally among the four CMG sets, there is no basis for doing otherwise. If the CMG torque $\dot{\tilde{H}}$ is replaced by the desired torque vector $\tilde{T}_c$, then conceivably each set could deliver the total required torque. To prevent overtorquing, the desired torque components are divided by four, that is, apportioned equally between the four sets. With $\tilde{T}_c/4$ being substituted into equation (85) with a negative sign, the four solution sets are obtained and the results for each CMG gimbal rate added together to obtain the Bendix three-inverse steering law. A flow diagram of the steering law is shown in Figure 8. The gimbal rate command to each CMG is composed of solutions from three of the four solution sets. In the event that one CMG fails, only that set which does not contain the failed CMG would be used to obtain the gimbal rate commands. For example, if CMG number 3 fails, then all the desired torque would be allotted to the A_3^{-1} solution. In this case, $\dot{\tilde{a}}_3$ would give the exact solution needed to generate the required control, if and only if k_1, k_2, k_4 are not coplanar. When three unit torque vectors are coplanar, the vector box product between them is zero. Moreover, the box product is identical to the value of the determinant formed by the vectors. When the determinant is zero, no solution exists, and the matrix is singular. With CMG number 3 out, the gain factor $1/4h$ would be changed to $1/h$ and the loops broken which lead to A_1^{-1}, A_2^{-1}, and A_4^{-1}. The resulting solution from A_3^{-1} should be, in this case, the exact solution.

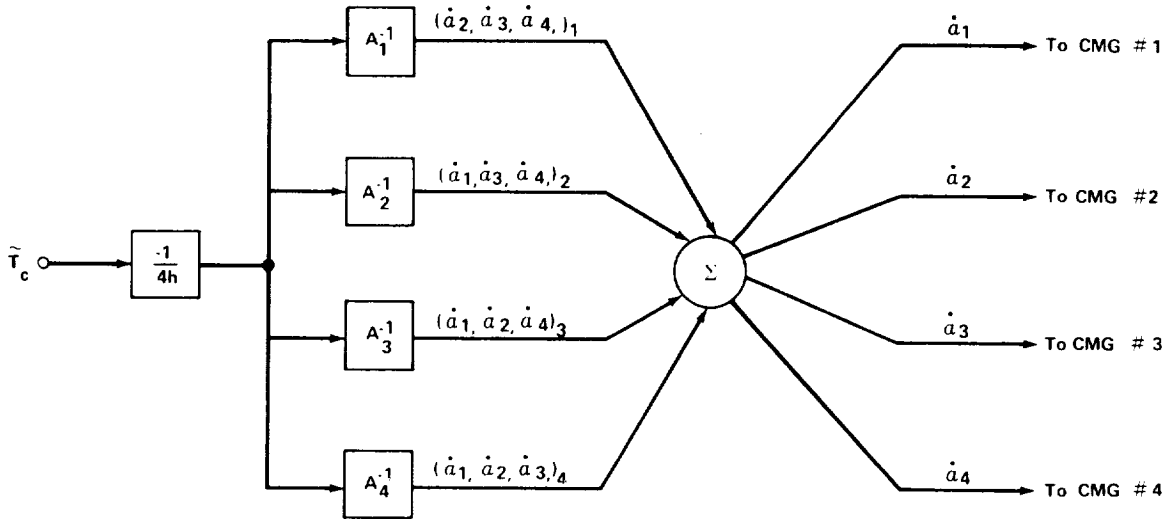

Figure 8. Three-gimbal inverse CMG steering law.

Assuming all CMGs operational, the four gimbal rate solutions from equations (88) are

$$\left.\begin{aligned}
\underset{\sim}{\dot{a}}_1 &= \begin{Bmatrix} \dot{\alpha}_2 \\ \dot{\alpha}_3 \\ \dot{\alpha}_4 \end{Bmatrix}_1 = (-1/4h)\, A_1^{-1} \begin{Bmatrix} T_{cx} \\ T_{cy} \\ T_{cz} \end{Bmatrix} \\
\underset{\sim}{\dot{a}}_2 &= \begin{Bmatrix} \dot{\alpha}_1 \\ \dot{\alpha}_3 \\ \dot{\alpha}_4 \end{Bmatrix}_2 = (-1/4h)\, A_2^{-1} \begin{Bmatrix} T_{cx} \\ T_{cy} \\ T_{cz} \end{Bmatrix} \\
\underset{\sim}{\dot{a}}_3 &= \begin{Bmatrix} \dot{\alpha}_1 \\ \dot{\alpha}_2 \\ \dot{\alpha}_4 \end{Bmatrix}_3 = (-1/4h)\, A_3^{-1} \begin{Bmatrix} T_{cx} \\ T_{cy} \\ T_{cz} \end{Bmatrix}
\end{aligned}\right\} \qquad (89)$$

$$\underset{\sim}{a}_4 = \begin{Bmatrix} \dot{\alpha}_1 \\ \dot{\alpha}_2 \\ \dot{\alpha}_3 \end{Bmatrix}_4 = (-1/4h)\, A_4^{-1} \begin{Bmatrix} T_{cx} \\ T_{cy} \\ T_{cz} \end{Bmatrix} \qquad (89)\ (\text{cont'd})$$

where the subscript on the gimbal rate solution sets are used for identification of the particular solution. The CMG gimbal rate commands can be written in vector matrix form by augmenting each solution with a null (zero) row which corresponds to the deleted torque vector:

$$\begin{Bmatrix} \dot{\alpha}_1 \\ \dot{\alpha}_2 \\ \dot{\alpha}_3 \\ \dot{\alpha}_4 \end{Bmatrix} = \begin{Bmatrix} 0 \\ \dot{\alpha}_2 \\ \dot{\alpha}_3 \\ \dot{\alpha}_4 \end{Bmatrix}_1 + \begin{Bmatrix} \dot{\alpha}_1 \\ 0 \\ \dot{\alpha}_3 \\ \dot{\alpha}_4 \end{Bmatrix}_2 + \begin{Bmatrix} \dot{\alpha}_1 \\ \dot{\alpha}_2 \\ 0 \\ \dot{\alpha}_4 \end{Bmatrix}_3 + \begin{Bmatrix} \dot{\alpha}_1 \\ \dot{\alpha}_2 \\ \dot{\alpha}_3 \\ 0 \end{Bmatrix}_4 \qquad (90)$$

That is, each gimbal rate command is composed of the three solution sets in which its torque vector appears:

$$\left.\begin{aligned} \dot{\alpha}_1 &= \dot{\alpha}_{12} + \dot{\alpha}_{13} + \dot{\alpha}_{14} \\ \dot{\alpha}_2 &= \dot{\alpha}_{21} + \dot{\alpha}_{23} + \dot{\alpha}_{24} \\ \dot{\alpha}_3 &= \dot{\alpha}_{31} + \dot{\alpha}_{32} + \dot{\alpha}_{34} \\ \dot{\alpha}_4 &= \dot{\alpha}_{41} + \dot{\alpha}_{42} + \dot{\alpha}_{43} \end{aligned}\right\} \qquad (91)$$

The matrix inverses can be incorporated into equation (90) by adding the null row to each inverse matrix to form B_c, a 4 by 3 matrix with its cth row zero, for example.

$$B_1 = \begin{bmatrix} 0 & 0 & 0 \\ & A_1^{-1} & \end{bmatrix} = \begin{bmatrix} 0 & 0 & 0 \\ a_{11} & a_{12} & a_{13} \\ a_{21} & a_{22} & a_{23} \\ a_{31} & a_{32} & a_{33} \end{bmatrix} \quad . \qquad (92)$$

Utilizing this somewhat superficial matrix definition, the three inverse steering laws can be written as

$$\begin{Bmatrix} \dot{\alpha}_1 \\ \dot{\alpha}_2 \\ \dot{\alpha}_3 \\ \dot{\alpha}_4 \end{Bmatrix} = (-1/4h)\,(B_1 + B_2 + B_3 + B_4) \begin{Bmatrix} T_{cx} \\ T_{cy} \\ T_{cz} \end{Bmatrix} \quad . \qquad (93)$$

Let $a_{ij}^{\,1}$, $a_{ij}^{\,2}$, $a_{ij}^{\,3}$, and $a_{ij}^{\,4}$ represent the elements of the inverse matrices A_1^{-1}, A_2^{-1}, A_3^{-1}, and A_4^{-1} respectively. Then, from equations (92) and (93), the gimbal commands are

$$\left.\begin{aligned}
\dot{\alpha}_1 &= (-1/4h)\left[(a_{11}^{\,2} + a_{11}^{\,3} + a_{11}^{\,4})\,T_{cx} + (a_{12}^{\,2} + a_{12}^{\,3} + a_{12}^{\,4})\,T_{cy} \right. \\
&\qquad \left. + (a_{13}^{\,2} + a_{13}^{\,3} + a_{13}^{\,4})\,T_{cz} \right] \\
\dot{\alpha}_2 &= (-1/4h)\left[(a_{11}^{\,1} + a_{21}^{\,3} + a_{21}^{\,4})\,T_{cx} + (a_{12}^{\,1} + a_{22}^{\,3} + a_{22}^{\,4})\,T_{cy} \right. \\
&\qquad \left. + (a_{13}^{\,1} + a_{23}^{\,3} + a_{23}^{\,4})\,T_{cz} \right] \\
\dot{\alpha}_3 &= (-1/4h)\left[(a_{21}^{\,1} + a_{21}^{\,2} + a_{31}^{\,4})\,T_{cx} + (a_{22}^{\,1} + a_{22}^{\,2} + a_{32}^{\,4})\,T_{cy} \right. \\
&\qquad \left. + (a_{23}^{\,1} + a_{23}^{\,2} + a_{33}^{\,4})\,T_{cz} \right]
\end{aligned}\right\} \quad . \qquad (94)$$

$$\dot{\alpha}_4 = (-1/4h)\left[(a_{31}^1 + a_{31}^2 + a_{31}^3) T_{cx} + (a_{32}^1 + a_{32}^2 + a_{32}^3) T_{cy} + (a_{33}^1 + a_{33}^2 + a_{33}^3) T_{cz} \right] \quad . \tag{94 (cont'd)}$$

If the inverse exists for all four gimbal sets, the desired torque will be obtained. However, if one or more of the A_c matrices are singular, special strategies must be devised to obtain the desired torque. The solution set whose determinant is zero could be disregarded and the desired torque apportioned to the remaining three sets. Bendix proposes a CMG singularity detection and avoidance scheme in their HEAO-A Phase B Final Study Report [6]. The box product between the column vectors of each A_c matrix is continuously calculated and, when any set value becomes less than some specified small value, a biased rate command is applied to one of the three CMGs in that set. The remaining CMGs must counteract the torque produced by the biased rate, hopefully driving the CMGs away from the singular condition.

Singularity detection is accomplished by continuously monitoring the triple scalar product between the column vectors of each torque matrix, A_c. The value of the determinant of A_c is identical to the triple scalar product. When the determinant of a torque matrix is zero, the three torque vectors [represented by k_c, $c = 1, 2, 3, 4$, in equation (87)] are coplanar and that particular matrix has no inverse at that instant of time. Singularities are detected by monitoring

$$\left.\begin{aligned} k_2 \cdot k_3 \times k_4 &= A_1 \\ k_1 \cdot k_3 \times k_4 &= A_2 \\ k_1 \cdot k_2 \times k_4 &= A_3 \\ k_1 \cdot k_2 \times k_3 &= A_4 \end{aligned}\right\} \quad . \tag{95}$$

When the absolute value of any determinant is less than a small positive constant, P_s, a near singularity has been detected for the cth torque matrix. That is, if

$$|A_c| < P_s \quad , \tag{96}$$

the singularity avoidance scheme is invoked.

The singularity avoidance scheme consists of applying a biased rate command, $\Delta\alpha_{ic}$, to any of the three CMG gimbals represented in the matrix whose determinant is less than P_s. The sign of the bias is opposite the polarity of the gimbal rate just previous to invoking singularity avoidance. Letting $\dot{\alpha}_s$ be the magnitude of the bias, the bias rate command to the ith CMG can be written as

$$\Delta\alpha_{ic} = -\dot{\alpha}_s \text{ sign } [\dot{\alpha}_{ic}(t-1)] \tag{97}$$

where t-1 indicates the rate measurement from the previous computational cycle. The remaining three CMGs, denoted by j, k, l are biased to counteract the bias applied to the ith CMG by defining

$$\begin{Bmatrix} \Delta\alpha_{jc} \\ \Delta\alpha_{kc} \\ \Delta\alpha_{lc} \end{Bmatrix} = -\alpha_s A_i^{-1} \tilde{k}_i \quad , \tag{98}$$

where k_i is the column vector corresponding to the biased CMG torque vector, equation (86), and A_i^{-1} is the inverse of the matrix that does not contain the ith torque matrix. For example, if $|A_1| < P_s$, then either gimbal 2, 3, or 4 may be selected for a bias rate command. Selecting the second CMG gimbal to apply a bias rate command yields

$$\Delta\dot{\alpha}_{21} = -\dot{\alpha}_s \text{ sign } [\dot{\alpha}_{21}(t-1)] \tag{99}$$

and

$$\begin{Bmatrix} \Delta\dot{\alpha}_{11} \\ \Delta\dot{\alpha}_{31} \\ \Delta\dot{\alpha}_{41} \end{Bmatrix} = -\dot{\alpha}_s A_2^{-1} \tilde{k}_2 \tag{100}$$

Then, the bias commands are added to the solution set rate commands, equation (91), to provide singularity avoidance. For the example given, the CMG gimbal rate commands are

$$\left.\begin{aligned} \dot{\alpha}_1 &= \dot{\alpha}_{12} + \dot{\alpha}_{13} + \dot{\alpha}_{14} + \Delta\dot{\alpha}_{11} \\ \dot{\alpha}_2 &= \dot{\alpha}_{21} + \dot{\alpha}_{23} + \dot{\alpha}_{24} + \Delta\dot{\alpha}_{21} \\ \dot{\alpha}_3 &= \dot{\alpha}_{31} + \dot{\alpha}_{32} + \dot{\alpha}_{34} + \Delta\dot{\alpha}_{31} \\ \dot{\alpha}_4 &= \dot{\alpha}_{41} + \dot{\alpha}_{42} + \dot{\alpha}_{43} + \Delta\dot{\alpha}_{41} \end{aligned}\right\} \tag{101}$$

Once initiated, the singularity avoidance slewing will continue until either another determinant drops below P_s or the first exceeds P_s. If another set drops below P_s, the bias commands are based on the second singularity condition. If all determinants exceed P_s, the avoidance is discontinued and normal operation is resumed.

In the preceding paragraphs, the Bendix three-gimbal inverse steering law with singularity detection and avoidance has been derived. If each solution set could contribute its allotted portion of the desired commanded torque, ideal control would be obtained. Depending upon the CMG gimbal positions and the desired torque at any instant of time, however, the solution sets cannot provide equal control authority in the required direction. For example, when any two CMG torque vectors, k_c, are colinear, at least two of the

solution set matrices are singular [equations (87)] and cannot provide their apportioned share of the desired control torque. Even if the other two solution sets could provide perfect commands, only half the needed torque would be produced since each set has been apportioned only one-fourth of the required torque commands. Moreover, when the singularity avoidance scheme starts working, the bias commands will produce undesirable torque components which will interfere with the normal torque needed for control, temporarily interrupting the vehicle's pointing accuracy. To help alleviate this deficiency, each solution set should be required to produce all the desired torque and the individual gimbal commands adjusted by dividing by one-fourth.

In comparing the Bendix three-gimbal inverse steering law with those derived in the previous sections, the Bendix law is far more complex then any of the other laws. Moreover, the Bendix scheme introduces mathematical singularities that are not otherwise present and do not correspond with ghu. For example, if any two CMG torque vectors are colinear, two of the solution set matrices become singular even if the total CMG system can provide perfect control through the remaining two solution sets.

Singularity detection and avoidance schemes are required to prevent program divergence. When the Bendix singularity avoidance scheme is invoked, unwanted torques are introduced which tend to disturb the vehicle's pointing performance. Four 3 by 3 matrices must be inverted to obtain the Bendix steering law, but only one 3 by 3 inversion is required in the pseudo inverse steering law. CMG failures must be identified and the correct solution sets deleted for proper failure mode operation with the Bendix steering law. Because of the complexity of the Bendix three-inverse steering law without corresponding increases in either reliability or performance, it is not recommended for use on HEAO.

Simulations indicate that the Bendix three-gimbal inverse steering law produces acceptable vehicle pointing performance. But, without the singularity detection and avoidance scheme, only about one-fourth of the available CMG momentum could be utilized before encountering a singular condition, after which the system diverged and exceeded the required pointing specifications. To utilize the Bendix steering law and the total CMG momentum envelope, it is absolutely necessary to also use their singularity detection and avoidance scheme, which will degrade performance. About four times more computer time was required for the Bendix steering law without singularity avoidance than for the pseudo inverse steering law.

F. The G.E. Transpose with Torque Feedback

As previously shown by equation (32), the CMG torque is

$$\dot{\tilde{H}} = hC\,\dot{\tilde{\alpha}} \quad , \tag{102}$$

where h is the momentum per CMG, C is the normalized 3 by 4 gimbal torque matrix, $\dot{\tilde{\alpha}}$ is a 4 by 1 column matrix representing the CMG gimbal rates, and $\dot{\tilde{H}}$ is a 4 by 1 column matrix for CMG torque. The matrix C has no unique inverse. However, the first approximation to the inverse of such a matrix is its transpose. The desired control torque, T_c, based on attitude error signals is substituted with a neagative sign for the CMG torque. Approximating the inverse of the torque matrix by the transpose, the CMG steering law is

$$\dot{\tilde{\alpha}} = (-1/h)\, C^{*}\, \tilde{T}_c \quad . \tag{103}$$

Expanding the transpose steering law, the gimbal rate commands are

$$\left.\begin{aligned}
\dot{\alpha}_1 &= -(C_{11}\, T_{cx} + C_{21}\, T_{cy} + C_{31}\, T_{cz})/h \\
\dot{\alpha}_2 &= -(C_{12}\, T_{cx} + C_{22}\, T_{cy} + C_{32}\, T_{cz})/h \\
\dot{\alpha}_3 &= -(C_{13}\, T_{cx} + C_{23}\, T_{cy} + C_{33}\, T_{cz})/h \\
\dot{\alpha}_4 &= -(C_{14}\, T_{cx} + C_{24}\, T_{cy} + C_{34}\, T_{cz})/h
\end{aligned}\right\} \quad . \tag{104}$$

There are no mathematical singularities in the steering law and it is easy to implement. The main disadvantages of this type steering law is that the desired torque is not produced and the gain through the CMGs depends upon the gimbal positions at that instant of time. For example, if the gimbal

angles are all zero and the elements of the torque matrix is evaluated at that condition, a unit torque command per axis produces a torque of $4s^2\beta$ on the X-axis and $2c^2\beta$ on both the Y- and Z-axis. More than twice as much torque is produced on the X-axis than was commanded, assuming a beta angle of 53.1 degrees. However, only about three-fourths of the commanded torque is produced on either the Y- or Z-axis. To alleviate this basic deficiency in control effectiveness, G. E. [2] has utilized CMG torque feedback in the transpose steering law. Since the actual CMG gimbal rate is proportional to the torque being produced, CMG tachometers measure the gimbal rates which are fed back in a minor loop illustrated in Figure 9. A first-order lag filter is installed in the loop to provide added rejection of mechanical noise errors.

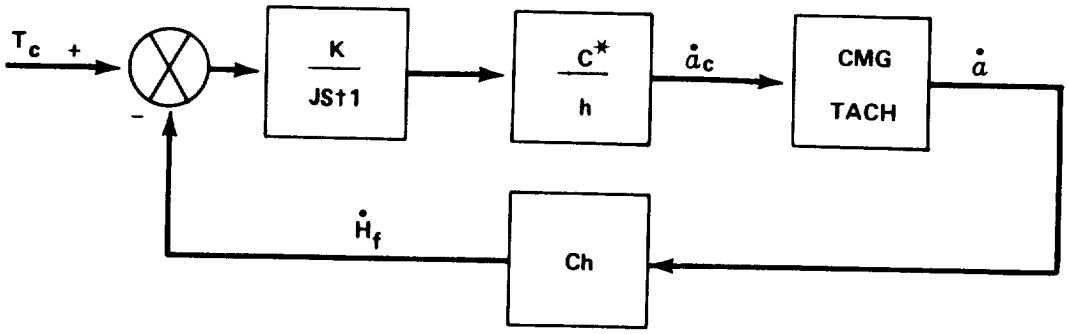

Figure 9. Transpose steering with torque feedback.

The modified transpose steering law with CMG torque feedback, $\dot{\bar{H}}_f$, becomes

$$\left.\begin{aligned}
\dot{\alpha}_1 &= -\left[C_{11}\left(T_{cx} - \dot{h}_x\right) + C_{21}\left(T_{cy} - \dot{h}_y\right) + C_{31}\left(T_{cz} - \dot{h}_z\right)\right]/h \\
\dot{\alpha}_2 &= -\left[C_{12}\left(T_{cx} - \dot{h}_x\right) + C_{22}\left(T_{cy} - \dot{h}_y\right) + C_{32}\left(T_{cz} - \dot{h}_z\right)\right]/h \\
\dot{\alpha}_3 &= -\left[C_{13}\left(T_{cx} - \dot{h}_x\right) + C_{23}\left(T_{cy} - \dot{h}_y\right) + C_{33}\left(T_{cz} - \dot{h}_z\right)\right]/h \\
\dot{\alpha}_4 &= -\left[C_{14}\left(T_{cx} - \dot{h}_x\right) + C_{24}\left(T_{cy} - \dot{h}_y\right) + C_{34}\left(T_{cz} - \dot{h}_z\right)\right]/h
\end{aligned}\right\} \quad (105)$$

Although the torque feedback provides constant gain for the rate loops, the total CMG system still has a variable gain as a function of the CMG gimbal angles. However, unless very fine control is required, adequate vehicle performance should be maintained. The torque feedback should help provide only the control authority required by the attitude error signals.

G. The BECO H-Distribution

As previously mentioned, equation (32) does not have a unique inverse for the CMG gimbal rates in terms of other parameters because the matrix C is not square and, therefore, is singular. An exact solution can be obtained by finding a constraint equation between the gimbal rates. This equation can be used to eliminate one of the gimbal rates from equation (32), thus reducing the C matrix to a 3 by 3 dimension which has an exact inverse, provided it is nonsingular. In lieu of a subsidiary condition between CMGs, BECO [3] has proposed the following scheme for obtaining a steering law.

Assume that CMG number 4 is arbitrarily gimbaled at a certain constant rate at each instant of time the matrix C is to be inverted. Moreover, assume that this rate can be determined just prior to each time step so that CMG saturation and ghu conditions are avoided. Under these conditions,

$$\dot{\alpha}_4 \quad \dot{\alpha}_4 \qquad (106)$$

is used as a fourth equation to augment equations (32)

$$\begin{Bmatrix} \dot{h}_x \\ \dot{h}_y \\ \dot{h}_z \\ \dot{\alpha}_4 \end{Bmatrix} \begin{bmatrix} C_{11} & C_{12} & C_{13} & C_{14} \\ C_{21} & C_{22} & C_{23} & C_{24} \\ C_{31} & C_{32} & C_{33} & C_{34} \\ 0 & 0 & 0 & 1/h_4 \end{bmatrix} \begin{Bmatrix} \dot{\alpha}_1 h_1 \\ \dot{\alpha}_2 h_2 \\ \dot{\alpha}_3 h_3 \\ \dot{\alpha}_4 h_4 \end{Bmatrix} . \qquad (107)$$

Let A be the augmented torque matrix in equation (107) and let Δ be its determinant. Using the elements of C [equation (31)], the determinant of A is

$$\Delta = (-S\beta/h)\left[2C^2\beta\ C\alpha_1\ C\alpha_2\ C\alpha_3 + S\alpha_2\ S(\alpha_1 + \alpha_3) - C\beta\ C\alpha_2\ S(\alpha_1 - \alpha_3)\right] \quad . \tag{108}$$

Assuming Δ is not zero, the solution of equation (107) is

$$\begin{Bmatrix} \dot{\alpha}_1 \\ \dot{\alpha}_2 \\ \dot{\alpha}_3 \\ \dot{\alpha}_4 \end{Bmatrix} = (-1/h)\,A^{-1} \begin{Bmatrix} T_{cx} \\ T_{cy} \\ T_{cz} \\ \dot{\alpha}_4 \end{Bmatrix} \quad , \tag{109}$$

where $\tilde{T}_c$ has been substituted for $\dot{\tilde{H}}$ with a negative sign.

The solution for CMG gimbal angles numbered 1, 2, and 3 [equation (109)] depends on both the gimbal rate and position of CMG number 4. As noted by equation (108), the determinant does not depend upon CMG number 4. The determinant goes to zero under the following conditions:

1. $\alpha_1 = -\alpha_3$ or $\alpha_1 = 180 - \alpha_3$ and $\alpha_2 = 90$ degrees.

2. $\alpha_1 = \alpha_3 = 90$ degrees.

3. $k_1 \cdot k_2 \times k_3 = |A_4| = 0$.

These conditions can occur without producing ghu. Thus, mathematical singularities not coinciding with ghu conditions are introduced by this formulation.

At this point the obvious problem is to suitably determine $\dot{\alpha}_4$. To prevent A from going singular, Δ must not be zero. It appears that singularities could be avoided by making the fourth gimbal rate, at each time step, inversely proportional to the determinant of A. However, to minimize the

total gimbal rates, the fourth gimbal should also be proportional to the root sum square of the other gimbal rates. Thus, $\dot{\alpha}_4$ may be determined by setting

$$\dot{\alpha}_4 = K(\dot{\alpha}_1^2 + \dot{\alpha}_2^2 + \dot{\alpha}_3^2)^{1/2}/\Delta \quad , \tag{110}$$

where K is a constant. A suitable value of K was found to be 0.001.

There are certain relative orientations of the spin momentum vectors of the four CMGs such that no torque can be produced in a particular direction. Such orientations will be referred to as gyro hang-up orientations and should be avoided if possible to have complete and independent control of the spacecraft axes at every instant of time.

The condition for the gyro hang-up orientation is that at any given instant of time, the torque vectors of the four CMGs happen to lie in a plane. If at that instant of time a torque normal to that plane is commanded, the CMGs cannot contribute any torque in the commanded direction and control is lost in that particular direction. Therefore, the only way to avoid gyro hang-up orientations is to not allow the torque vectors of the four CMGs to go into a plane. The following analysis is conducted to determine the conditions in terms of the known quantities like α_1, α_2, α_3, and α_4 when gyro hang-up orientations may occur and a scheme to avoid these orientations.

The determinant Δ vanishes both at ghu orientations and at mathematical singularities. In principle, if Δ is positive, the fourth CMG can be used to cause Δ to increase, remain the same, or decrease as slowly as possible. Hopefully, this will delay the occurrence of ghu or singularity as long as possible.

To get an explicit expression for $\dot{\alpha}_4$ which will make the derivative $\dot{\Delta}$ positive semidefinite, the following procedure may be adopted:

1. Differentiate Δ with respect to time [equation (108)] to get an expression in terms of gimbal angles and gimbal rates.

2. Substitute the values of the various gimbal rates from equation (109) into the above expression for $\dot{\Delta}$. The resulting expression is equated

to zero and solved for $\dot{\alpha}_4$. This expression for $\dot{\alpha}_4$ is in terms of gimbal angles, spacecraft rates, commanded control torques, and the CMG angular momentum resolved into spacecraft body axes. Thus the value of $\dot{\alpha}_4$ is completely known at every instant of time.

It may happen at certain instances that the gimbal rate $\dot{\alpha}_4$ calculated from the above procedure will give higher values than the upper limit of one degree per second allowed. In such instances, the upper limit value of one degree per second for $\dot{\alpha}_4$ will be used and in that case the value of Δ will tend to decrease.

Figure 10 shows an outline of the information flow diagram for this CMG control law. The following are important features of the proposed CMG control law:

1. Provides control torques exactly as commanded in all three axes.

2. No interaxis cross coupling.

3. Involves only one matrix (4 by 4) inversion. Three of the elements of this matrix are identically zero; this further reduces the complex matrix inversion computations.

4. Tends to distribute the momentum between each CMG and, for this reason, is referred to as the H-distribution steering law.

Digital simulations show that the BECO steering law [using equations (109) and (110)] gave performance equaling that of the pseudo inverse; however, it is more complicated than the pseudo inverse. For each CMG failure, the failure would have to be identified, the BECO steering law deleted, and an exact inverse inserted which would depend upon the failed CMG.

SECTION IV. STEERING LAW SUMMARY AND SELECTION

The problems in selecting a steering law are caused primarily by the fact that there are more unknowns than there are equations between the unknown variables. For example, the four-skewed CMG configuration baselined

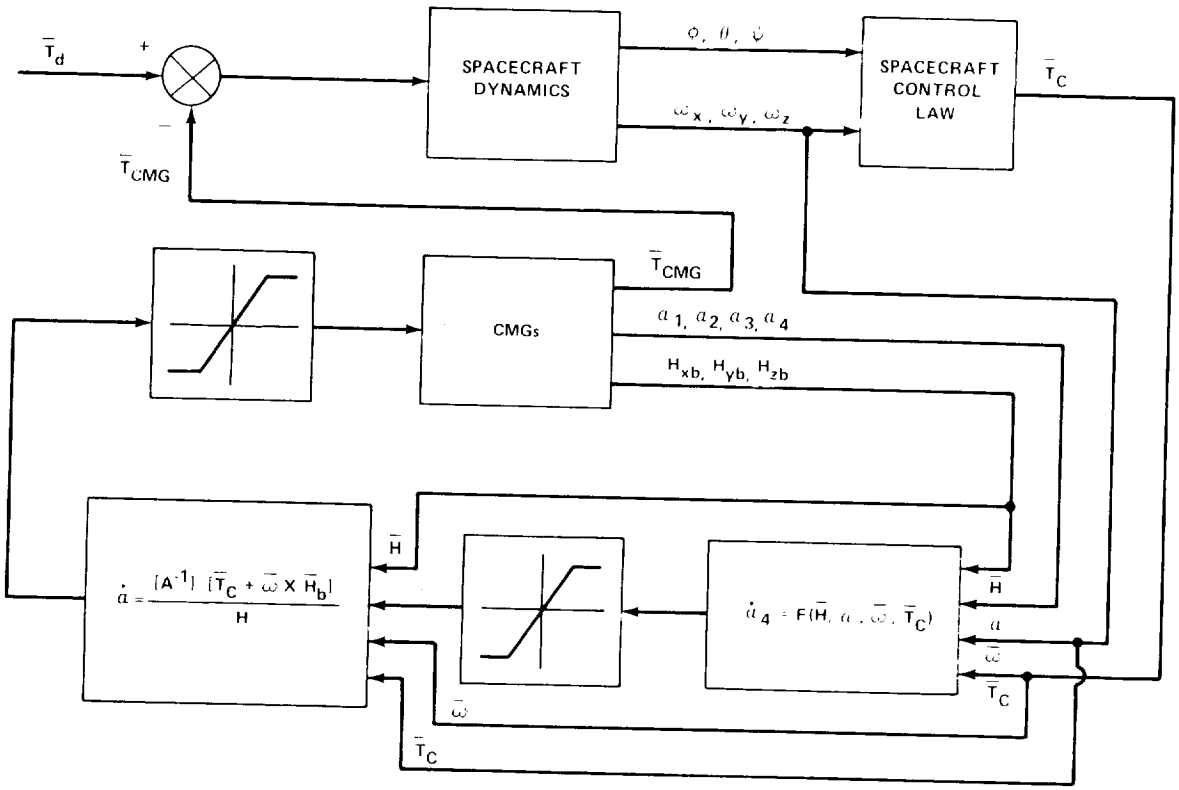

Figure 10. H-distribution steering law.

for HEAO-C has four gimbal rate commands as unknowns. However, there are only three equations from which to obtain a gimbal rate solution. These equations are obtained by equating the three components of the torque command vector to the CMG torque vector. Although there are many solutions, an exact solution in the usual sense does not necessarily exist. At this point, each designer will devise his own scheme for obtaining a solution. What is needed, of course, is a constraint equation between variables so that an exact solution can be obtained. For each constraint or assumption that is made, a different solution will be obtained for the gimbal rates. Whatever the solution, it is referred to as the CMG steering law. Several candidate steering laws were derived and compared on the basis of their effectiveness in producing the desired control torque. Each was derived for the four-skewed CMG configuration which has been baselined for HEAO-C, and each was implemented in digital simulations. The candidate steering laws were:

1. Constant gain.

2. Maximum contribution.

3. Pseudo inverse.

4. The Bendix summation of three-gimbal inverses.

5. The BECO momentum vector distribution.

6. The G.E. transpose with torque feedback.

Given any CMG configuration and steering law, there are certain conditions that can produce problems in either the performance of the system or in the ability to obtain the commanded torque. As previously defined, the CMG torque is related to the gimbal rates by a torque matrix whose columns are unit vectors along each CMG torque output axis. Since there are four CMGs, there are four columns in the torque matrix. When all four columns are coplanar, no torque can be produced perpendicular to that plane. This condition has been defined as gyro hang-up. That is, when the commanded torque is perpendicular to the total CMG torque vector, it cannot be produced. The ultimate in gyro hang-up is CMG saturation. Obviously, if the CMGs have produced all the momentum possible in a given direction and the commanded torque vector asks for more in that direction, it is impossible to produce the required change in momentum and, subsequently, control is lost. For an inertially oriented spacecraft, a component of the gravity gradient (g.g.) torque is usually offset from its zero reference, producing a momentum component that tends to saturate the CMGs over a period of time. Before the CMGs are saturated, the prevailing condition must be detected and stored CMG momentum must be interchanged with that produced by a second source, such as RCS or electromagnets. In so doing, the CMG gimbal positions are normally returned to their reference position, usually a zero momentum state.

Each steering law was compared on the basis of complexity, accuracy, mathematical singularities, failure adaption, performance after failure, and growth potential. No attempt was made to weigh the importance of each comparative factor and the ratings shown in Table 2 are somewhat subjective. However, on the basis of an elaborate digital simulation (Appendices A, B, and C) the pseudo inverse consistently gave better performance than the other steering laws, especially when various CMG failures were simulated, and was relatively easy to implement. The context in which the comparative factors were used are as follows:

1. Complexity — The mathematical manipulation and logic required for implementation.

2. Accuracy — The pointing and jitter performance obtained through simulations.

TABLE 2. CMG STEERING LAW COMPARISON[a]

Law \ Comparative Factor	Complexity	Accuracy	Singularity	Failure Adaption	Pert. After Failure	Growth Potential	Gyro Hang-Up	Cross Coupling	Efficiency	Rating
Constant Gain	1	3	1	3	3	3	3	3	3	23
Max. Contribution	2	2	1	1	2	1	2	3	2	16
Pseudo Inverse[b]	2	1	2	1	1	2	2	1	2	14
Bendix 3 Gimbal	3	2	3	2	1	3	3	2	3	22
BECO H-Distribution	3	1	2	3	1	3	1	1	1	16
G. E. Transpose	2	3	1	1	2	1	2	3	2	17

a. Each comparative factor is evaluated by 1, 2, or 3 with low numbers being best. The rating is the sum of all factor ratings.

b. The pseudo inverse is recommended for HEAO-C.

3. Singularity — Combinations of gimbal angles which can cause zeros in the denominator of the steering law, hence, program divergence.

4. Failure Adaption — The corrective actions that must be taken in the event of a CMG failure, in particular, changes in the steering law.

5. Performance After a Failure — Pointing and jitter performance with one CMG out.

6. Growth Potential — Minimum modifications required to accommodate more than four CMGs.

7. Gyro hang-up — A combination of gimbal angles which prevents the desired torque from being produced: (a) cannot transfer attitude error through the steering law, and (b) the commanded torque is perpendicular to the instantaneous CMG torque vector ($\dot{\bar{H}} \cdot \bar{T}_c = 0$) . The ultimate in gyro-hang-up is CMG saturation.

8. Cross Coupling — Not being able to produce a torque about one axis without also torquing a transverse axis.

9. Efficiency — Capability of using the total momentum available without gyro hang-up or cross coupling.

The "constant gain" steering law is derived by assuming small gimbal angles and assuming that the CMGs operate similar to scissored pairs. As implied by the name, the constant gain steering law contains constants which can easily be implemented on an analog computer. It is the simplest of all laws but is valid for gimbal angles less than ±90 degrees. It contains no singularities. With one CMG failed, the CMG null position must be redefined and a new constant gain steering law derived which is valid about the new null position. After a failure, the gimbal angles tend to become larger and the performance degrades.

The "maximum contribution" is derived by assuming that each CMG operates independently. The gimbal rate of each CMG is commanded to produce as much as possible of the desired torque. In complexity, it compares favorably with the constant gain steering law. Excellent performance is obtained as long as the gimbal angles stay small. However, as the gimbal angles become large, gyro hang-up conditions are approached and the performance is degraded due to cross coupling torques. There are no singularities in the maximum contribution steering law and no changes are required for failure adaption. With only three CMGs operating, the performance is degraded due to cross coupling CMG torques.

The "pseudo inverse" steering law basically minimizes the norm between gimbal rates and is based on the work of R. Penrose [8]. A 3 by 3 matrix inversion is required to get the inverse, along with several matrix multiplications. It represents the ultimate accuracy in performance. With one CMG failed, the pseudo inverse reduces to an exact inverse without program modifications, and its performance is not degraded. Since the pseudo inverse tends to produce exactly what is commanded, there are no cross coupling torques. However, gyro hang-up conditions can be approached as the gimbal angles become large. The pseudo inverse is recommended for HEAO-C.

The "Bendix summation of three gimbal" solutions is much more complex than any of the other candidate steering laws. Basically, the CMG torque vectors are arranged in combinations of three. There are four possible combinations, each having an exact inverse. The solutions to each combination are summed to produce the steering law. It is not known what the equivalent constraint equation would be or what, if anything, is being minimized. The Bendix law introduces several singularities that are inherent only to their scheme. In addition, gyro hang-up conditions can be attained. Singularity detection and avoidance techniques are required which compound the complexity. Failure detection and corrective actions are required. However, after a failure only one of the three gimbal inverses would be used, in which case the steering law reverts to an exact inverse and the performance improves. The Bendix steering law is not recommended for HEAO.

The "BECO H-distribution" is derived by assuming a constraint between the gimbal rates that tend to distribute the CMG momentum to avoid gyro hang-up conditions. In addition to a constraint equation, a 4 by 4 matrix must be inverted, increasing its complexity. It performed well in simulations; however, complete reprogramming is required to accommodate a CMG failure. With one CMG out, supposedly the exact inverse would be used, improving performance.

The "G. E. transpose with torque feedback" is a variation of the maximum contribution steering law. Basically, each CMG is commanded individually with the CMG torque signal being fed back to prevent overcontrol and provide stability. It is more complex than the maximum contribution with about the same performance capabilities. As the gimbal angles become large, gyro hang-up conditions can also be attained. Both the maximum contribution and G. E. steering laws offer maximum growth potential. As more CMGs are added, the cross coupling between CMGs becomes less and the performance improves. The main objection to this type steering law is that the system bandwidth varies as a function of the CMG gimbal position.

Each steering law was evaluated through digital simulations of vehicle pointing performance. Based on factors such as complexity, accuracy, CMG failure adaption, performance after failure, mathematical singularities, and singularity avoidance, the pseudo inverse CMG steering law is preferred over the other steering laws. As a specific comparison, the Bendix steering law introduces several singularities that are inherent to their law and make necessary a rather complex singularity detection and avoidance scheme. By far, the Bendix three-gimbal inverse steering law is more complex than any other candidate steering law without a corresponding increase in either accuracy or reliability. In contrast, the pseudo inverse is more accurate than any of the other laws, adapts to a failure mode without software modification, and performs after a failure (assuming failure identification) without any degradation.

With the magnetic system continuously dumping CMG momentum, the candidate CMG steering laws were simulated. In all cases, the stored CMG momentum remains near zero; consequently, the gimbal angles stay very small. Even under worst environmental torque conditions, the deviation of the angles from their null position was only about 3 degrees. As a result, all steering laws performed equally well and all produced excellent pointing and jitter performance. Since the gimbal angles stay very small, a constant gain steering law is adequate for HEAO with magnetic momentum dump. However, if rapid slewing is commanded, the gimbal angles became large during the maneuver. If HEAO is required to maneuver rapidly (for example, solar flare viewing in an antisolar direction), the pseudo inverse or maximum contribution steering law is recommended. Moreover, either steering law does not require any modification in the event of a CMG failure, providing fail operational capability. Assuming one CMG has failed, the magnetic system will automatically drive the remaining CMGs to a new null (zero momentum) position, without any changes being made in the software.

As long as the gimbal angles stay small, as with continuous momentum dump against the earth's magnetic field by electromagnets, all steering laws perform about equally well. As the gimbal angles become large there are significant differences in performance. These differences are due to the steering laws' ability to cope with singularities, gyro hang-up, and cross coupling CMG torques. Based on a comparison of the candidate steering laws for HEAO, the pseudo inverse is recommended for HEAO-C. As an alternate, the maximum contribution should be considered, especially if more CMGs were added for greater reliability over the two year mission.

The HEAO-C control system is described in Appendix A, including electromagnet sizing for continuous momentum dump. Euler's equations for HEAO-C with the four-skewed CMG configuration illustrated in Figure 2 are derived in Appendix B. The digital simulation of HEAO-C is described in Appendix C along with typical performance results using the various CMG steering laws. The spacecraft inertia properties, orbital parameters, and feedback gains are also given.

APPENDIX A. SYSTEM DESCRIPTION

An alternate actuator system proposed for HEAO-C is composed of the four skewed CMGs for maneuvering and attitude hold during normal operations, a cold gas RCS for control during orbit adjust stage (OAS) burn and initial stabilization, and three orthogonal electromagnets for momentum management of the CMGs and for direct control torque in the event of two CMG failures. Such a system will be more reliable, weigh less, and provide greater depth of failure without degrading system performance than the RCS-CMG system baselined for HEAO-C. For long lifetime missions such as HEAO, a considerable amount of RCS fuel is required to dump the accumulated CMG momentum due to biased environmental forces. It seems only natural to consider the productive use of environmental forces such as gravity gradient or the earth's magnetic field. Previous studies for the Skylab program show that gravity gradient can be utilized to dump CMG momentum. However, during dump, the spacecraft's pointing requirements must be ignored and the vehicle maneuvered in a specific sequence such that the gravity gradient counteracts the accumulated momentum. For HEAO, experiment viewing time takes priority and precludes the use of gravity dump except perhaps as a backup measure. Currently, the earth's magnetic field offers the greatest growth potential for utilizing the HEAO environment for control purposes, without sacrificing experiment viewing time by imposed maneuvers or restricting the observatory's orientation.

MAGNETIC TORQUER

Basically, the advantage of utilization of controlled interactions with ambient fields is that no fuel need be carried aboard the vehicle for CMG momentum dump. However, the use of electromagnets to react against the earth's magnetic field does require additional power to drive the coils. The magnetic system proposed for HEAO consists of three electromagnets aligned orthogonally with each vehicle control axis which is assumed to be a principal axis. When current is passed through the coils, a dipole moment, $\overline{M}$, is generated which reacts with the earth's magnetic field, $\overline{B}$, to produce a torque, $\overline{T}_m$. The torque produced obeys the vector cross product

$$\overline{T}_m = \overline{M} \times \overline{B} \quad . \tag{A-1}$$

It is apparent that the torque produced is perpendicular to both the dipole moment and the earth's field. Although limited in magnitude by the electromagnet size, the direction of the dipole can be produced in any direction. At any instant of time, the magnitude and direction of the earth's field depends on the observatory's orbital position relative to the surface of the earth. The vector components of $\overline{B}$ would be obtained by onboard magnetometers. The magnitude of $\overline{M}$ varies as a function of the currents being passed through the coils at any time. To maximize the torque produced by a given current, the dipole generated should be perpendicular to the earth's field. Moreover, it is apparent that a torque cannot be produced in the direction of $\overline{B}$.

At some instant of time, the desired torque may be aligned with $\overline{B}$, in which case it cannot be produced. However, these periods are relatively short because, as the orbital position of the observatory changes, a corresponding change occurs in the direction of the earth's field. Over any time interval during an orbit, the CMGs produce the desired torque required for fine control and the magnetic torque, if available, is used to dump the momentum accumulated in the CMGs. The magnetic system proposed for HEAO provides a torque proportional to the stored momentum. As such it is a secondary control torque and, if it cannot momentarily be produced, the vehicle performance is not degraded.

MAGNETIC CONTROL LAW

Let the CMG momentum be denoted by the vector

$$\overline{H} = h_x i + h_y j + h_z k \quad . \tag{A-2}$$

Then, if a proportional system is considered, the magnetic torque required to dump the CMG momenta must be proportional to $\overline{H}$ but opposite in direction; therefore,

$$\overline{T}_m = -K_m \overline{H} \quad , \tag{A-3}$$

where K_m is an arbitrary constant to be determined. Equating equations (A-1) and (A-3) and taking the vector cross product of $\overline{B}$ with both sides gives

$$\overline{B} \times (-K_m \overline{H}) \quad \overline{B} \times (\overline{M} \times \overline{B}) \quad B^2 \overline{M} - (\overline{M} \cdot \overline{B}) \overline{B} \quad . \tag{A-4}$$

The maximum torque for a given magnitude of $\bar{B}$ and $\bar{M}$ is obtained when $\bar{M}$ is normal to $\bar{B}$, implying that $\bar{M} \cdot \bar{B} = 0$. For this case, equation (A-4) can be solved for $\bar{M}$ to give

$$\bar{M} = -K_m(\bar{B} \times \bar{H})/B^2 \quad . \tag{A-5}$$

Equation (A-5) gives the dipole moment required to dump the CMG momentum $\bar{H}$. In expanded form, the vector components of the required magnetic control law for momentum dumping are

$$\left.\begin{aligned} M_x &= (-K_m/B^2)(B_y h_z - B_z h_y) \\ M_y &= (-K_m/B^2)(B_z h_x - B_x h_z) \\ M_z &= (-K_m/B^2)(B_x h_y - B_y h_x) \end{aligned}\right\} \quad . \tag{A-6}$$

Of course, the magnetic dipole can be directly related to current and voltage. For use on HEAO, the power has been arbitrarily limited to 10 watts per electromagnet. Substituting the dipole commands into the torque equation [equation (A-1)] produces

$$\bar{T}_m = (-K_m/B^2)(\bar{B} \times \bar{H}) \times \bar{B} = (-K_m/B^2)[B^2\bar{H} - \bar{B}(\bar{B} \cdot \bar{H})] \tag{A-7}$$

as the magnetic torque produced to dump the CMG momentum. If $\bar{H}$ is perpendicular to $\bar{B}$, then $\bar{B} \cdot \bar{H} = 0$ and the exact torque needed for momentum dump is produced. Consider the other extreme and assume that $\bar{H}$ is aligned with $\bar{B}$. In this case, $\bar{H}$ can be expressed as a constant k times $\bar{B}$ ($\bar{H} = k\bar{B}$) and equation (A-7) becomes zero. That is, no magnetic torque is produced when the earth's field is unfavorable for dumping momentum. Only that portion of the desired torque which is perpendicular to the earth's field will be produced at any given time. However, momentum can be dumped on one axis at the expense of increasing momentum on another axis, but the total magnitude will always be reduced by the magnetic system.

In the event of two CMG failures, the magnetic system could be used to provide direct torque in addition to dumping CMG momentum. For direct torque control, the magnetic torque would be set proportional to the desired control torque, $\bar{T}_c$. The desired torque is based upon attitude error signals

which have been weighted by appropriate feedback gains. Normally, the CMGs would provide this torque through the CMG steering law. The dipole moment required for direct torque commands is obtained by setting

$$\bar{T}_m = K_c \bar{T}_c \quad . \tag{A-8}$$

In a manner similar to that used to obtain the dipole commands for momentum dump, the dipole command for direct torque control is

$$\bar{M} = K_c(\bar{B} \times \bar{T}_c)/B^2 \quad . \tag{A-9}$$

Assuming two CMGs have failed, the dipole commands would be a combination of that required for momentum dump and direct control. The magnetic torque would be set equal to

$$\bar{T}_m = -K_m \bar{H} + k_c \bar{T}_c \quad . \tag{A-10}$$

The corresponding dipole solution is

$$\bar{M} = \frac{\bar{B} \times (-K_m \bar{H} + K_c \bar{T}_c)}{B^2} = \frac{-K_m}{B^2} (\bar{B} \times \bar{H}) + \frac{K_c}{B^2} (\bar{B} \times \bar{T}_c) \quad . \tag{A-11}$$

Hence, the form of the dipole command changes according to the type actuation desired. Appropriate values for the constants are $K_m = 0.01$ and $K_c = 1.0$.

Electromagnet Sizing

The maximum dipole is physically limited by the shape and volume of the electromagnet, the number of turns in the coil, current passed through the coils, and physical properties of the materials used. In sizing the electromagnets, low power usage is selected over weight as a design criterion. A maximum of 10 watts per coil has been arbitrarily selected as an upper limit and the rest of the magnetic system has been sized accordingly to meet the required torque and/or momentum dump capability. The magnetic system would be installed in the OAS and, for this reason, the length of the electromagnet has been limited to 60 inches.

Based on simulation results for which the dipoles per axis were limited to selected values, it was found that a dipole moment per axis of 0.2 ft-lb/gauss was adequate to dump the expected secular momentum due to gravity gradient torque. However, under worst-case conditions, the magnetic system could not dump all the accumulated momentum and the CMGs could saturate in about one day. For direct torque control, the magnetic system must produce a torque equal to or greater than that of gravity gradient, in which case a dipole moment of 0.4 ft-lb/gauss is desirable. With a properly sized magnetic system, two out of four CMGs can be failed and still maintain acceptable HEAO-C performance. For this reason a value of 0.4 ft-lb/gauss was selected as a basis for designing electromagnets for HEAO-C. A candidate electromagnetic torquer design to meet the above specifications is shown in Table A-1. In this case, an AEM 4750 Core was assumed to be utilized.

TABLE A-1. ELECTROMAGNET TORQUER DESIGN DATA

	Total (1 torquer)	Total (3 torquers)
Weight, lbm	110	330
Max Power, W	10	30
Outside Diameter, in.	2.45	
Core Diameter, in.	2.11	
Core Volume, in.^{3}	209.5	628.5
Max Magnetic Moment, amp-turn-m^2	5440	9422
Torque Produced in a 0.35 gauss field, ft-lb	0.14	0.24
Flux Density, gauss	12 000	
Field Intensity, oersted	20	
Core Material	AEM 4750	
Winding Material	Aluminum	

As simulation data were obtained using coils for CMG momentum dump, an improvement in observatory performance was noted. A linear analysis of the HEAO-C equations of motion proved that magnetic momentum dump introduced the integral of attitude error through the control loop, improving both pointing and jitter performance of HEAO-C. Moreover, since momentum is continuously dumped, the CMG gimbal angles stay very small, permitting the use of a constant gain steering law. Since the coil commands are based on the CMG momentum state, when one CMG is failed, the remaining CMGs are automatically driven to a new null (zero momentum) state without reprogramming or software modification. The following are some of the advantages of using electromagnets for continuous momentum management:

1. No fuel or RCS required for momentum dump.

2. Lifetime not limited by expendables.

3. Saturation detection not required.

4. Very small gimbal angles permit use of a constant gain steering law.

5. One CMG fail operational capability.

6. Operation with two CMGs failed is possible.

7. Small size CMGs (50 ft-lb-sec each) could be used.

8. Improved pointing performance.

There are, however, some possible disadvantages in the use of electromagnets. These are possible magnetic contamination, which may require that certain components such as photomultiplier tubes be shielded, or power usage, which would be limited to 30 watts for the three coils. Overall, the system should be more reliable than one using RCS dump.

SYSTEM COMPONENTS

The attitude sensing and control system components are shown in Figure A-1. The sensors provide attitude information which is processed in a central computer to generate attitude error signals. The control laws and

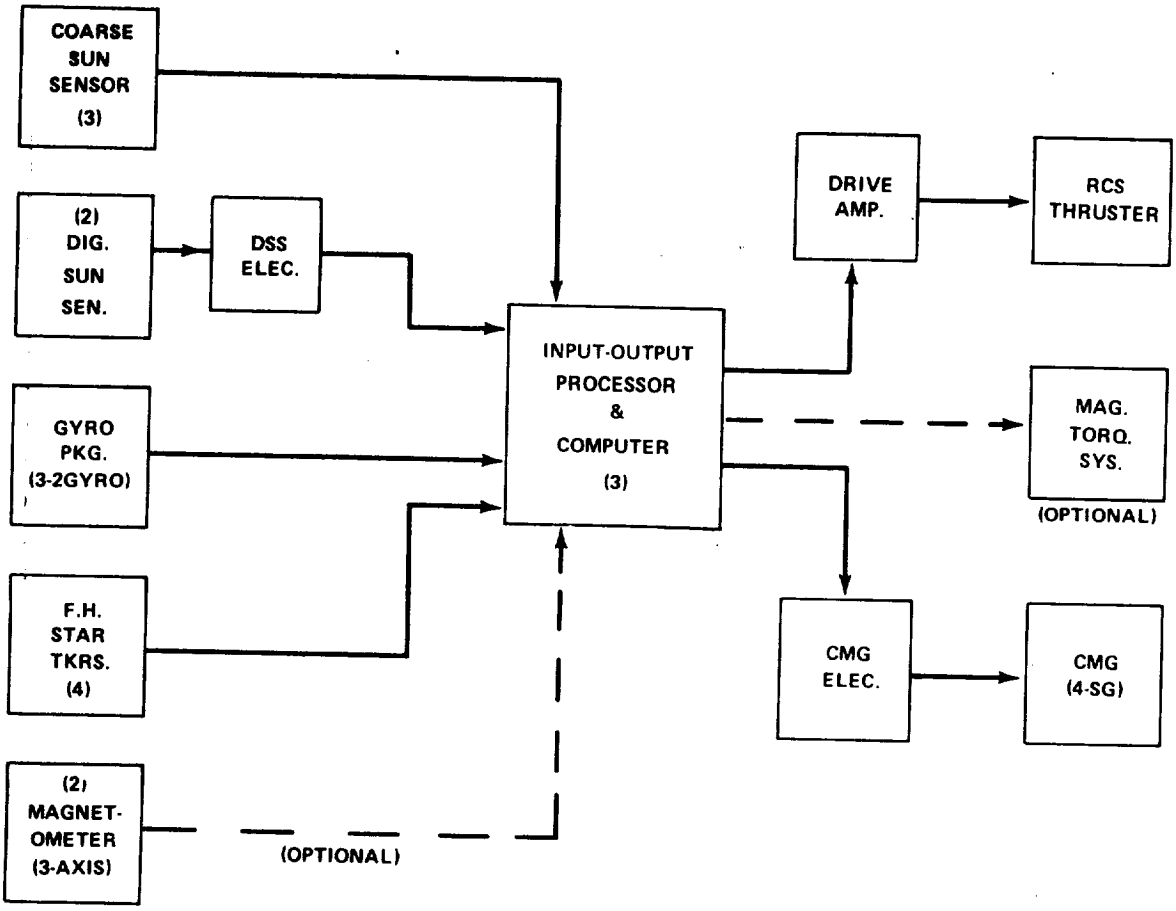

Figure A-1. HEAO-C attitude sensing and control system.

algorithms are generated within the computer to drive the actuator systems. The actuators (CMGs, RCS, and electromagnets) provide the torque required for attitude hold against environmental disturbances and for maneuvering. Most of the components are redundant so that fail operational capability exists for most subsystem failures. As illustrated, there are three coarse sun sensors, two digital sun sensors, six rate gyros, four fixed head star sensors, and two 3-axis magnetometers. There are three input-output processors and computers with only one operational at any time. The RCS is completely dual redundant with only half the system normally in use. There are three orthogonal bar torquers in the magnetic system, each with separate drive electronics and all are normally operating. All four skewed CMGs are also normally operating. However, any bar torquer or CMG can be failed without degrading system performance. If two CMGs fail, control can be maintained if the magnetic system is used to provide direct torque as well as CMG momentum management.

The interaction between the attitude sensing and control system and the HEAO spacecraft is shown in Figure A-2. Ground commands for pointing to various target sources are used to program and/or drive the guidance, navigation, and sequencing logic in the control computer. Based on the attitude commands and the present vehicle attitude from the onboard sensors, the vehicle control law forms an attitude error signal, usually denoted as the commanded torque, $\overline{T}_c$. Then, the commanded torque must be processed by an appropriate actuator steering law to obtain signals to drive the actuators. The actuators (CMGs, RCS, or magnetic torquers) produce a control torque on the vehicle that counteracts the disturbance torques, $\overline{T}_d$, and forces the attitude errors to zero. Based on the CMG accumulated momentum status and the earth's magnetic field, the magnetic coils are energized to produce a dipole moment which reacts with the earth's magnetic field to produce a magnetic torque, $\overline{T}_m$. The magnetic torque is normally used continuously to keep the CMG momentum near zero, thus, preventing CMG saturation. With the magnetic system, the RCS is not used in normal operational modes after the orbit has been established. Either with or without the magnetic system, however, an RCS is still required for initial stabilization, control during orbital adjust stage burn, initial solar acquisition, establishing the first celestial reference, and attitude hold during checkout before and while the CMGs are activated. While establishing the orbit and during initial checkout phases, the RCS is used continuously as required. After the CMGs are operational, the RCS is only used periodically for CMG momentum dump or emergencies. Normal maneuvering and attitude control is done by gimbaling the CMGs.

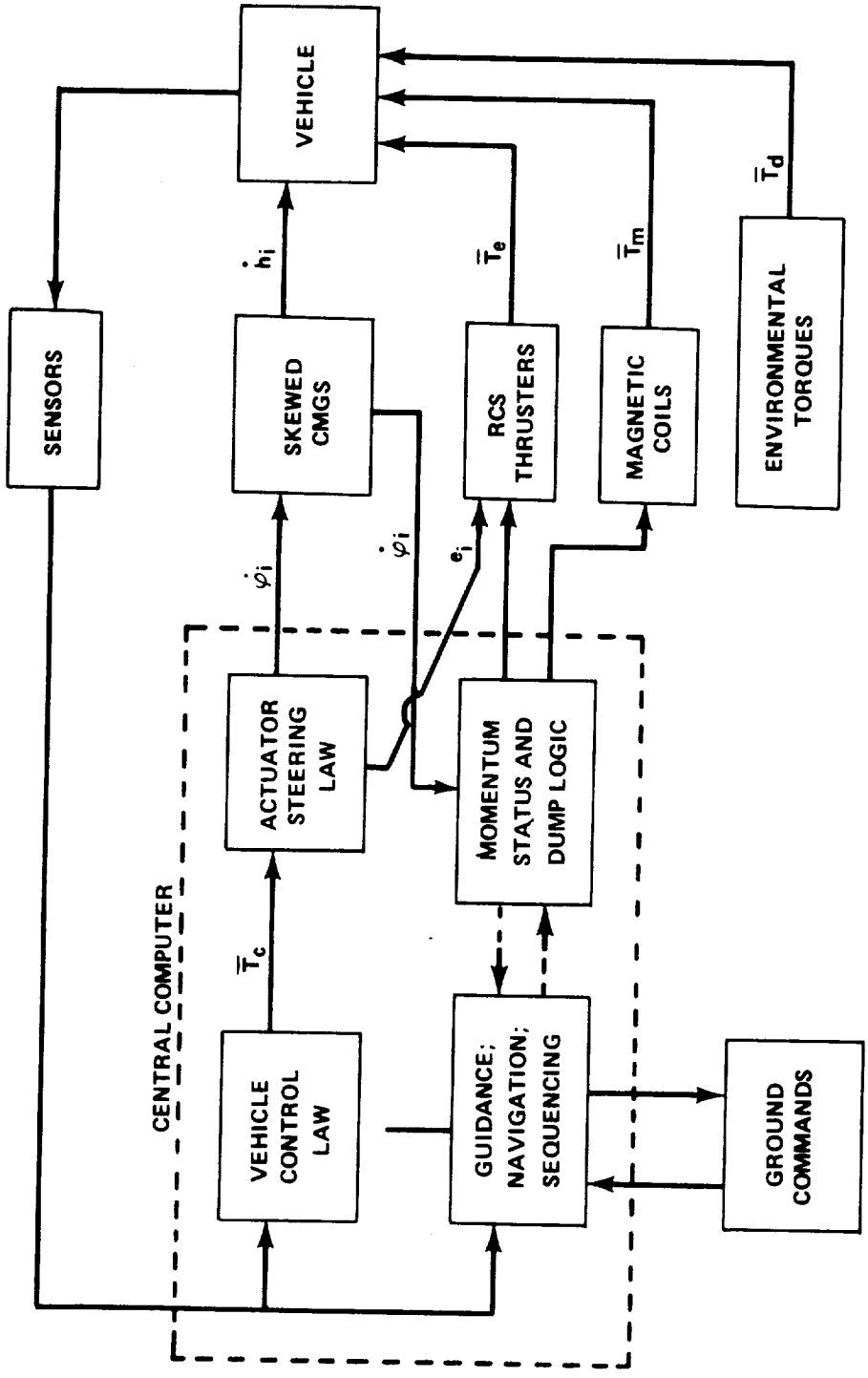

Figure A-2. Simplified attitude control system block diagram.

APPENDIX B. EULER'S EQUATIONS FOR HEAO-C

The dynamic equations which govern the rotational motion of a rigid HEAO with four skewed single gimbal CMGs are obtained by equating the time derivative of the total system angular momentum to the sum of the applied torques:

$$\dot{\bar{H}}_t = \sum \bar{T}(\text{applied}) = \bar{T}_m + \bar{T}_g \quad . \tag{B-1}$$

The applied torques are due to environmental forces such as gravity, aerodynamic and electromagnet interactions, and to onboard actuators such as reaction jets which expel mass from the spacecraft. Simulations have shown that for higher orbits, the dominant environmental torque is gravity gradient, T_g, and the others can be ignored during preliminary design studies. Normally, torque due to electromagnet interaction with the earth's ambient field is very small. But, since an electromagnet system is proposed for continuous momentum management of the CMGs, the magnetic torque given by the equation

$$\bar{T}_m = \bar{M} \quad \bar{B} \tag{B-2}$$

must be included as an applied torque. Although a reaction jet control system will be of the ON-OFF type, its torque is not considered as a part of the Euler equations since the basic objective is to show the performance of the CMG system along with bar torquers.

The total system angular momentum is composed of two parts: that due to the spacecraft motion and that due to the CMGs. The spacecraft angular momentum $\bar{H}_v$ is the product of its inertia tensor, I, and angular rate, ω.

$$\bar{H}_v = I \cdot \bar{\omega} \quad . \tag{B-3}$$

For study purposes, the products of inertia are assumed to be zero, in which case

$$\bar{H}_v = I_x \omega_x i + I_y \omega_y j + I_z \omega_z k \tag{B-4}$$

is the vector form of the spacecraft momentum relative to its reference coordinates. The CMG momentum has previously been derived in the spacecraft reference coordinates as:

$$\bar{H}_c = h_x \underset{r}{i} + h_y \underset{r}{j} + h_z \underset{r}{k} \quad , \tag{B-5}$$

whose components are given by equation (28). The total vehicle momentum is

$$\bar{H}_t = \bar{H}_v + \bar{H}_c \quad . \tag{B-6}$$

The time derivative of any vector relative to inertial space is equal to its derivative relative to its reference coordinates plus the cross product of the angular motion of the reference coordinates relative to inertial space and the vector. The angular motion of the spacecraft body reference coordinates is given by

$$\bar{\omega} = \omega_x \underset{r}{i} + \omega_y \underset{r}{j} + \omega_z \underset{r}{k} \quad . \tag{B-7}$$

Selecting body reference coordinates as a basis in which to perform the vector operations, equation (B-1) becomes

$$\left(\dot{\bar{H}}_t\right)_{\text{inertial}} = \left(\dot{\bar{H}}_t\right)_{\text{reference}} + \bar{\omega} \times \bar{H}_t = \bar{T}_m + \bar{T}_g \tag{B-8}$$

or

$$\dot{\bar{H}}_v + \bar{\omega} \times \bar{H}_v + \dot{\bar{H}}_c + \bar{\omega} \times \bar{H}_c = \bar{T}_m + \bar{T}_g \quad . \tag{B-9}$$

Performing the indicated vector operations produces the Euler equations for HEAO-C. The vector components of equation (B-9) produce three equations which govern the rotational motion:

$$\left.\begin{aligned} I_x \dot{\omega}_x + (I_z - I_y)\,\omega_y \omega_z + \dot{h}_x + h_z \omega_y - h_y \omega_z &= T_{my} + T_{gx} \\ I_y \dot{\omega}_y + (I_x - I_z)\,\omega_x \omega_z + \dot{h}_y + h_x \omega_z - h_z \omega_x &= T_{my} + T_{gy} \\ I_z \dot{\omega}_z + (I_y - I_x)\,\omega_x \omega_y + \dot{h}_z + h_y \omega_x - h_x \omega_y &= T_{mz} - T_{gz} \end{aligned}\right\} \quad . \tag{B-10}$$

As derived in the main text, equations (28) and (30),

$$\left.\begin{aligned} h_X &= S\alpha_2(h_1S\alpha_1 + h_2S\alpha_2 + h_3S\alpha_3 + h_1S\alpha_1) \\ h_Y &= h_1C\alpha_1 - h_2C\alpha_2 = C\beta(h_1S\alpha_1 - h_2S\alpha_2) \\ h_Z &= h_2C\alpha_2 - h_1C\alpha_1 = C\beta(h_1S\alpha_1 - h_3S\alpha_3) \end{aligned}\right\} \qquad \text{(B-11)}$$

and

$$\left.\begin{aligned} \dot{h}_X &= S\beta(\dot{\alpha}_1h_1C\alpha_1 - \dot{\alpha}_2h_2C\alpha_2 + \dot{\alpha}_3h_3C\alpha_3 + \dot{\alpha}_1h_1C\alpha_1) \\ \dot{h}_Y &= \dot{\alpha}_1h_1S\alpha_1 - \dot{\alpha}_2h_2C\beta C\alpha_2 - \dot{\alpha}_3h_3S\alpha_3 + \dot{\alpha}_1h_1C\beta C\alpha_1 \\ \dot{h}_Z &= \dot{\alpha}_1h_1C\beta C\alpha_1 - \dot{\alpha}_2h_2S\alpha_2 - \dot{\alpha}_3h_3C\beta C\alpha_3 - \dot{\alpha}_1h_1S\alpha_1 \end{aligned}\right\} \qquad \text{(B-12)}$$

are the CMG momentum and torque components.

The gravity torque components are given by

$$\left.\begin{aligned} T_{gX} &= 3\omega_O^2(I_Y - I_Z)R_ZR_Y \\ T_{gY} &= 3\omega_O^2(I_X - I_Z)R_XR_Z \\ T_{gZ} &= 3\omega_O^2(I_Y - I_X)R_YR_X \end{aligned}\right\} \quad , \qquad \text{(B-13)}$$

where R_Z, R_X, and R_Y are the components of the local vertical unit vector projected [illegible] coordinates and ω_O is the orbital angular rate. The magnetic torque components, equation (B-2), are

$$\left.\begin{aligned} T_{mX} &= M_YB_Z - M_ZB_Y \\ T_{mY} &= M_ZB_X - M_XB_Z \\ T_{mZ} &= M_XB_Y - M_YB_X \end{aligned}\right\} \quad , \qquad \text{(B-14)}$$

where M_X, M_Y, and M_Z are the electromagnet dipole components and B_X, B_Y, and B_Z are the earth's magnetic field components, all expressed in body coordinates.

The spacecraft is related to solar inertial coordinates by a Euler angle sequence. The solar coordinates are defined by having the X_s-axis pointing to the sun, the Z_s-axis perpendicular to the ecliptic plane directed northward, and the Y_s-axis completing a right-hand triad in the ecliptic plane. The transformation between coordinates is derived by first rotating about the X_s-axis by the angle ϕ, then rotating about the once transformed Y'_s-axis by the angle θ and, finally, about the twice transformed Z''_s-axis by the angle ψ. In vector matrix form,

$$\tilde{X}_r = B_{rs}\tilde{X}_s \quad . \tag{B-15}$$

The elements of B_{rs} (a 1, 2, 3 rotation order) are

$$\left.\begin{aligned}
B_{11} &= C\theta\, C\psi \\
B_{12} &= C\phi\, S\psi + S\phi\, S\theta\, C\psi \\
B_{13} &= S\phi\, S\psi - C\phi\, S\theta\, C\psi \\
B_{21} &= -C\theta\, S\psi \\
B_{22} &= C\phi\, C\psi - S\phi\, S\theta\, S\psi \\
B_{23} &= S\phi\, C\psi - C\phi\, S\theta\, S\psi \\
B_{31} &= S\theta \\
B_{32} &= -S\phi\, C\theta \\
B_{33} &= C\phi\, C\theta
\end{aligned}\right\} \quad . \tag{B-16}$$

The body angular rates, equation (B-7), are related to the Euler angular rates by the kinematic relations

$$\left.\begin{aligned}
\omega_x &= \dot{\phi} C\theta\, C\psi + \dot{\theta} S\psi \\
\omega_y &= \dot{\theta} C\psi - \dot{\phi} C\theta S\psi \\
\omega_z &= \dot{\psi} + \dot{\phi} S\theta
\end{aligned}\right\} \quad . \tag{B-17}$$

The inverse relations are

$$\left.\begin{aligned} \dot{\phi} &= (\omega_X C_\psi - \omega_Y S_\psi)/C\theta \\ \dot{\theta} &= \omega_Y C_\psi + \omega_X S_\psi \\ \dot{\psi} &= \omega_Z - \dot{\phi} S\theta \end{aligned}\right\} \quad . \tag{B-18}$$

Additional coordinates and transformations between coordinates are required to generate the earth's magnetic field and the local vertical vector components. These are contained in the HEAO-A summary report NASA TMX-53976 [1] and the simulation definition document prepared by Computer Sciences Corporation, Huntsville, Alabama [9]. Also, additional information on the transformations and gravity torque are contained in NASA TMX-53829 [10].

For study purposes, the HEAO body reference coordinates are defined by X_r which is perpendicular to the hard-mounted solar panels, Y_r which is along the axis of minimum inertia (long axis), and Z_r which completes a right-hand triad. When the Euler angles are zero, the body reference and solar coordinates are aligned. Vehicle pointing performance is measured by the solar offset angle, δ_s, the target pointing error, δ_p, and the spacecraft angular rate, ω.

The solar offset angle is given by

$$\delta_s = \cos^{-1}(B_{11}) = (\theta^2 + \psi^2)^{1/2} \tag{B-19}$$

and the target pointing error by

$$\delta_p = [(\phi - \phi_c)^2 + (\theta - \theta_c)^2]^{1/2} \tag{B-20}$$

where ϕ_c, θ_c, and ψ_c are the commanded Euler angles required for target pointing the long spacecraft axis to an experiment target source. The total spacecraft stability, commonly referred to as jitter, is given by

$$\omega = (\omega_X^2 + \omega_Y^2 + \omega_Z^2)^{1/2} \quad . \tag{B-21}$$

The roll error about the line-of-sight, long observatory axis, is given by

$$\delta_r = \phi - \phi_c \quad . \tag{B-22}$$

During normal operations, the HEAO-C performance requirements are

$$\left.\begin{aligned} \delta_s &\leq 37 \text{ degrees} \\ \delta_p &\leq 1 \text{ arc minute} \\ \delta_r &\leq 5 \text{ arc minutes} \\ \omega &\leq 1 \text{ arc second/second} \end{aligned}\right\} . \qquad \text{(B-23)}$$

APPENDIX C. PERFORMANCE SIMULATIONS

INTRODUCTION

A digital computer program was written to simulate the dynamic behavior of the HEAO-C spacecraft in a circular earth orbit. The program is basically a modification of the program [9] used for HEAO-A with the addition of CMG dynamics and steering law. The equations which were programmed were Euler's equations for rotational motion about the principal observatory body axes, Euler's kinematical relations which relate the observatory body principal axes to the solar reference, transformational matrices which relate the environmental forces to the observatory body axes, control logic which relates the HEAO spacecraft's attitude errors and rates through appropriate feedback gains to applied torques about the observatory body axes, a spherical harmonic expansion of the earth's magnetic field, CMG dynamics, several selected steering laws, and magnetic control torque logic for CMG momentum management.

For added realism, the program included all natural movements which could affect the spacecraft's attitude motion. These movements include the earth's revolution about the sun (1 deg/day), regression of the ascending line of orbital node (6 deg/day) and the earth's rotation (360 deg/day). The environmental forces acting on the spacecraft were gravity gradient, aerodynamic, and [illegible].

The dominant environmental torque is that caused by g.g. effects. To simulate the gravity torque, the vector components of the local radius vector must be projected into body coordinates. The effects of orbital position, inclination, orbital regression, time of year, and position of the ascending line of nodes were considered in deriving the required transformational matrices. The magnitude of the g.g. torque also depends upon the vehicle inertia properties, in particular the difference between the inertia values. Both spacecraft inertia values and orbital conditions were selected such that the g.g. torque attained its maximum value.

Figure C-1 illustrates a simplified block diagram of the HEAO-C digital simulation. The simulation contains four nonlinearities: (1) limits on the CMG gimbal rates; (2) limits on the CMG gimbal positions, which are not shown; (3) limits on each position feedback channel (not shown); and (4) limits on the electromagnet dipole moments. During the simulation runs, the limits on the CMG gimbal positions were deleted since the CMGs were assumed to have unlimited angular positions.

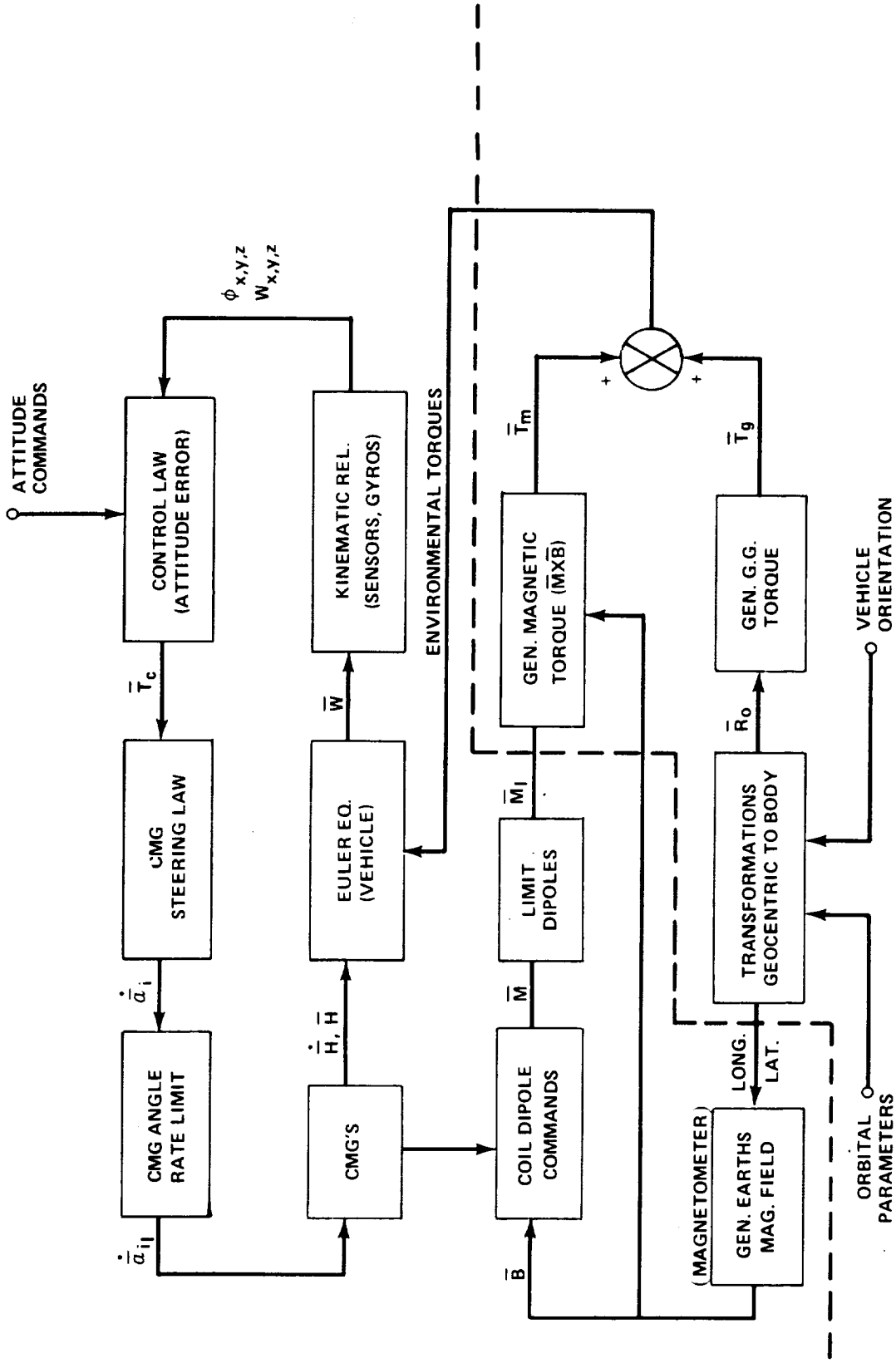

Figure C-1. Simulation block diagram.

Parameters and Cases Simulated

The parameters utilized in the simulation for base runs are listed below.

I_x — 2598 slug-ft^2, long (pointing) axis inertia

I_y — 82 119 slug-ft^2, intermediate inertia axis

I_z — 82 669 slug-ft^2, maximum (sunward) inertia axis

AA — 270 n. mi., orbital altitude

i — 28.5 deg, orbital inclination

λ — 270 deg, winter solstice time of year

Ω — 180 deg, morning terminator line of nodes

Ω_G — 315 deg, position of Greenwich meridian relative to Aries

H — 250 ft-lb-sec, momentum per CMG

[illegible] — 1 gauss, assumed dipole limit

K_{px} — .256, X-axis position feedback gain

K_{py} — .8097, Y-axis position feedback gain

K_{pz} — .4159, Z-axis position feedback gain

K_{rx} — .4142, X-axis rate feedback gain

K_{ry} — .55 100, Y-axis rate feedback gain

K_{rz} — .56 333, Z-axis rate feedback gain

$L_{x_{max}}$ — 15 ft-lb/rad, X-axis position feedback limit

$L_{y_{max}}$ — 478 ft-lb/rad, Y-axis position feedback limit

L_{zm} = 481 ft-lb/rad, Z-axis position feedback limit

$\dot{\alpha}_l$ = 1 deg/sec, CMG gimbal rate limit

K_m = 0.01, magnet dipole gain for momentum dumping

β = 53.1 deg, CMG skew angle

K_c = 1.0, magnet dipole gain for direct torque if two CMGs have failed

More than 100 cases were simulated for various HEAO-C configurations, orbital conditions, and control gains. Utilizing the base run parameters, with the g.g. torque near its maximum value, six CMG steering laws were evaluated. On the basis of this evaluation, the pseudo inverse steering law is recommended for HEAO-C. Most of the simulation results shown are based on the pseudo inverse CMG steering law and all on one set of the base run parameters. During the study period, several configurations were evaluated. These were a HEAO configuration with distributed subsystems, a configuration with a subsystems module, and several configurations which had the orbital adjust stage (OAS) attached. The inertia values shown above represent a growth version of the HEAO with distributed subsystems and with the OAS attached.

The feedback control gains were selected to give a damping ratio of 0.7 and a natural frequency of 0.314. The corresponding time period is 20 sec and the system time constant is 10 sec/rad. As shown in Reference 11, the pointing error is proportional to the disturbance torque magnitude and inversely proportional to the position feedback gain. In essence, the greater the required pointing accuracy, the higher the feedback gains. Introduction of integral position feedback permits the use of lower position and rate gains. However, HEAO-C pointing performance can be obtained with only position and rate feedback terms in the attitude error signal. As an alternate, electromagnets are used to dump the accumulated momentum against the earth's magnetic field. In this case, the magnetic loop also provides integral feedback of the attitude error signal which improves vehicle pointing performance as an added bonus. The objective of the attitude error signal is to formulate some desired vehicle torque command.

The objective of the CMG steering law is to convert the torque commands into CMG gimbal rate commands. When the CMG gimbal positions are moved, a corresponding change occurs in the CMG momentum vector, hence,

producing a control torque which acts on the vehicle to counteract the disturbing torque due to the environment. Ideally, the steering law should make the CMGs produce exactly the torque which is commanded.

All the simulation data have been plotted as a function of orbit time as measured from the ascending line of nodes, which for all cases shown is at the morning terminator. At a circular altitude of 270 nautical miles, the orbital rate is 1.10502×10^{-3} rad/sec with a period of 5686 sec. The orbital time is scaled in 1000-sec increments on all graphs. The time step used in the digital simulation was 0.5 sec; that is, at each half-second of orbit time, the equations in the simulation were solved. The printout was on each 50-sec interval. Although not important for attitude control purposes, the minimum period of orbital darkness is about 26 minutes per orbit and the maximum about 36 minutes. There are about 15.2 orbits per day.

The vehicle performance is measured by three Euler angles: ϕ about the sunline (X_S-axis), θ about the once transformed solar Y_S-axis, and ψ about the twice transformed solar Z_S-axis. For small angular deviations the Euler angles ϕ, θ, and ψ correspond to rotations about the spacecraft Z_V, X_V, and Y_V axes respectively. The pointing performance is measured by the angle between the long spacecraft axis (X_V) and the desired target and is given by

$$[\quad)^2 + (\quad)^2]^{1/2} \quad ,$$

where the subscript c indicates the commanded rotations required to point to the selected target. The roll error is about the target line-of-sight (experiment axis):

$$\phi_E = \phi - \psi_c \quad .$$

The pointing stability (jitter) is given by

$$\omega = (\omega_X^2 + \omega_Y^2 + \omega_Z^2)^{1/2}$$

where ω is the body angular rate. To meet HEAO performance requirements, the errors must be less than 1 arc min pointing, 5 arc min roll, and 1 arc sec/sec jitter.

Response Capabilities

The maximum vehicle maneuver capabilities are determined by both the CMG system torque and available momentum for making the maneuver. Assuming 250 ft-lb-sec per CMG with the gimbal rate limited to 1 deg/sec, each CMG has a torque capability of 4.36 ft-lb. Utilizing a four-skewed CMG configuration with a skew angle of 53.1 degrees, the maximum torque per vehicle axis is about 14 ft-lb on the sun pointing axis and 5 ft-lb on the two transverse axes, as shown in Table C-1. The maximum rotational rate imparted to the vehicle is 2.66 rpm about the axis of minimum inertia (X_V-axis). On the sun pointing (Z_V) axis, the momentum capacity of 800 ft-lb-sec allows the CMGs to spin up the vehicle to 0.109 rpm. Several runs were made with HEAO-C operating in a spinup mode similar to that required for HEAO-A. In all cases, HEAO-A performance requirements [1] were attained with a wide margin. Maximum CMG torque on the Z_V-axis permits rapid movement about the sunline for initial spinup or for small maneuvers about that axis as in normal HEAO-C operation. In case of unusual maneuvers, as in solar flare viewing, the spacecraft could be rotated about the Y_V-axis by 90 degrees. If a time optimal maneuvering command were issued, the rotation for this antisolar viewing would take about three minutes plus another three minutes estimated for settling out time to attain HEAO-C pointing requirements. This gives a total time of about six minutes. However, a time optimal maneuver scheme was not incorporated into the HEAO simulation and this is an area for future study. Normal maneuvers of 90 degrees or less were

TABLE C-1. VEHICLE RESPONSE CAPABILITIES

Axes	CMG Momentum (ft-lb-sec)[a]	CMG Torque (ft-lb)[b]	Max Turning Rate (rpm)[c]	Time for 180 deg Turn (min)[d]
X_V	800	5.24	2.66	2.18
Y_V	800	5.24	0.110	6.54
Z_V	800	13.95	0.109	6.59

a. Four 250 ft-lb-sec CMGs skewed at 53.1 degrees.

b. Max torque with gimbals at null; 1 deg/sec gimbal rates.

c. At CMG saturation.

d. Time optimal maneuver, settling out time not included.

satisfactorily conducted through the HEAO simulation by position commands only. Each position feedback channel was limited to 20 deg/min equivalent spacecraft rotation per axis. The time required to go from one X-ray source to another is short for small angle maneuvers and the CMGs do not have time to reach saturation. Normal pointing maneuvers can be made by position commands only, without utilizing a more complicated time optimal scheme.

Orbit Environmental Conditions

Although many cases were run with the orbital parameters as variables, the simulation results to be shown are all for only one type orbit so that each steering law can be compared under the same environmental conditions. The orbit and spacecraft orientations relative to the solar reference coordinates are shown in Figure C-2. The sun is at its winter solstice position (λ 270 degrees), the ascending line of nodes is at the morning terminator (Ω 180 degrees), and the earth (not shown) has its north magnetic pole tilted toward the sun (Ω_e [illegible] degrees). The spacecraft is oriented with its Z_V-axis pointing to the sun, the Y_V-axis directed northward perpendicular to the ecliptic plane, and the X_V-axis completing a triad in the ecliptic plane. With this type orbit and vehicle orientation, the gravity gradient disturbance torque is [illegible] momentum component appears on the [illegible] axis. This axis has the greatest potential for [illegible] oscillation will saturate the CMGs quicker than any other and represents a worst case for attitude hold.

Figure C-3 illustrates the g.g. torque vector components and magnitude relative to the observatory reference axes in ft-lb. The Y_V-component is biased [illegible] ft-lb. Other orbital conditions, however, can cause the biased torque to appear on either the X_V- or Z_V-axis, or to be [illegible] all axes equally. Both the X_V and Z_V axes have cyclic components and, due to vehicle symmetry, the X_V-component is near zero. The magnitude of the g.g. torque is about 0.16 ft-lb. The vehicle's pointing error is directly proportional to [illegible]. With a control system that performs well, the pointing error takes on the shape of the disturbance torque. The observatory momentum components corresponding to the torque shown in Figure C-3 are shown in Figure C-4. Due to X_V-axis symmetry both the g.g. torque and momentum are near zero on that axis. The cyclic Z_V-axis torque

produces biased but cyclic momentum. However, the biased Y_V-axis torque produces a linear buildup of momentum with time that will eventually saturate the CMGs. This momentum buildup over a period of time is denoted as secular

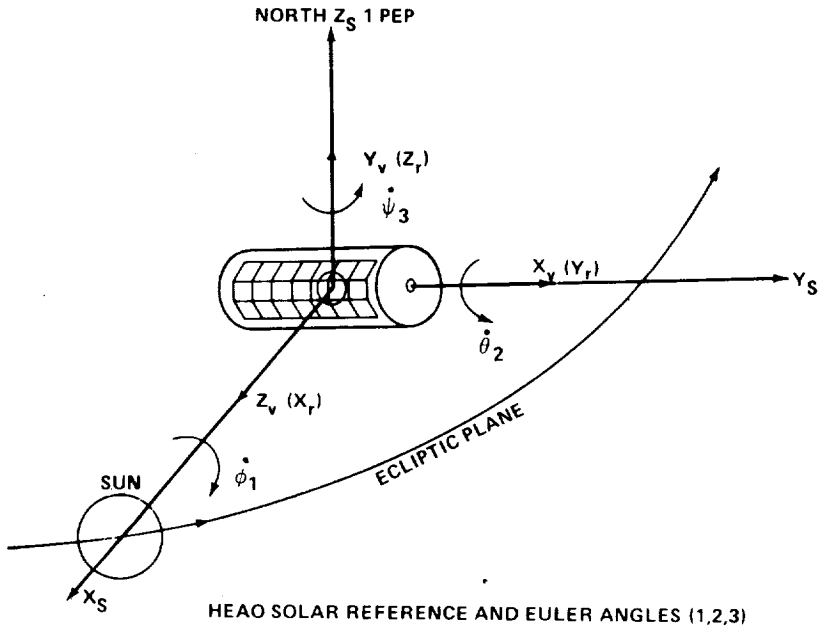

HEAO SOLAR REFERENCE AND EULER ANGLES (1,2,3)

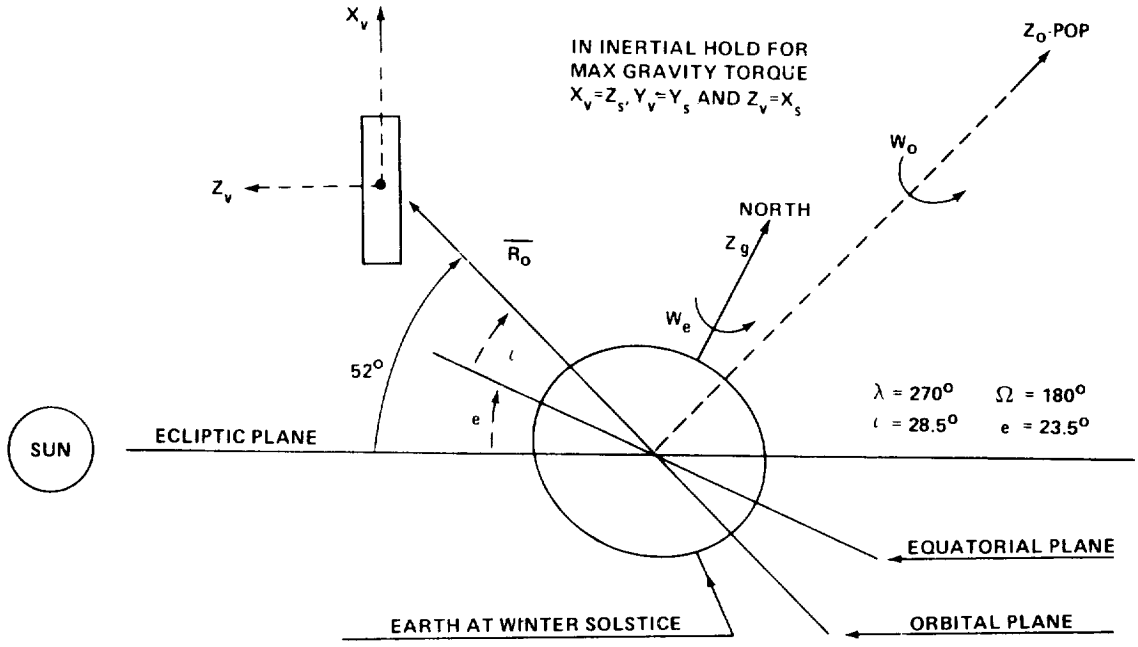

Figure C-2. Solar reference, standard orbital position and spacecraft orientation.

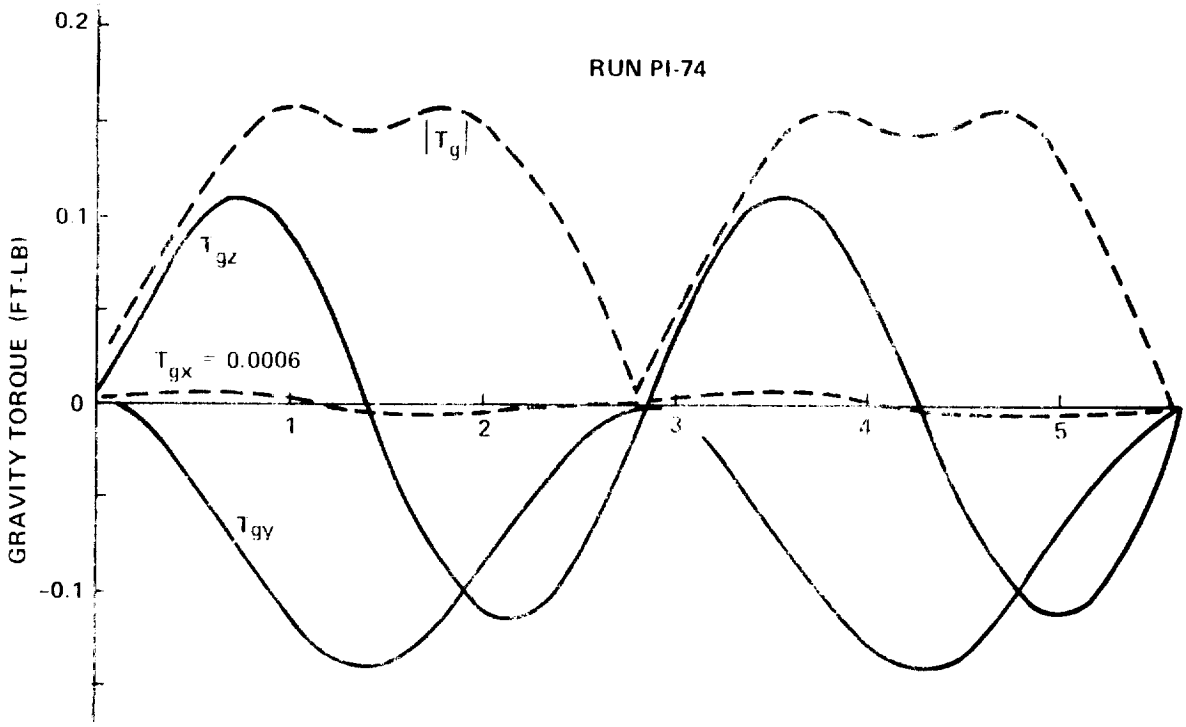

Figure C-3. Gravity torque versus orbit time (10^4 sec).

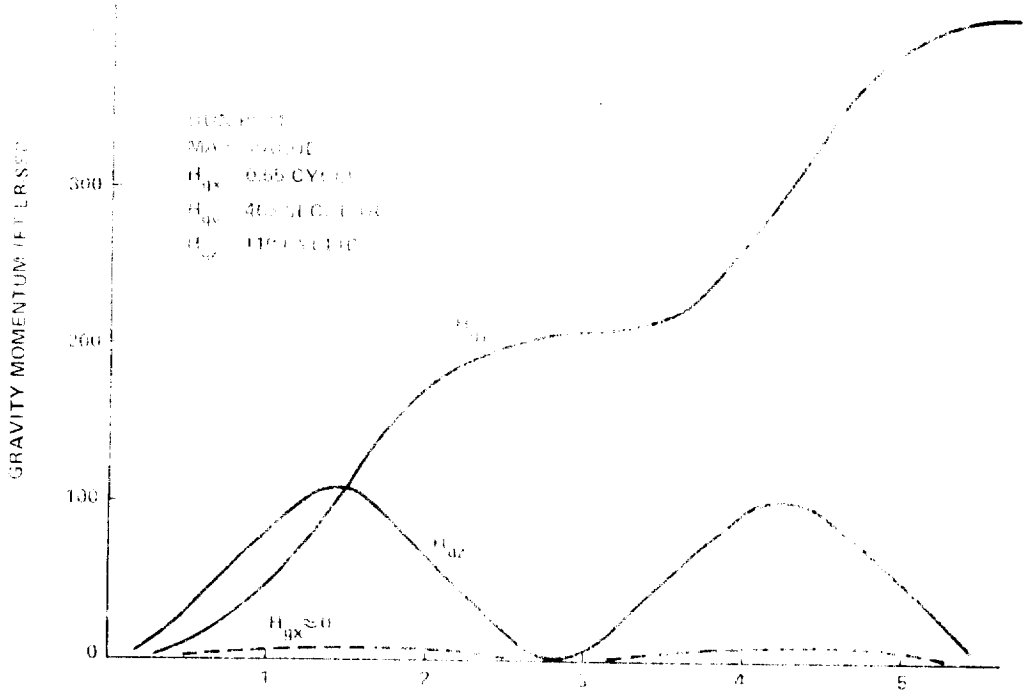

Figure C-4. Gravity momentum versus orbit time (10^4 sec).

momentum and must be dumped to prevent CMG saturation. As shown, the secular momentum is 405 ft-lb-sec per orbit and, as previously shown by the CMG momentum envelope, four 250 ft-lb-sec CMGs produce a maximum capability of about 800 ft-lb-sec in the Y_v-axis direction. Therefore, if momentum is not dumped, the CMGs will saturate in about two orbits. Computer runs verified the CMG saturation time. If, however, the CMGs' momentum size were doubled to a value of 500 ft-lb-sec per CMG, then, under worst-case conditions, about four orbits are required to reach saturation. One general problem area for future study research is to investigate techniques for dumping only the secular momentum without also dumping the cyclic portions. Starting with zero initial conditions, the CMG momentum components are identical to the g.g. momentum up to saturation, at which time the two diverge.

The Earth's Magnetic Field

The earth's magnetic field is generated by a subroutine, "B-Field." For proper operation, the spacecraft's latitude and longitude relative to the Greenwich meridian must be input at each time of calculation, along with the altitude and the time of year. The B-Field outputs are the vector components and magnitude of the earth's magnetic field relative to a geocentric coordinate system (eastward, southward, and outward directions). The parameters λ, Ω, and Ω_e, and the orbital position are used to calculate the latitude and longitude. The B-Field outputs are operated upon by appropriate transformations to obtain the field components in solar and in spacecraft body reference coordinates. Essentially, the B-Field[2] and its subroutines perform the functions of a magnetometer for measuring the earth's magnetic field in body coordinates.

Figure C-5 gives the components of the earth's magnetic field for the standard type orbit predominantly used during the simulation. The year 1974 was used as a reference for calculations. The southward component is always negative since the field dipole is directed from south to north. Near the magnetic equator at orbital times 0, 2800, and 5700 seconds both the eastward and outward components are near zero. Since the orbit starts at the morning terminator and the north magnetic pole is tilted toward the sun, the maximum outward component, B_r, is attained at an orbital time corresponding to

2. The B-Field, with its spherical harmonic coefficients, digital program can be obtained from the National Space Science Data Center, Goddard Space Flight Center, Code 601, Greenbelt, Maryland 20771.

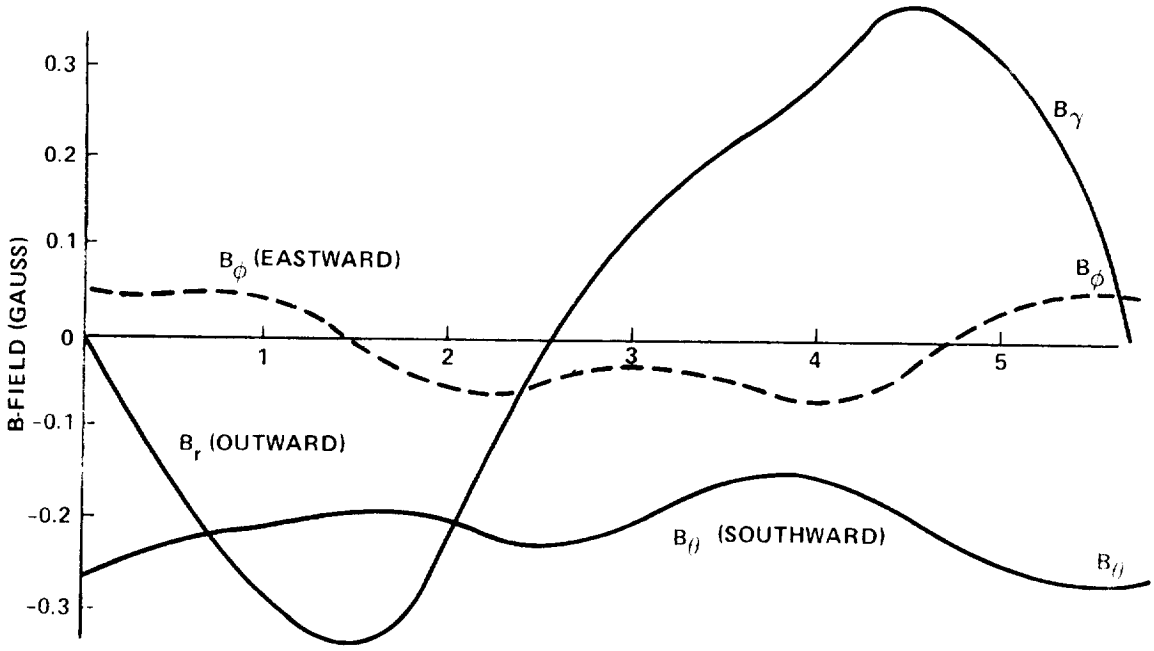

Figure C-5. B-Field in geocentric coordinates versus orbital time (10^3 sec).

about one-fourth (1400 sec) and three-fourths (4400 sec) orbit. Since the spacecraft's latitude (Fig. C-6) only attains 28.5 degrees (equal to its orbital inclination) the southward component never goes to zero. However, the eastward component is always near zero. The spacecraft longitude did not attain a value of 180 degrees during the orbit because of the earth's rotation of about 23 degrees per orbit. Both the spacecraft's longitude and latitude are shown in Figure C-6 with the corresponding B-Field outputs shown in Figure C-5 in gauss units.

The B-Field components shown in Figure C-5 are projected into solar coordinates and from there to observatory body reference coordinates by the Euler angle sequence shown in Appendix B. The earth's magnetic field components, as would be measured by an onboard magnetometer, are shown in Figure C-7. The sunward component B_z is, in this case, always negative and attains a magnitude of -0.39 gauss, the northward (perpendicular to the ecliptic) component, B_x, is slightly biased positively with a maximum value of 0.26 gauss, and the B_y component in the ecliptic plane perpendicular to the sunline is near-cyclic. The maximum field magnitude is 0.43 gauss at 4400 sec and the minimum is 0.24 gauss at 2700 sec. The minimum occurs

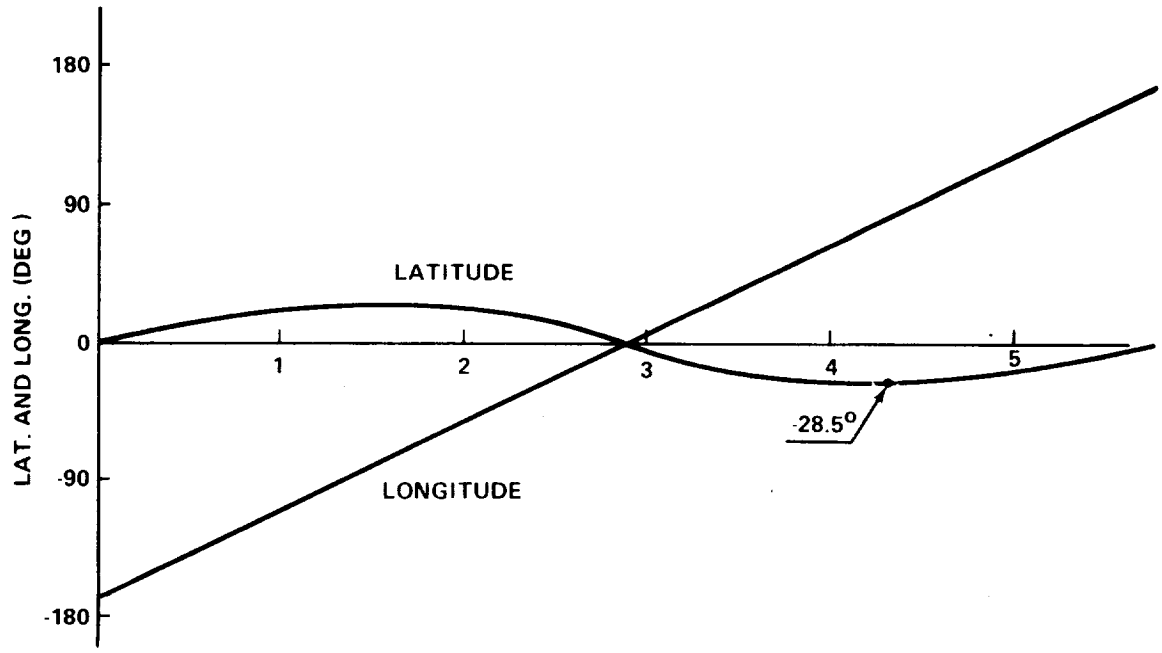

Figure C-6. Spacecraft longitude and latitude versus orbital time (10^3 sec).

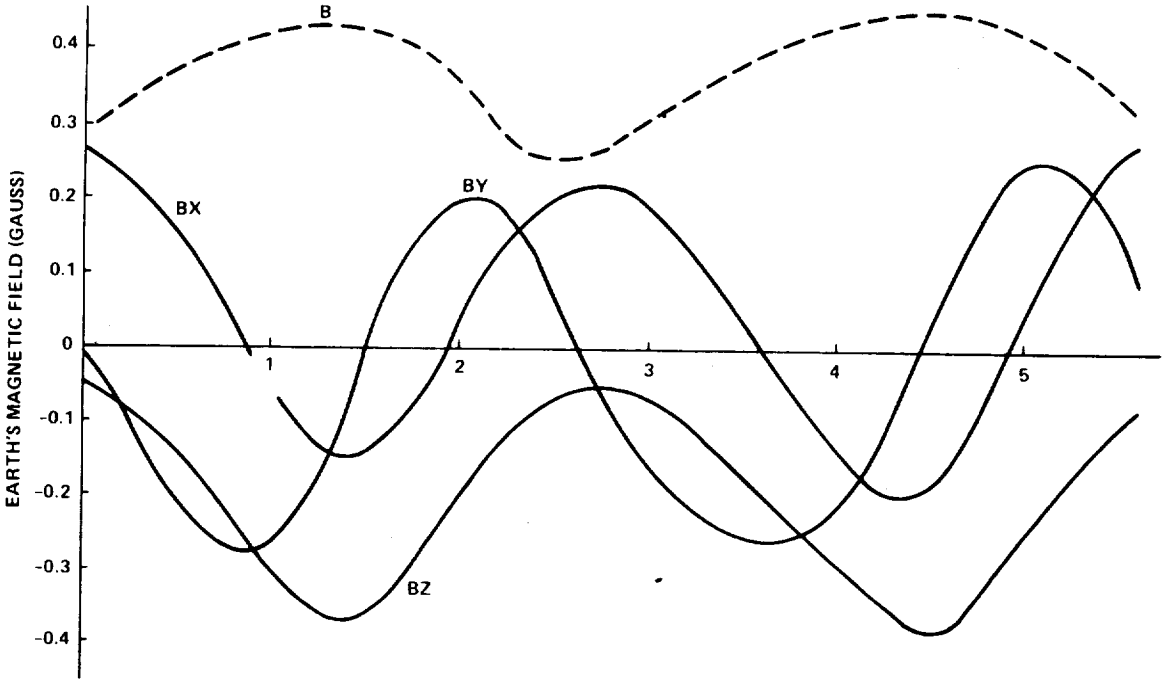

Figure C-7. Earth's magnetic field components in vehicle coordinates versus orbital time (10^3 sec).

when the spacecraft crosses the equatorial plane which is also near the magnetic and equatorial plane line of nodes. The maxima occur when the latitude is greatest, at about the one-fourth and three-fourths points of the orbit. The components given are for a standard reference. However, by reorienting the vehicle, completely different values could be obtained. But the total magnitude curve, B , would remain the same regardless of orientation because it depends only upon altitude and position of the center of mass in orbit.

CMG STEERING LAW SIMULATION

The Constant Gain Steering Law

The constant gain steering law was the one first implemented because of its simplicity. The CMG gimbal rate commands are

$$\dot{\alpha}_1 = K_A T_{cx} + K_B T_{cz} \quad ,$$

$$\dot{\alpha}_2 = K_A T_{cx} - K_B T_{cy} \quad ,$$

$$\dot{\alpha}_3 = K_A T_{cx} - K_B T_{cz} \quad ,$$

and

$$\dot{\alpha}_4 = K_A T_{cx} + K_B T_{cy} \quad ,$$

where

$$K_A = -0.00125047 \quad ,$$

and

$$K_B = -0.00333111 \quad .$$

for a skew angle of 53.1 degrees and 250 ft-lb-sec CMGs. Because the gains K_A and K_B have been derived to linearize the system when operating about the CMG null position, pointing performance is expected to deteriorate when the CMG gimbal angles get large. Figure C-8 illustrates typical performance obtained by using the constant gain steering law. As long as the gimbal angles are small, the pointing error is about equal to that obtained with the pseudo inverse. On the first half-orbit the peak error is less than 0.07 arc min and the gimbal angles (Fig. C-9) are less than 45 degrees. As the gimbal angles become larger during the second half of the orbit, a corresponding increase occurs in pointing performance. At about 4400 seconds, gimbal angle number 3 attains a value of 90 degrees at which time control is lost and the system diverges. At this time, the CMGs have only accumulated 338 ft-lb-sec momentum (Fig. C-10). Using a constant gain steering law, less than one-half of the total CMG momentum can be used for control purposes. For the HEAO inertias and CMG size, momentum would have to be dumped each half-orbit to prevent the gimbal angles from becoming too large. By increasing the momentum per CMG to 500 ft-lb-sec, excellent control over a full orbit under worst-case conditions could be maintained without dumping CMG momentum.

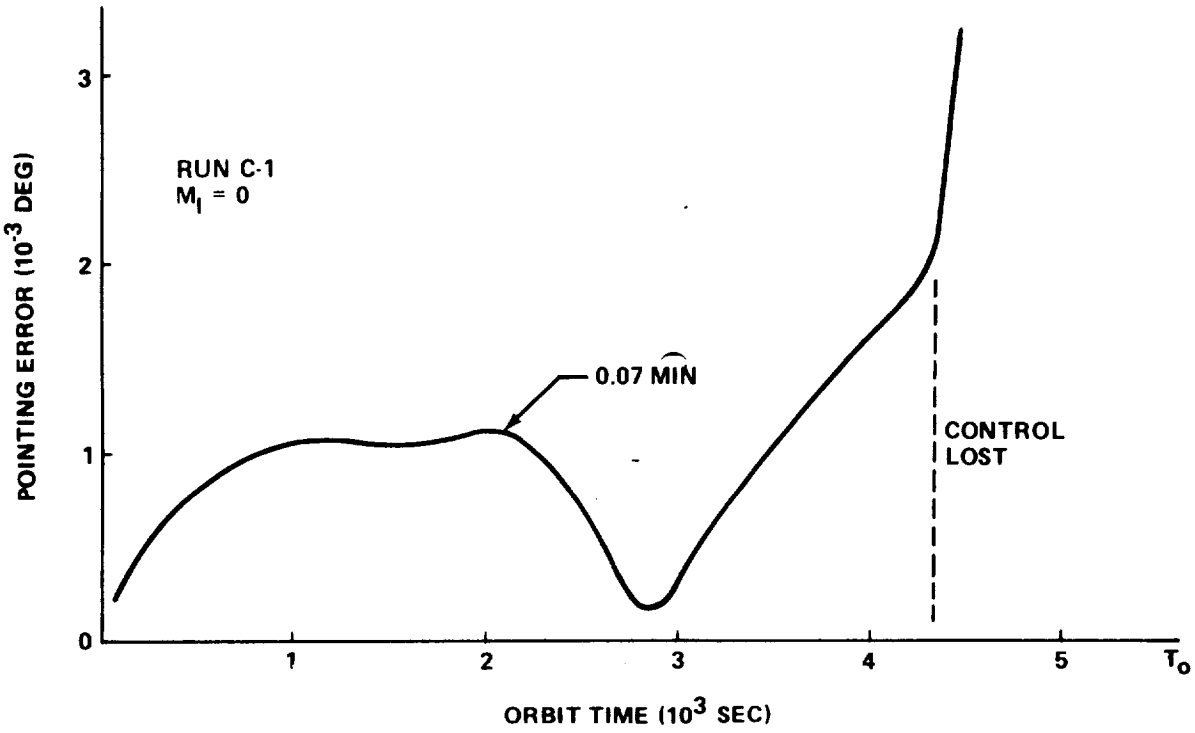

Figure C-8. Constant gain pointing performance.

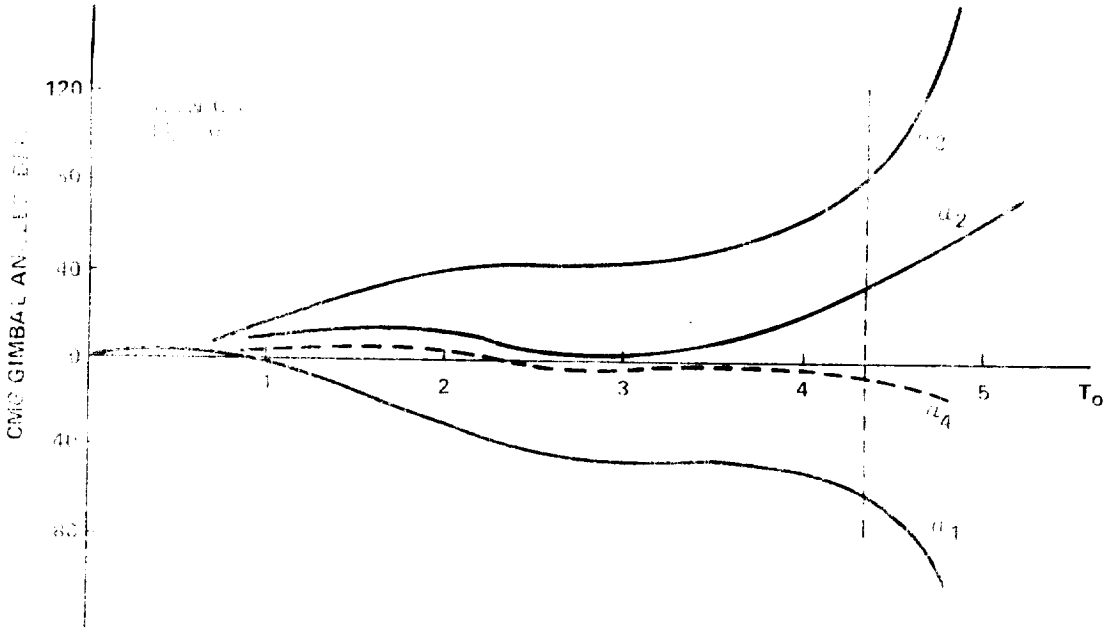

Figure [illegible] CMG gimbal angles with constant gain steering law.

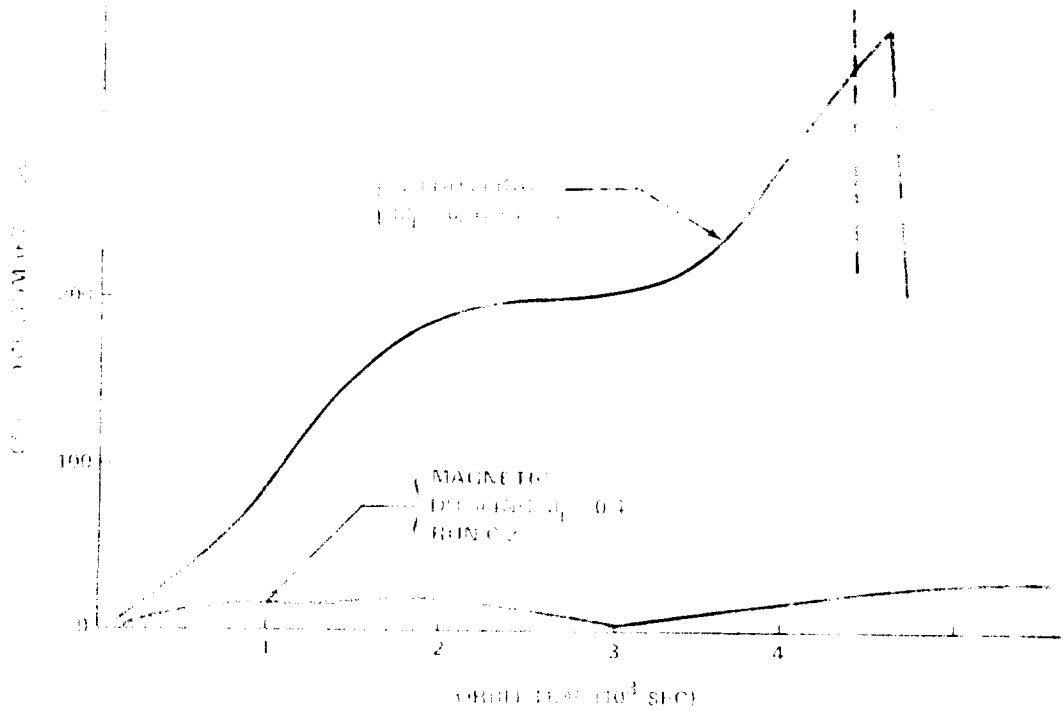

Figure [illegible] Accumulated CMG momentum with the constant gain steering law.

Using three orthogonal electromagnets to generate a magnet dipole which reacts against the earth's magnetic field, continuous CMG momentum dumping is provided. As shown in Figure C-11, the pointing performance improves considerably by using continuous momentum dumping by magnetics. The peak error is 0.022 arc min at 4500 seconds. The gimbal angles (not shown) deviate less than 4 degrees from their null position. As long as the gimbal angles are less than 15 degrees, the constant gain steering law performs as well as the most complicated laws or the pseudo inverse. The accumulated CMG momentum is shown in Figure C-10 for the constant gain steering law, both with and without continuous momentum dump. Without magnetics, the momentum value is 338 ft-lb-sec at 4400 seconds after which time control is lost, the vehicle rotates violently, and the momentum is absorbed by increased vehicle angular rates. With magnetic dumping, the accumulated CMG momentum is less than 30 ft-lb-sec, indicating that very small CMGs could have been used for pointing control.

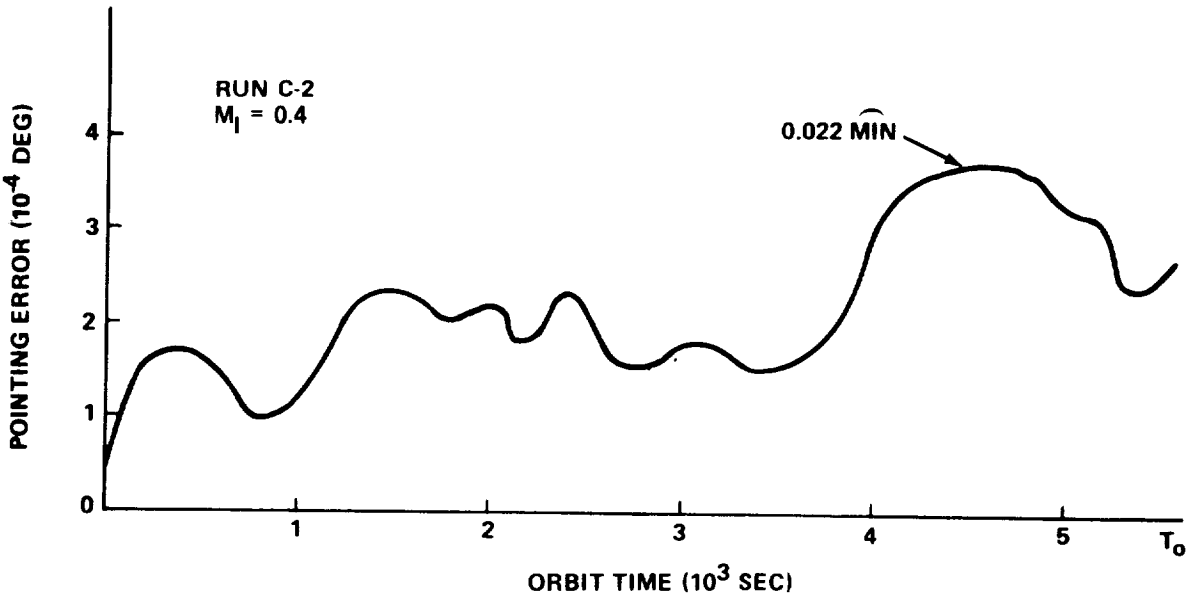

Figure C-11. Constant gain pointing error with magnetic momentum dump.

Maximum Contribution

The maximum contribution (MC) steering law has been derived such that each gimbal rate is commanded independently of the other gimbal rates or positions. The steering law is

$$\left.\begin{aligned}
\dot{\alpha}_1 &= K_A C\alpha_1 T_{cx} - K_C S\alpha_1 T_{cy} + K_B C\alpha_1 T_{cz} \\
\dot{\alpha}_2 &= K_A C\alpha_2 T_{cx} - K_B C\alpha_2 T_{cy} - K_C C\alpha_2 T_{cz} \\
\dot{\alpha}_3 &= K_A C\alpha_3 T_{cx} + K_C S\alpha_3 T_{cy} - K_B C\alpha_3 T_{cz} \\
\dot{\alpha}_4 &= K_A C\alpha_4 T_{cx} + K_B C\alpha_4 T_{cy} + K_C S\alpha_4 T_{cz}
\end{aligned}\right\}$$

where

$$K_A = -0.00125047 \quad ,$$

$$K_B = -0.00333111 \quad ,$$

and

$$K_C = -0.00554815$$

are constants that have been derived to provide unity gain through the CMG loop.

Using the MC steering law, each CMG gimbal rate is commanded (as if it alone were controlling) to contribute as much as possible to the commanded torque. Simulations indicate that when the gimbal angles get large, certain combinations of angles can momentarily prevent the desired torque from being produced without also producing unwanted torque components that will disturb the pointing accuracy. This is indicated in Figure C-12 by run number MC-68: All the CMGs are operating and no momentum is being dumped. At 4600 seconds, the pointing error is 1.26 arc min which exceeds HEAO-C pointing specifications. The roll error attains a peak amplitude of 4.45 arc min. However, by using higher feedback gains, the error can be reduced to an acceptable value (shown by a later run not included herein). After the peak error, acceptable performance was maintained after CMG saturation near the two-orbit time point. Near the peak attitude errors, the gimbal angles, shown in Figure C-13, are changing rapidly. After one orbit, the third gimbal angle attains a value of 142 degrees. The other angles also deviate considerably from their null position. The CMG

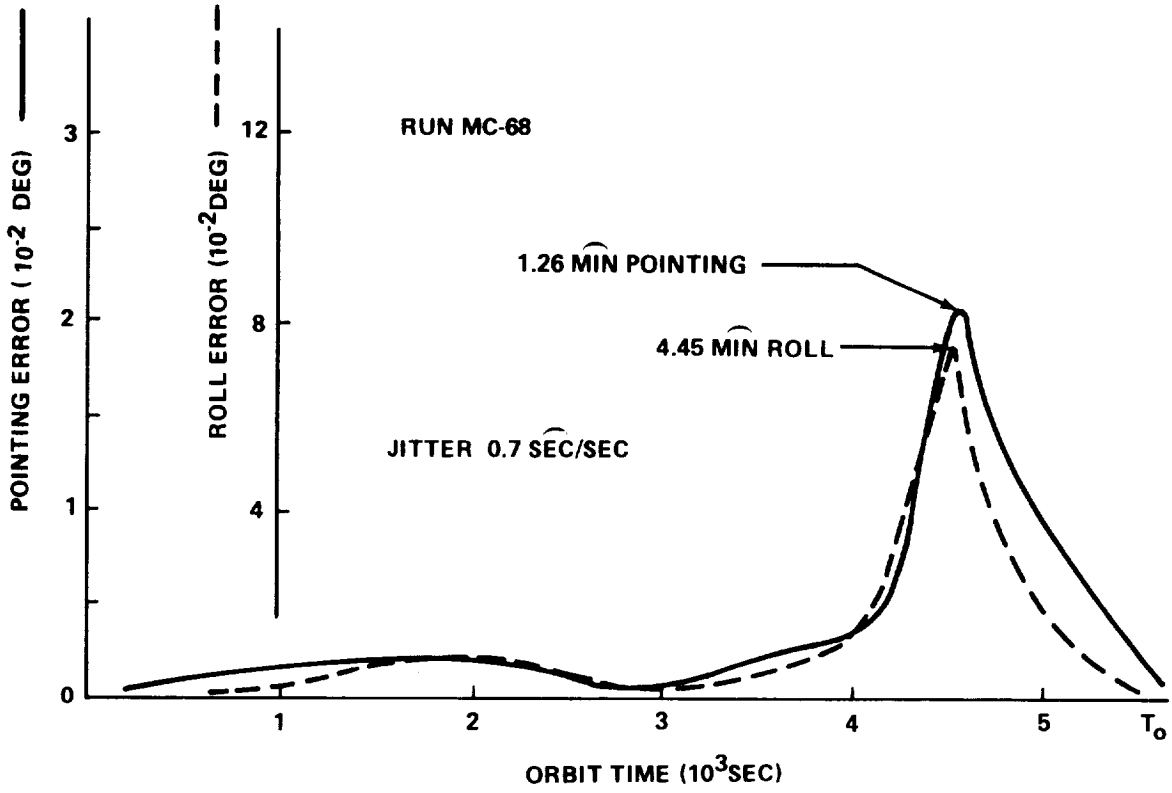

Figure C-12. Maximum contribution performance.

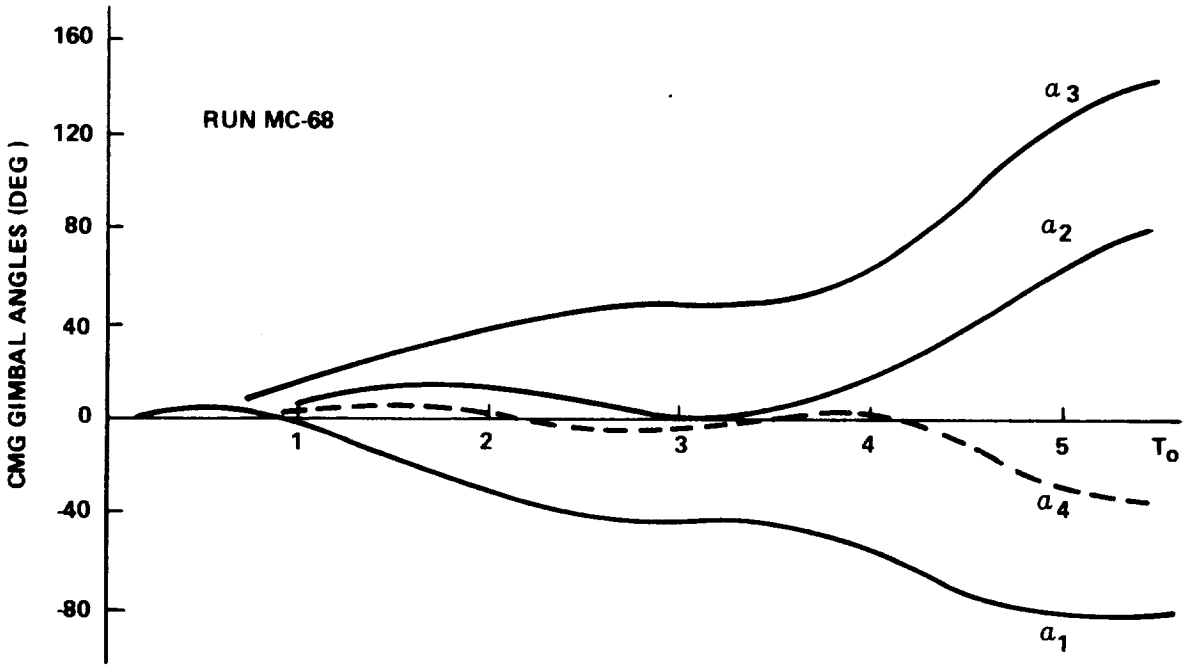

Figure C-13. CMG gimbal angles for the maximum contribution steering law.

gimbal rates are all hard limited at 1 deg/sec (0.017453 rad/sec). However, the limit is not approached during normal attitude hold modes. The gimbal rates shown in Figure C-14 correspond to the angles previously shown in Figure C-13. These rates are typical for all steering laws (except the transpose with torque feedback). In this particular run, a peak value of 0.055 deg/min, occurs at 4500 seconds.

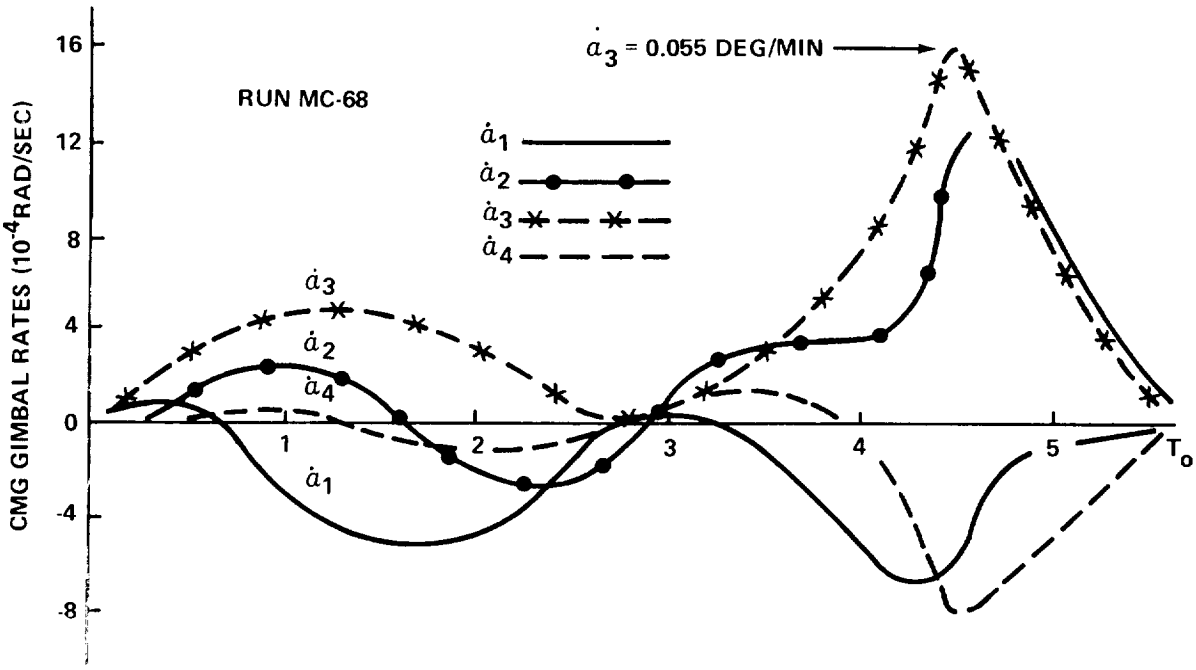

Figure C-14. CMG gimbal rates with maximum contribution steering.

CMG number 3 was failed by setting its momentum to zero. However, no change was made in computing the gimbal rate command for the remaining CMGs. They were initialized to a new zero momentum state by setting $\alpha_1 = 0$, $\alpha_2 = 56.4$, and $\alpha_4 = -56.4$ degrees. The resulting pointing performance is shown in Figure C-15. The three CMG system hit a gyro hang-up condition at 4100 seconds after which pointing control was lost. Before saturation, both the gravity gradient and stored CMG momentum are identical but differ once the CMGs have saturated. As shown in Figure C-16, about 300 ft-lb-sec have been stored in the CMG system when control was lost. The momentum envelope for the three CMGs shown in Figure 7 has an indenture centered around the gimbal axes of each CMG, at which point the maximum momentum is only about 368 ft-lb-sec along a CMG gimbal axis. The CMGs have been driven into ghu near this minimum momentum state.

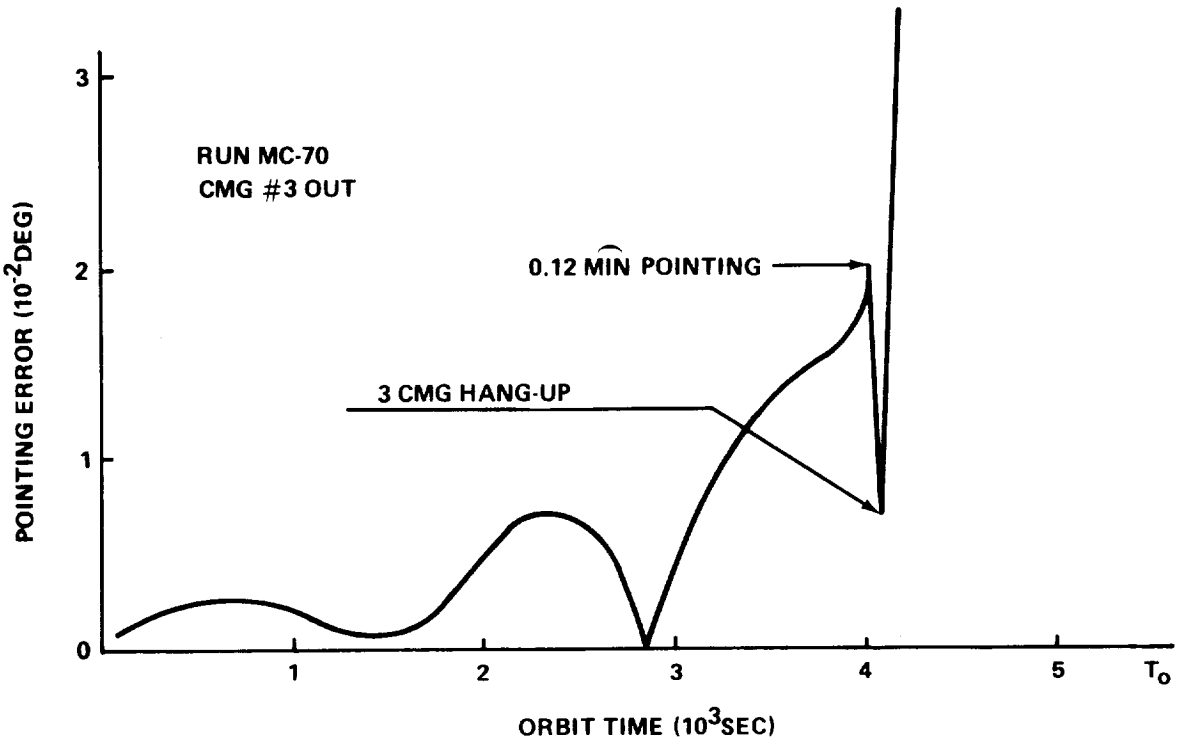

Figure C-15. Maximum contribution performance with only three CMGs.

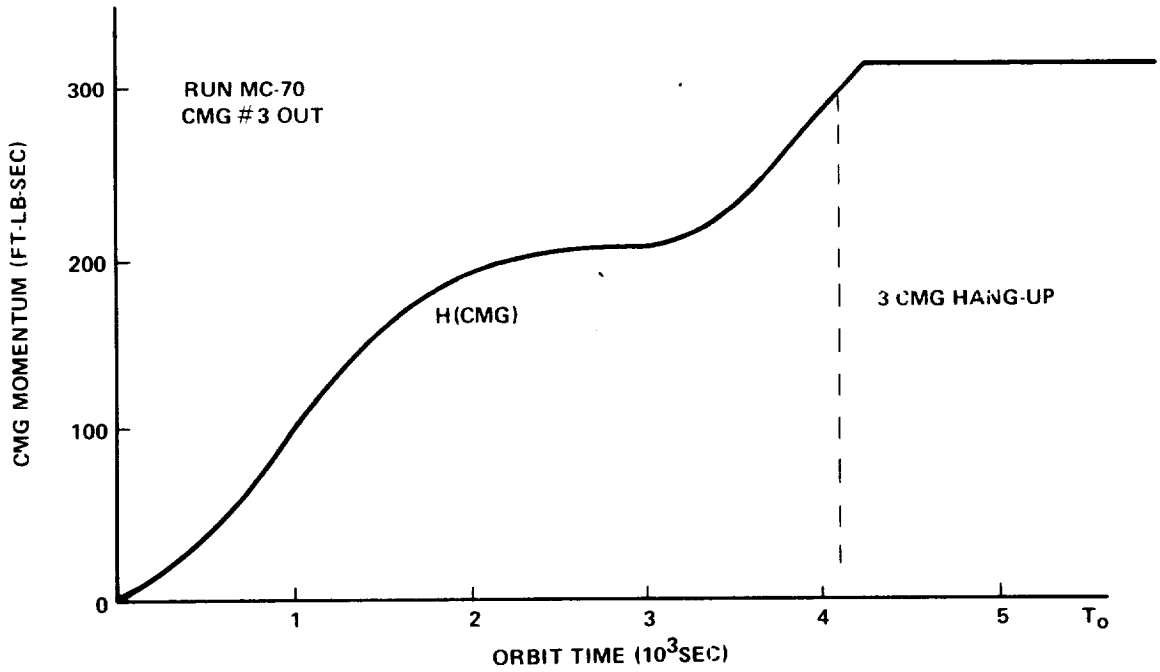

Figure C-16. Stored CMG momentum with CMG number 3 out.

Additional runs in which other CMGs were failed indicate that the HEAO performance specifications can be met using any three CMGs. In each case the CMGs must be initialized to a new null state. If, however, a full orbit under worst conditions must be attained before CMG desaturation or gyro-hang-up, the CMG momentum must be increased to 500 ft-lb-sec per wheel. Runs with the momentum per CMG raised to 500 ft-lb-sec illustrate that the gimbal angles stay relatively small over one orbital period, even with one CMG failed, and both pointing and jitter specifications are more than satisfied. If more than four CMGs are used, the induced cross coupling effects (see Figure C-12 at 4600 seconds) become less and the maximum contribution steering law performance is enhanced. The MC offers maximum growth potential because more CMGs can be added without altering the basic form of the steering law or the mathematical manipulations.

With the addition of magnetic torquers for CMG momentum management, the pointing improves by a factor of about 100 and the jitter by a factor of 4. As illustrated in Figure C-17, the maximum peak values are 0.022 arc min pointing, 0.16 arc min roll, and 0.19 arc sec/sec jitter. The gimbal angles stay less than 4 degrees over the orbit and the magnetic system dumps about 400 ft-lb-sec momentum. After failing any CMG, the magnetic system

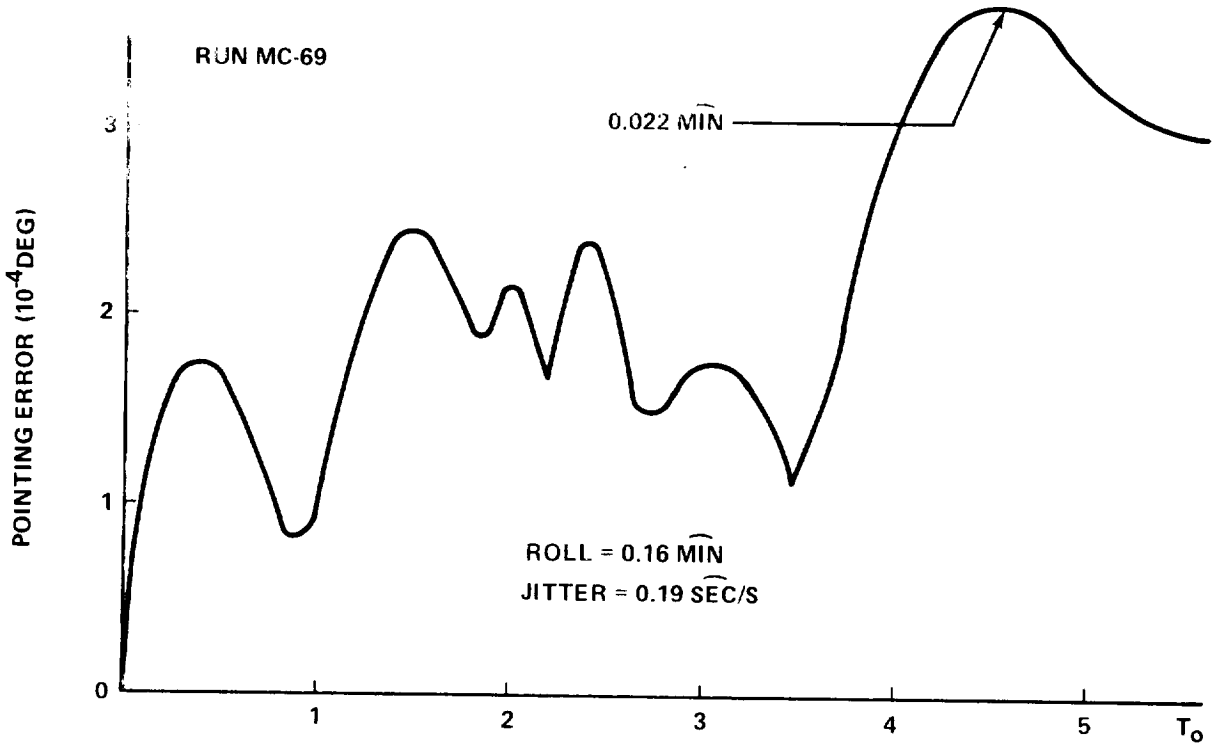

Figure C-17. Maximum contribution performance with magnetic momentum dump.

will automatically force the CMGs to a new null position. No reprogramming or changes are required in the MC steering law. After finding a new null, the three-CMG system with magnetics performs the same as the four-CMG system shown in Figure C-17. If two CMGs are failed, direct magnetic torque must be used in addition to magnetic momentum dumping for control of a vehicle axis. Most of the time, HEAO performance requirements can be maintained. However, there are short time intervals of about 50 seconds during some orbits that 1 arc min pointing is exceeded. The MC steering law with magnetics is the simplest way of providing fail operational capability.

In run MC-102, CMG number 3 and number 4 were failed by setting their momentum to zero. No changes were made in the steering law, nor were the remaining two CMGs set to a new null position. Without magnetics the program diverged. There was an initial momentum of 250 ft-lb-sec on both the Y and Z axes that produced initial vehicle rotations. The two operational CMGs could not correct the situation without additional torque from either the RCS or bar torquers. In the next run (MC-103), the magnetic system was used to provide both direct torque and CMG momentum management. The performance is shown in Figure C-18. During the first quarter orbit, the CMGs are automatically driven to a new null position by the magnetic system, during which time the initial pointing error is about 0.16 degree and the roll error peaks at 15.6 arc min at 1000 seconds. The new null position is with CMG angles $\alpha_1 = -59$ and $\alpha_2 = 59$ degrees. At these angles the CMG momentum vectors are opposite each other on the intersection of their momentum planes. The axis that cannot be controlled by the two CMGs is approximately aligned with the momentum vectors at their null position. The magnetic system must provide torque about the uncontrolled axes. After the new null is attained, the peak errors are 0.48 arc min pointing and 0.36 arc min roll. The jitter is well within the bounds specified for HEAO. The CMG gimbal angles are shown in Figure C-19. Dashed lines represent the null position for the two operational CMGs. The angular excursions from the null are less than 10 degrees once it has been established. The accumulated CMG momentum oscillates proportional to the gimbal angle deviations with peak values of about 100 ft-lb-sec (not shown).

The maximum contribution is the only steering law that provided fail operational capability when any two CMGs were failed. No logic is required to detect the failures and no modifications to the steering law are necessary with magnetics. The magnetic system permits any CMG-out type failure without any detection and logic required to define a new CMG null position. With the MC steering law, each gimbal is commanded independently of the others; therefore, no modifications are required when any CMG fails.

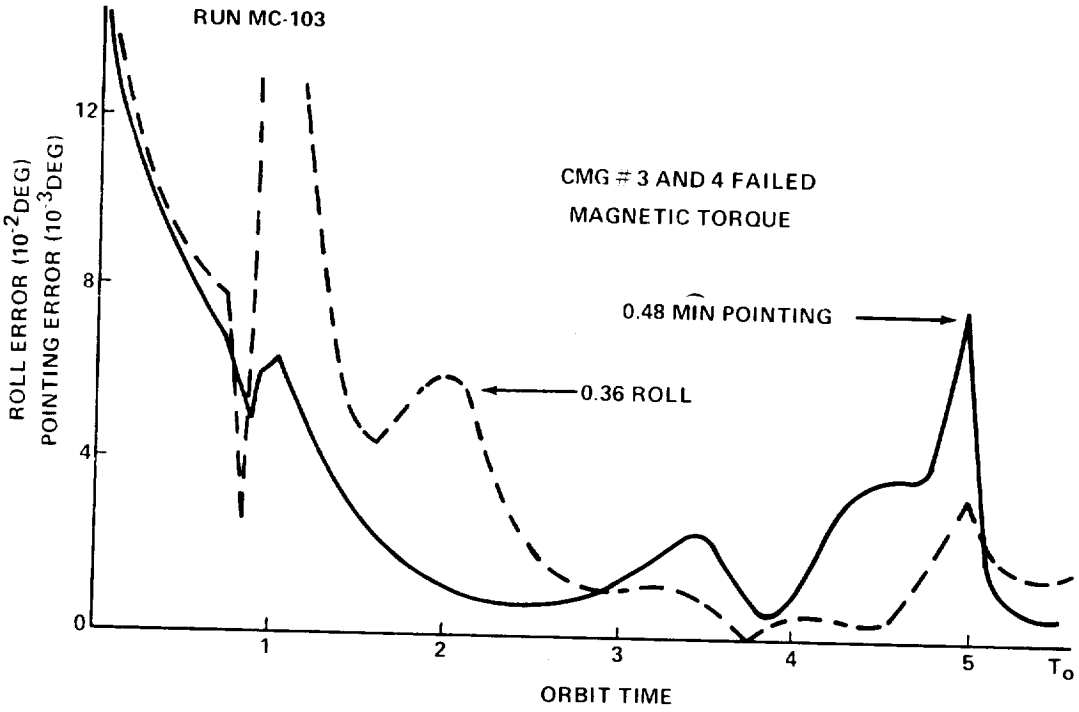

Figure C-18. Maximum contribution performance with two CMGs failed and magnetics.

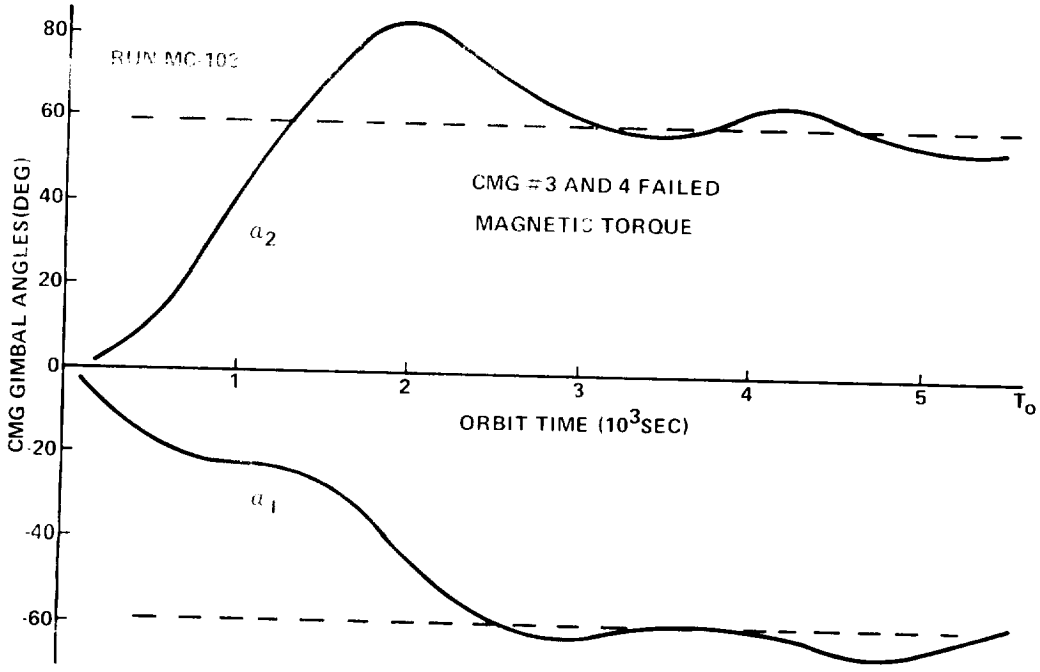

Figure C-19. CMG gimbal angles for the MC law with two CMGs failed and magnetics.

Pseudo Inverse Steering Law

Typical performance with all CMGs operating using the pseudo inverse (PI) steering law is shown in Figure C-20. The maximum deviations are 0.062 arc min on both the experiment and solar pointing axes and less than 0.004 arc sec/sec jitter which clearly meet HEAO-C specifications. No momentum has been dumped. As a result of secular g.g. momentum, the CMG gimbal angles get rather large. As shown in Figure C-21, gimbal angle number 3 attains a value of 142 degrees at the end of one orbit, T_o, while CMG gimbals one and two reach a magnitude of 82 degrees. Although not shown, saturation is attained near two orbits with $\alpha_1 = -90$, $\alpha_2 = 180$, $\alpha_3 = 90$, and $\alpha_4 = 0$ at which time control is lost.

Using the pseudo inverse steering law, the vehicle angular rates stay very small, consequently the pointing performance is very smooth. The pointing error (Fig. C-20) has the same shape as the gravity gradient disturbance torque (Fig. C-3). The momentum accumulated by the CMGs is the same as the gravity gradient momentum shown in Figure C-4 but opposite in sign, and total magnitudes are identical until the time of CMG saturation after which the two diverge and pointing control is lost. CMG saturation also corresponds to gyro hang-up and to a mathematical singularity in the steering law algorithm. Using the pseudo inverse, those gimbal angle combinations which produce gyro hang-up will also cause the determinant of the $|CC^*|$ matrix to go to zero. Although there are an infinite number of CMG gimbal conditions that can produce gyro hang-up internal to the maximum momentum envelope, these conditions were not encountered under normal pointing conditions. But by replacing the cyclic g.g. torque by a properly directed constant torque, gyro hang-up could always be encountered. Much more work is needed to characterize the gyro hang-up problem associated with SG CMGs and to assess its impact on vehicle pointing performance.

With the addition of electromagnets for continuous momentum dump, the performance improves by about a factor of four, as shown in Figure C-22. With the magnetic torquers sized at 0.4 ft-lb/gauss and a magnetic loop gain K_m equal to 0.01 sec^{-1}, the maximum pointing error is 0.019 arc min.

Since momentum is being continuously dumped, the stored CMG momentum stays near zero. Consequently, the CMG gimbal angles, shown in Figure C-23, deviate less than 4 degrees from their null position. Both

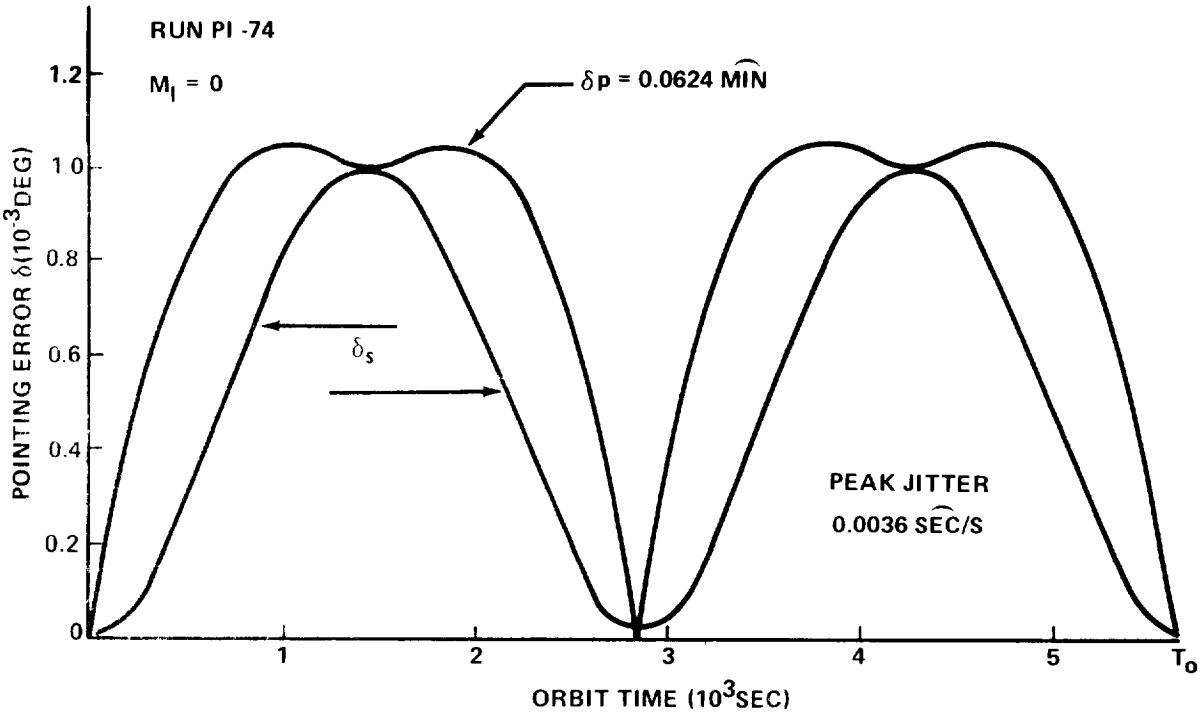

Figure C-20. Pseudo inverse pointing performance.

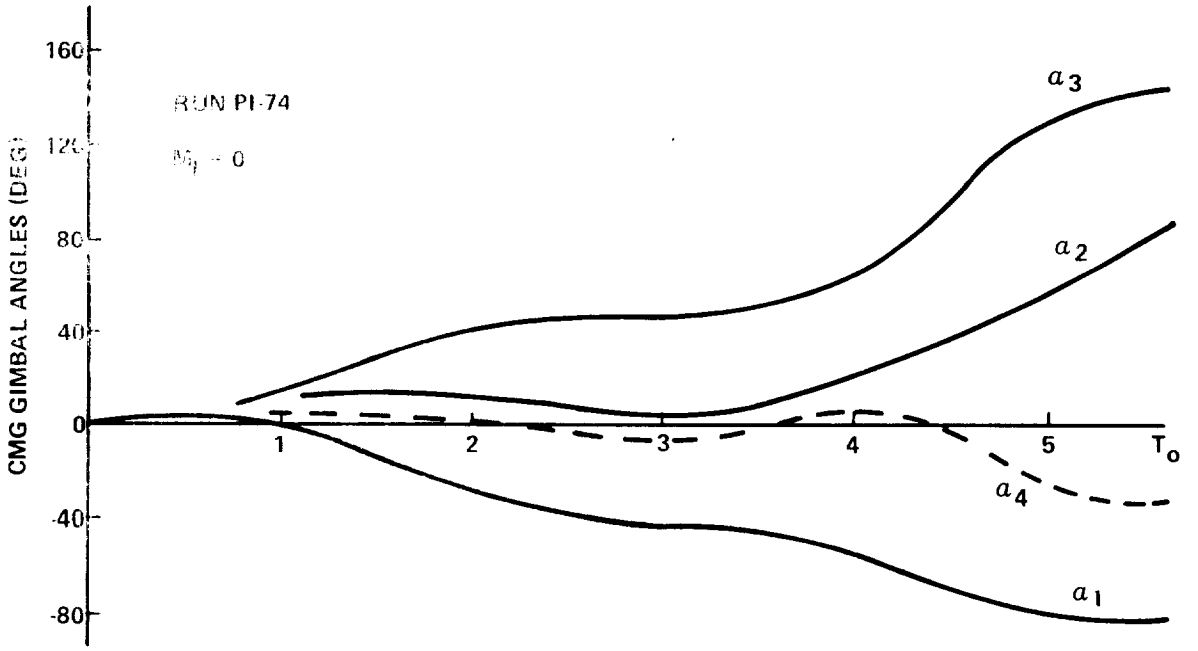

Figure C-21. CMG gimbal angles for the pseudo inverse.

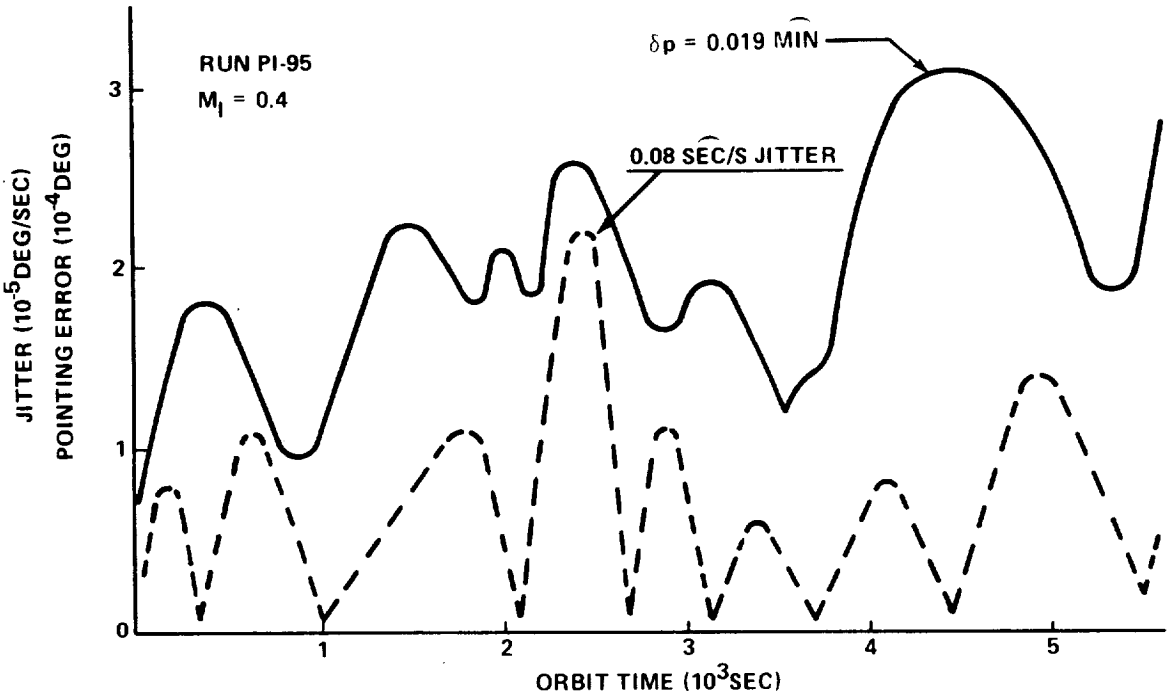

Figure C-22. Pseudo inverse performance with magnetics.

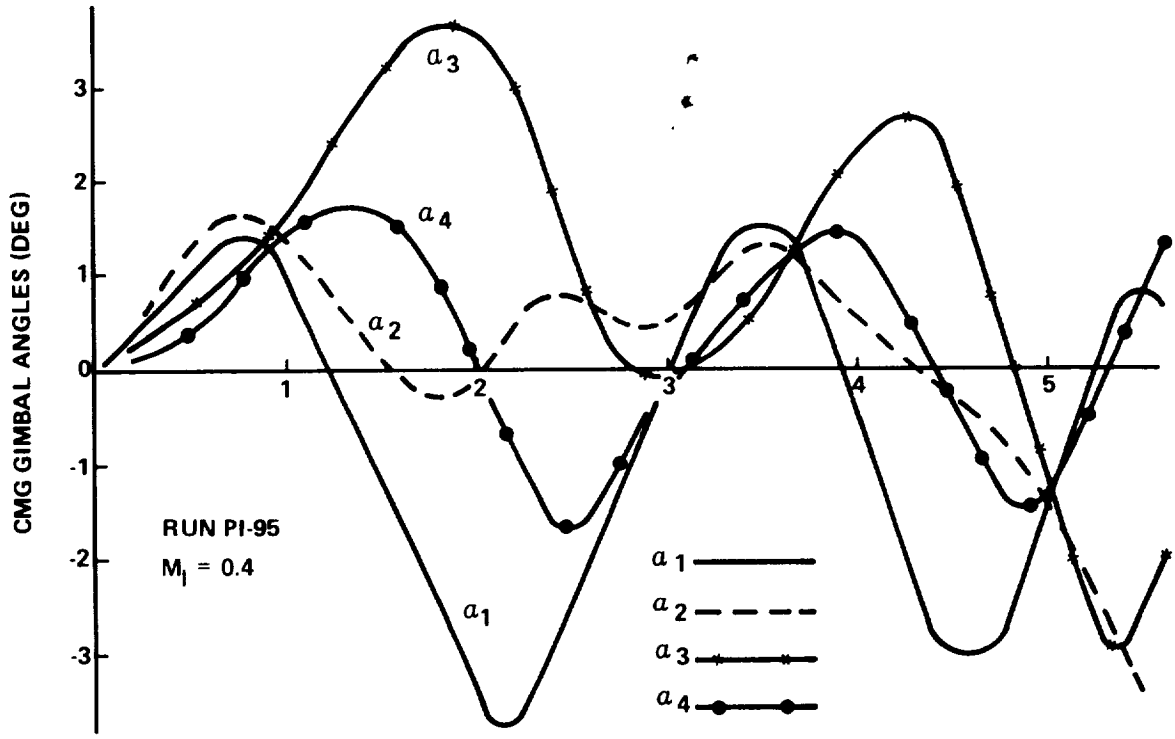

Figure C-23. CMG gimbal angles with magnetics.

the gravity gradient and the accumulated CMG momenta are shown in Figure C-24. The difference between the curves represents the momentum that has been dumped by the magnetic system, about 400 ft-lb-sec per orbit. The coil dipoles, shown in Figure C-25, have been hard limited to 0.4 ft-lb/gauss and commanded proportionally to the vector components of the stored CMG momentum. The dipole commands were derived in Appendix A. As noted, the X_v-axis component saturates during the orbit. By decreasing K_m to 0.001, the coils do not saturate, but not as much momentum is dumped and a corresponding increase occurs in CMG gimbal angles. The pointing performance is relatively unchanged. However, by increasing K_m to 0.1, all the coils reach saturation values. Both the stored momenta and gimbal angles stay near zero, but the pointing performance is degraded slightly. Using still higher K_m values causes the coil dipoles to react in a bang-bang manner that produces a magnetic torque which greatly degrades the pointing performance. Based on several runs in which K_m was varied, a magnetic loop gain of 0.01 is recommended for continuous momentum dump. Figure C-26 illustrates the magnetic torque applied to the spacecraft as the result of the coil dipoles shown in Figure C-25. The components of the magnetic torque are about equal to that of gravity gradient in both magnitude and shape, indicating that the magnetic system is, indeed, counteracting the environmental torque, leaving the CMGs with relatively little to do.

The roll error about the experiment axes (long vehicle axis) is shown in Figure C-27. Without magnetics, the roll error peaks at about 0.072 arc min, but with magnetics it increases to 0.4 arc min. These data are in contrast to those generally observed when comparing performance with and without the magnetic system. In all cases where errors about two axes were root-sum-squared to get the pointing error, the use of continuous electromagnetic momentum dumping improved performance.

CMG number 3 was failed by setting its momentum to zero. However, no change was made in computing the gimbal rate commands for the remaining CMGs, and the elements of the column vector in the CMG torque matrix corresponding to the failed CMG were not set to zero. In run PI-63 the gimbal angles were not initialized to a new null position (position at which the CMG momentum is zero) for the three operational CMGs. The effect was to produce a biased momentum component of 250 ft-lb-sec on the positive Y-axis. Without magnetics, pointing control was lost after 1000 sec orbit time and did not recover. The CMGs had to be initialized to a new null position using the RCS system after which control was maintained until CMG saturation.

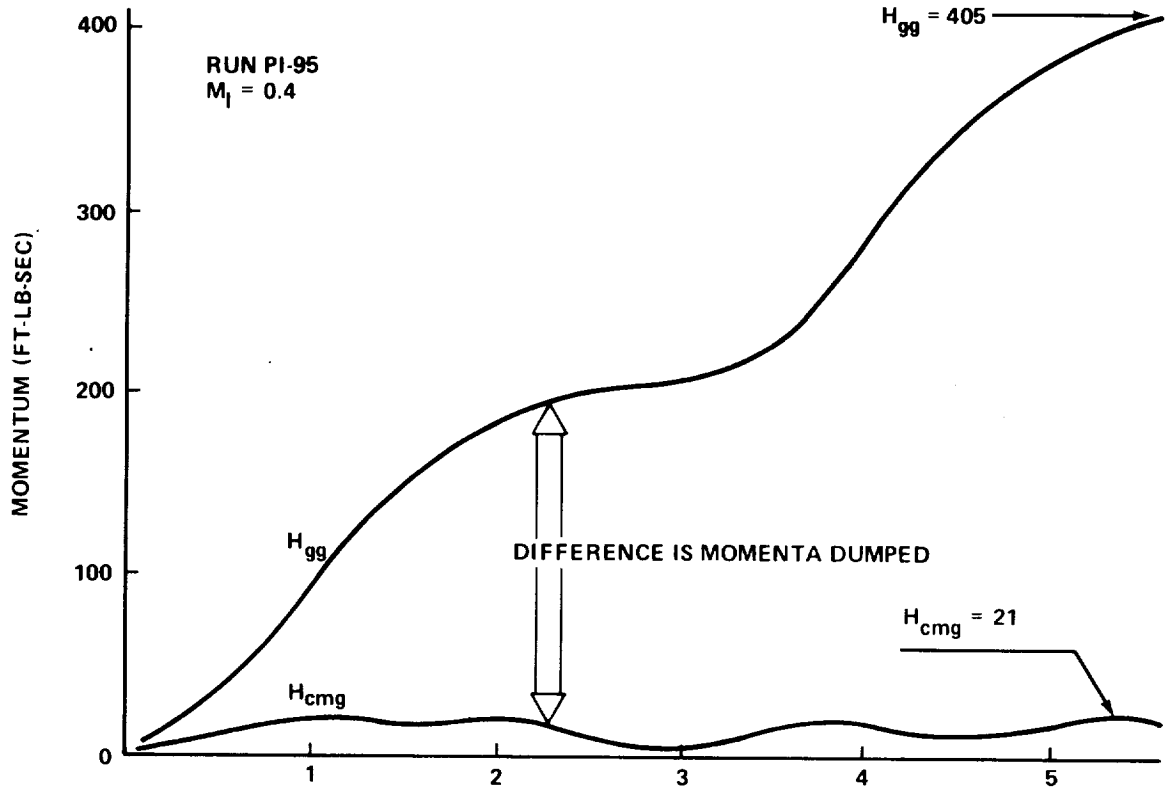

Figure C-24. CMG accumulated momentum with magnetics.

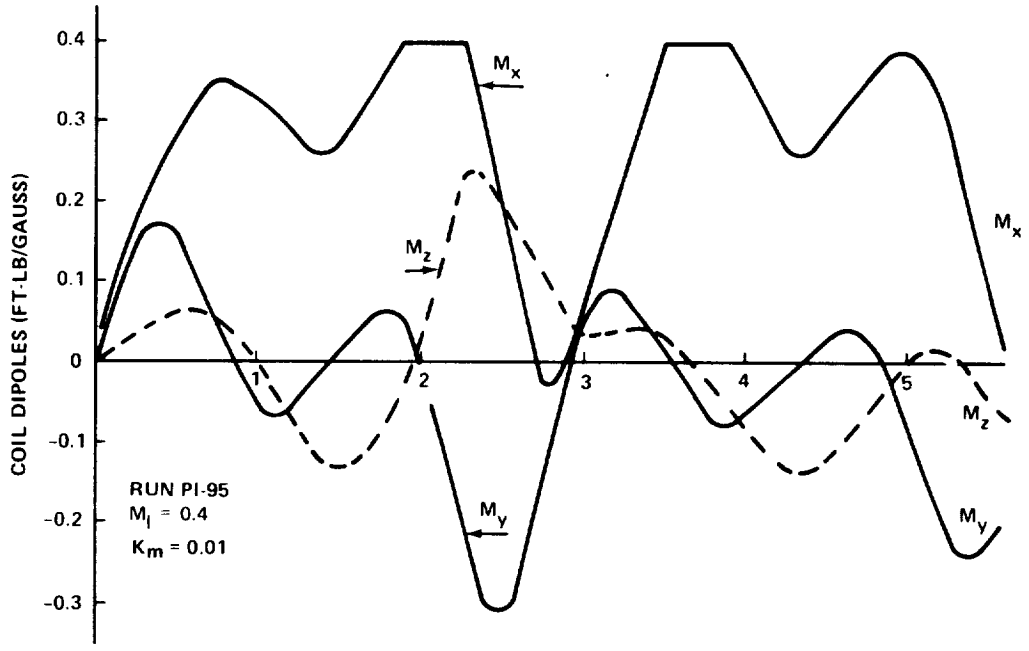

Figure C-25. Magnetic dipoles for CMG momentum management.

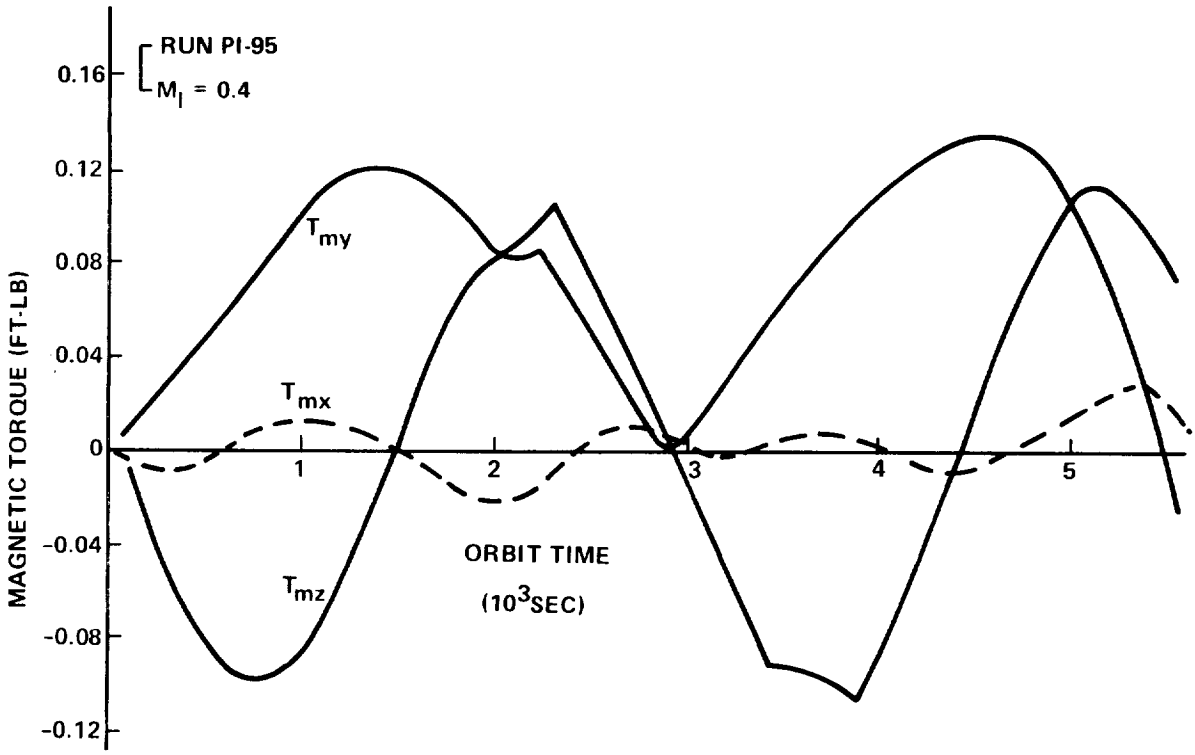

Figure C-26. Magnetic torque components dumping CMG momentum.

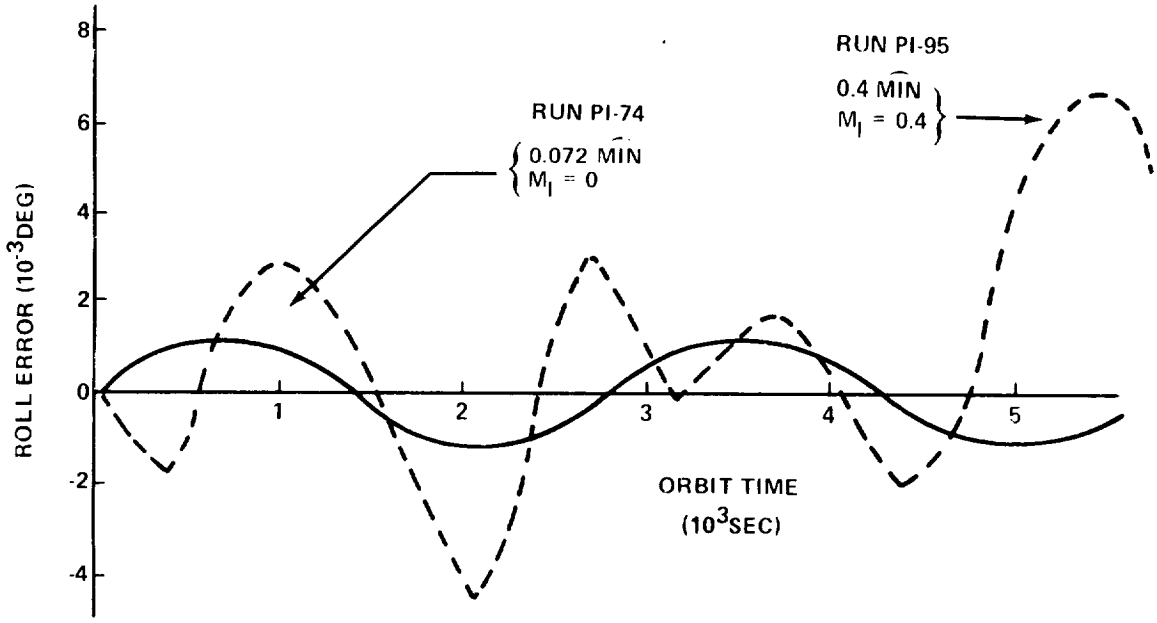

Figure C-27. Roll error with and without magnetics.

In an attempt to find a new null with CMG number 3 failed, maximum use was made of the magnetic system by setting $K_c = 1$ for direct magnetic torque control and $K_m = 0.01$ for CMG momentum dump. The results are summarized by Figures C-28 through C-31. The magnetic system forced the CMGs to a new null position while maintaining HEAO-C pointing requirements. The peak pointing error (Fig. C-28) was 0.084 arc min and the jitter was 0.72 arc sec/sec. The new null position was attained after about 2000 seconds (Fig. C-29) with $\alpha_1 = 0$, $\alpha_2 = 56.4$, and $\alpha_4 = -56.4$ degrees. As shown in Figure C-30, the initial CMG momentum was 250 ft-lb-sec but the magnetic system rapidly reduces it to less than 40 ft-lb-sec after 2000 seconds time. In so doing, the magnetic system was continuously exercised and all the dipoles were saturated at 1000 seconds (Fig. C-31), but toward the end of the orbit were operating in their linear regions. In addition to dumping the initial momentum of 250 ft-lb-sec, the accumulated g.g. momentum of about 400 ft-lb-sec has also been dumped. During this orbit, the magnetic torque components which were generated attained magnitudes of 0.22 ft-lb, a value greater than the gravity disturbance torque. With the magnetic system, the CMGs continued to operate about the new null with less than 4 degrees gimbal variation over the next several orbits (not shown). The pointing performance was only slightly degraded from that shown in Figure C-22 with all four CMGs operating.

In additional cases (runs PI-98 and -99) the elements of the torque matrix corresponding to the failed CMG were set to zero. The performance of the three operational CMGs equaled that obtained with all four operating once the new null had been established. With one CMG out, there are three remaining gimbal angles and three equations that relate them to the commanded torque, in which case an exact inverse can be used to obtain the CMG steering law. Additional cases (not shown) were programmed with exact inverses for three CMG configurations. Data from these cases were compared with those of the pseudo inverse with one CMG out. The results were identical. That is, with one CMG out, the pseudo inverse steering law reduces to an exact inverse. Again, the simulation data agree with the theory of the pseudo inverse [8 and 12].

With continuous momentum dump, the CMGs do not accumulate much momentum. In a subsequent run (not shown) four 25 ft-lb-sec CMGs were used to maintain satisfactory performance. In general, the electromagnet aligned with the axis of minimum inertia does more work than the dipoles along the other axes. In the next run (not shown) the X_v-axis coil was failed, as well as CMG number 3, and the pointing performance was relatively unchanged.

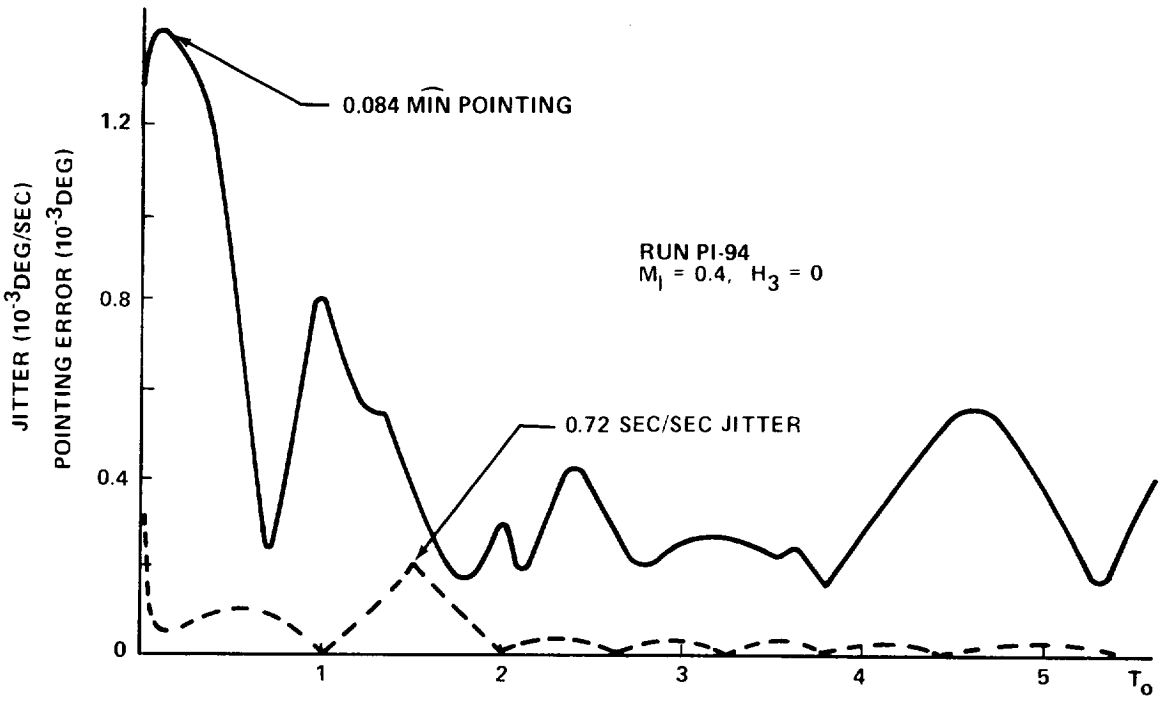

Figure C-28. Performance while finding a new CMG null with CMG number 3 out.

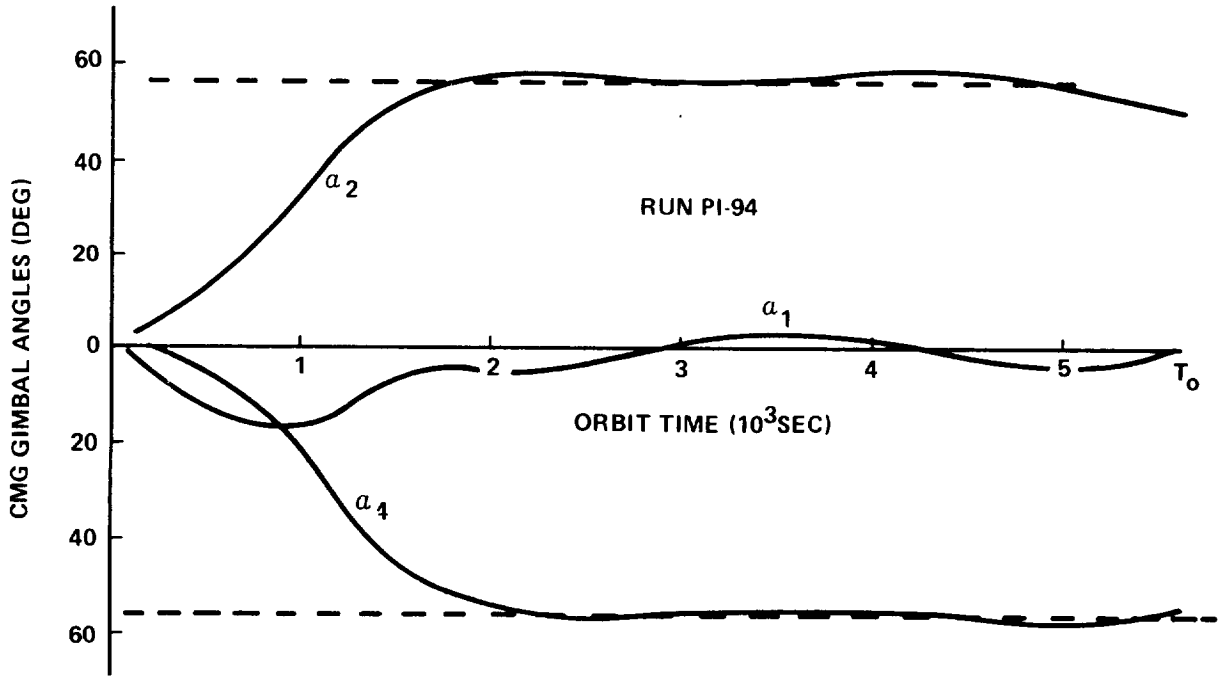

Figure C-29. Magnetics force CMGs to a new null with CMG number 3 out.

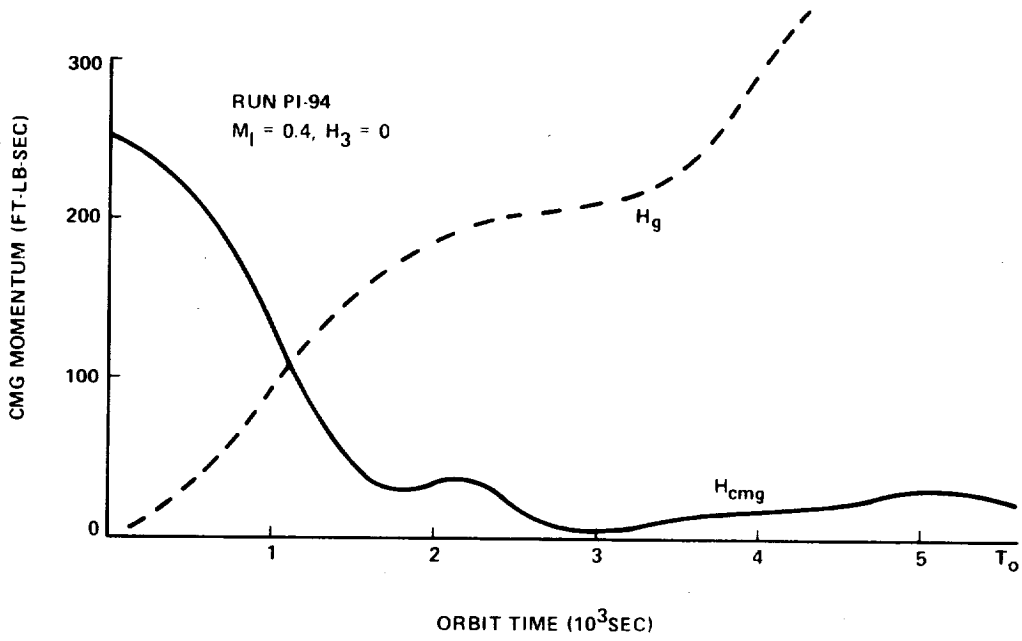

Figure C-30. Magnetics force the CMG momentum to zero as a new null is found.

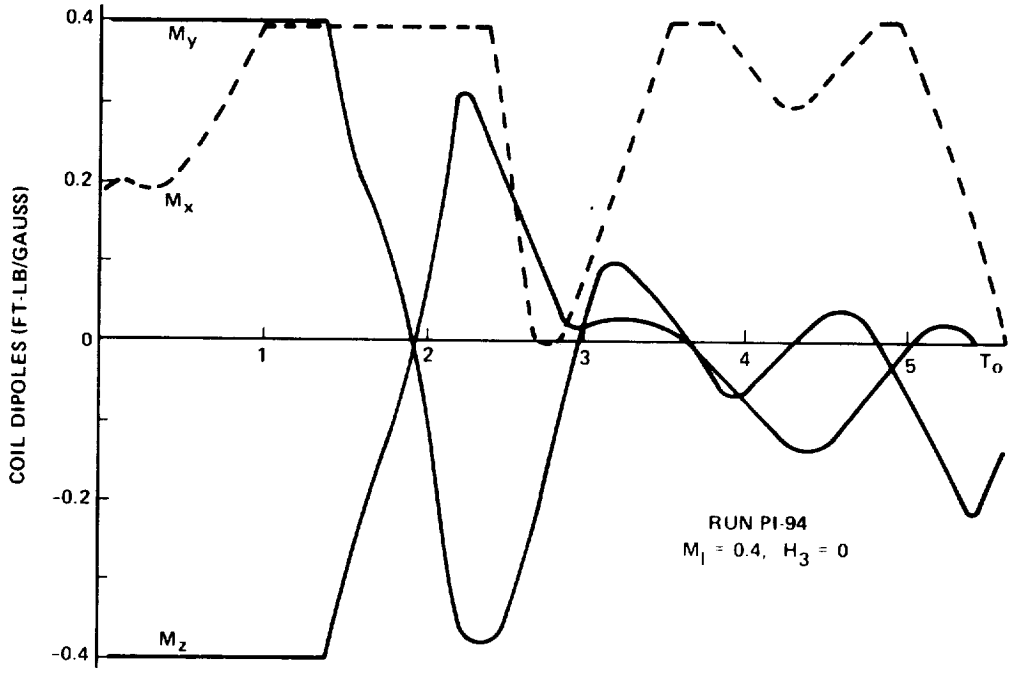

Figure C-31. Coil dipoles with CMG number 3 failed versus orbit time (10^3 sec).

However, only about two-thirds of the accumulated gravity momentum was dumped. The system could saturate in about four orbits if a worst-case attitude hold were maintained with one CMG and one coil failure.

With the magnetic system dumping momentum, two CMGs were failed and, without modifying the steering law, control was lost. With two CMGs failed, the remaining two CMGs can provide only two-axis control. The third axis must be controlled by magnetics or the RCS. Moreover, the pseudo inverse must be reprogrammed. Since there are only two unknowns (gimbal rates) and three known quantities (commanded torque components), the pseudo inverse has the form

$$C^{+} = (C^{*} C)^{-1} C^{*}$$

and the gimbal rates are

$$\dot{\tilde{\alpha}} = C^{+} \tilde{T}_{c} \quad .$$

In this case, the torque matrix C is a 3 by 2 matrix and the pseudo inverse, C^{+}, is 2 by 3 matrix. To obtain maximum use of the magnetic system, both direct torque ($K_{c} = 1.0$) and momentum dump ($K_{m} = 0.01$) commands were used to drive the coils. The pointing performance is shown in Figure C-32 with CMGs number 2 and number 4 failed. The pointing error peaks at 2550 seconds with a value of 0.22 arc min. In this particular case, the roll error about the experiment axis is 4.8 arc min. The magnetic system is providing roll control and at 2750 seconds the earth's field is unfavorable for roll control (Fig. C-7). Both the Y_{v} and Z_{v} axes components (B_{y} and B_{z}) are near zero and the X_{v} axis component (B_{x}) cannot be used to produce roll control torque. Therefore, at 2750 seconds, the roll axis is not being controlled and the roll error is building up. However, this condition lasts only for about 50 seconds during the orbit before the earth's magnetic field changes and roll control is re-established. Although the roll error is large compared to the pointing error, it is still within the 5 arc min goal baselined for HEAO-C. Additional runs were made with only two CMGs operational and augmented with magnetic torques. In most cases, the HEAO-C pointing requirements were maintained. In those cases where the errors exceeded requirements, the excess errors were only for very short time intervals during the orbit, less than 100 seconds per orbit. It is concluded that, in all but the most unfavorable pointing orientations and orbit conditions, two CMGs augmented with direct magnetic torque can meet the HEAO-C pointing requirements.

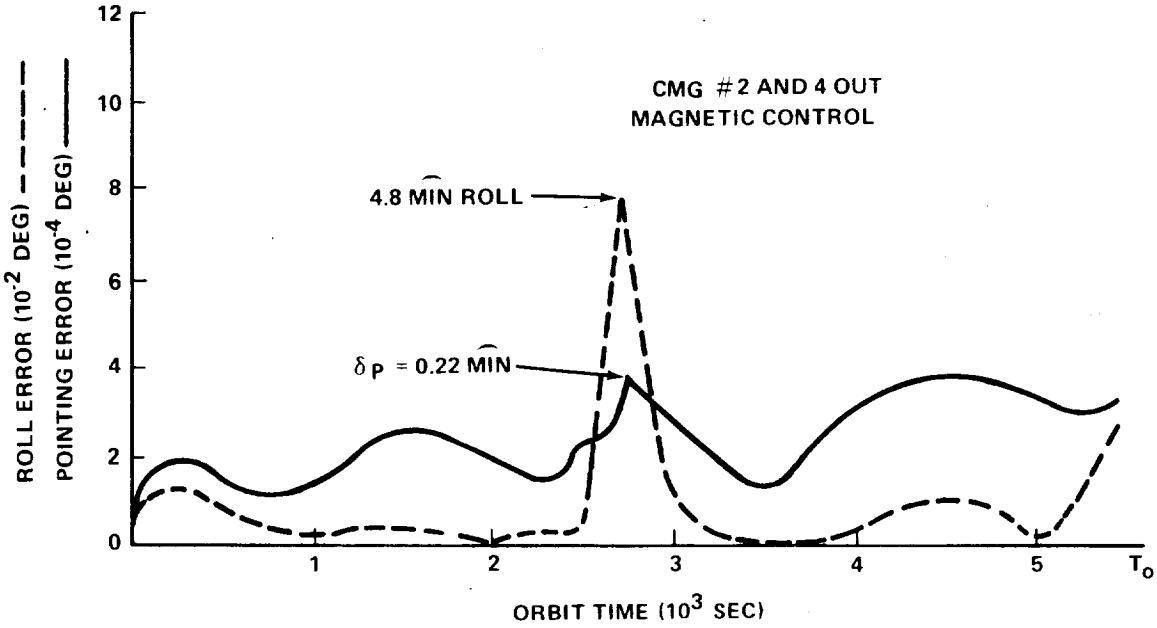

Figure C-32. Performance with CMG number 2 and number 4 out using the pseudo inverse with magnetic control.

With CMG number 2 and number 4 out, the momentum vectors of CMG number 1 and number 3 are equal but opposite in direction. The two-CMG system is, therefore, at a null position. The variation in gimbal angles, shown in Figure C-33, is less than 10 degrees over the orbital period and the accumulated momentum (not shown) is less than 100 ft-lb-sec.

The Bendix Three-Gimbal Inverse

The three-gimbal inverse steering law proposed by Bendix [6] is more complex than any of the other laws. Consequently, more time and effort were required for simulation. The four 3 by 3 matrices were inverted by several methods: (1) a subroutine for matrix inversion, (2) direct programming for each inverse, and (3) an iterative technique for which the matrix elements were updated at each time step. Each method gave somewhat different results. All, however, produced similar trends without magnetic dump. At about 1200 seconds in the orbit, the torque vectors for CMG number 1 and number 3 became colinear causing the determinants of matrices A_2 and A_4 to approach zero. Even though a three-dimensional space was still spanned by CMG torque vectors number 2 and number 4 and a vector aligned with number 1 and number 3, the program diverged due to mathematical singularities. For the three-gimbal inverse to perform properly, it is absolutely essential that singularity

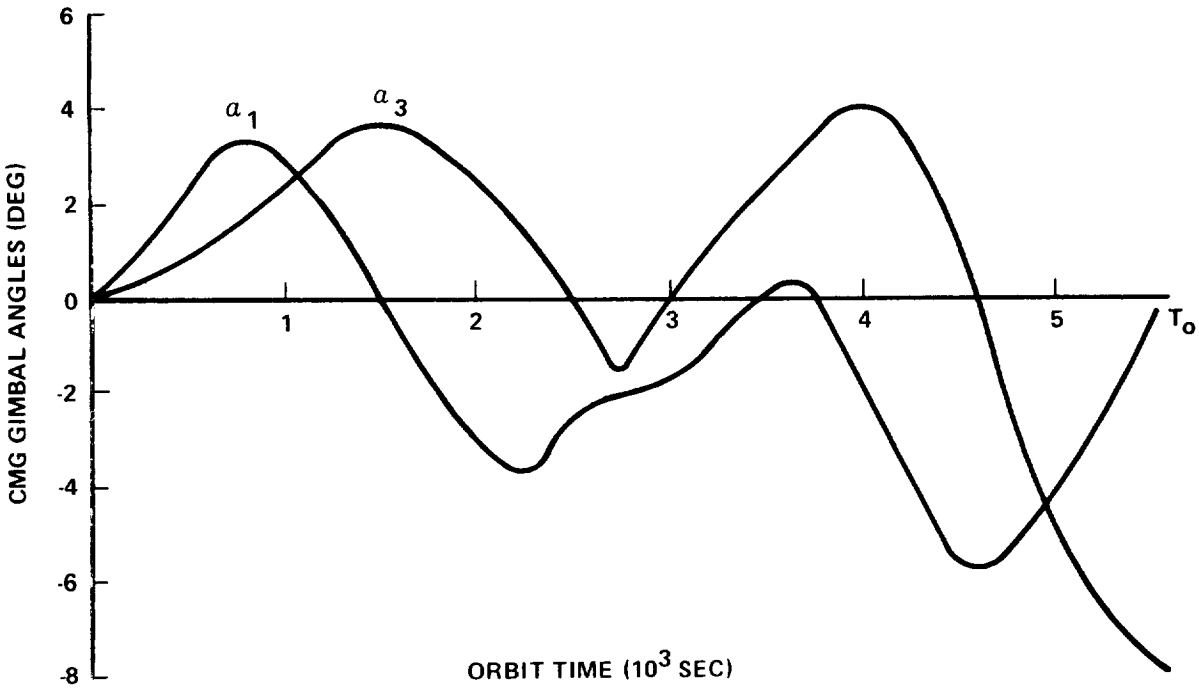

Figure C-33. CMG gimbal angles with CMG number 2 and number 4 out and magnetic control.

detection and avoidance schemes be incorporated into the steering law. However, due to the complexity of such schemes, this was not done during the simulation.

With the directly programmed inverse, the singularities occurred at 1200 seconds. In contrast, the subroutine for matrix inversion used an iterative method and, hence, was not quite as sensitive to singularities. With this subroutine, the program diverged at 1700 seconds. However, with the iterative technique utilizing matrix element update, the determinants were not used in obtaining the inverse. With this inverse, oscillations occurred at 1800 seconds after which control was regained and pointing performance maintained over most of the orbit. Figure C-34 shows pointing performance using the iterative technique. The peak error of 5.4 arc min occurs at a time (1900 seconds) just after the time the matrices would have singularity. As illustrated, the performance is not smooth and, many times during the three-fourths orbit period, the jitter exceeded HEAO requirements.

The gimbal angles are shown in Figure C-35. Notice the sharp breaks where the singularities occurred (1900 seconds). The movements are irregular especially at 1700 and 4000 seconds, although the general trends are similar to those obtained with the other steering laws.

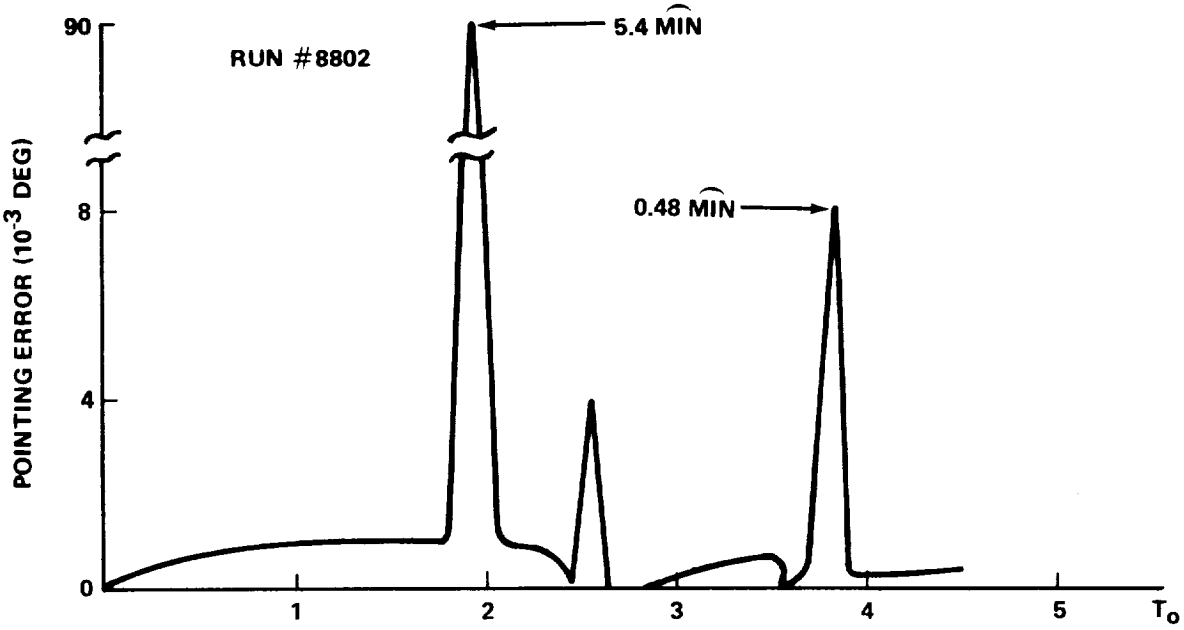

Figure C-34. Three-gimbal inverse pointing performance.

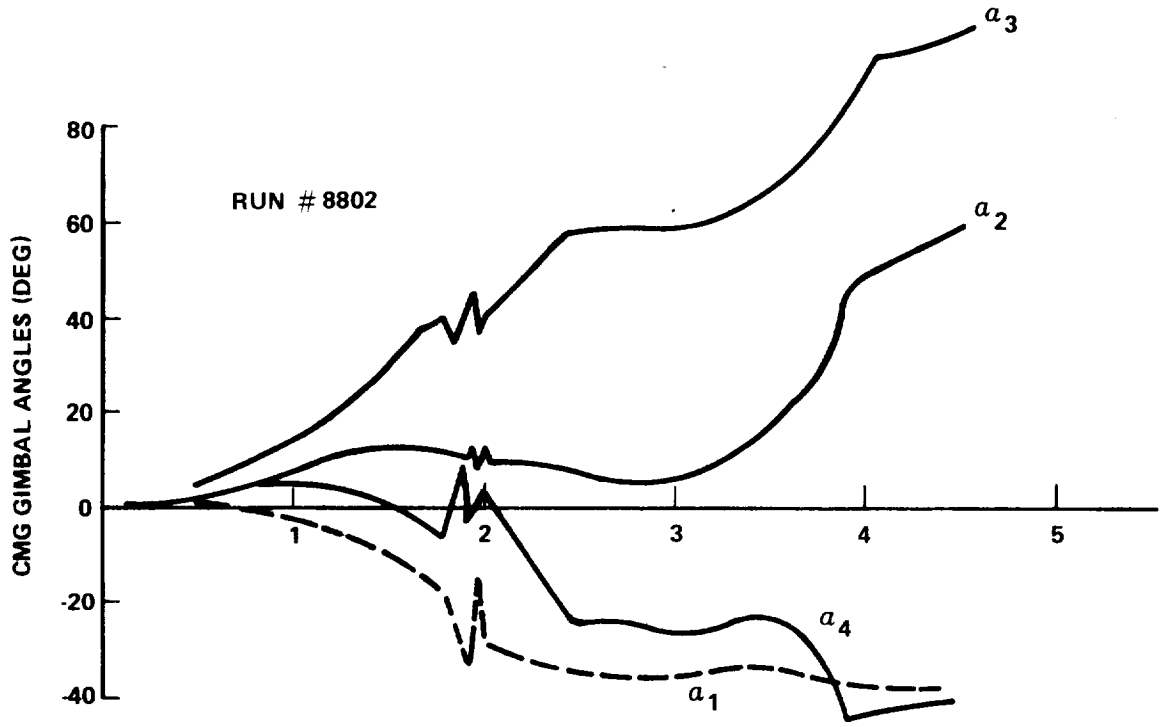

Figure C-35. CMG gimbal angles for the three-gimbal inverse versus orbit time (10^3 sec).

With electromagnets inserted and used for continuous CMG momentum management, the gimbal angles stay small, thus, avoiding the singular condition. In these cases, the performance of the three-gimbal inverse was comparable with that obtained by the other steering laws and, therefore, is not shown.

The shortcoming of the three-gimbal inverse is that most of its singularities are self-induced. That is, the basic law itself permits mathematical singularities that are not singularities for the other steering laws. However, with a suitable singularity detection and avoidance scheme, the full momentum envelope could probably be utilized for control purposes. Nevertheless, the complexity of the scheme with the associated matrix inversion procedures appears to prohibit its use.

Transpose with Torque Feedback

The transpose type steering law is derived by taking the transpose of the CMG torque matrix as an approximation for its inverse. The gimbal rate commands are:

$$\dot{\alpha}_1 = -(C_{11}T_{cx} + C_{21}T_{cy} + C_{31}T_{cz})/H \quad ,$$

$$\dot{\alpha}_2 = -(C_{12}T_{cx} + C_{22}T_{cy} + C_{32}T_{cz})/H \quad ,$$

$$\dot{\alpha}_3 = -(C_{13}T_{cx} + C_{23}T_{cy} + C_{33}T_{cz})/H \quad ,$$

and

$$\dot{\alpha}_4 = -(C_{14}T_{cx} + C_{24}T_{cy} + C_{34}T_{cz})/H \quad ,$$

where C_{ij} are the elements of the torque matrix, $T_{cx,y,z}$ are the components of the commanded torque, and H is the momentum per CMG. Typical performance is shown in Figure C-36. The pointing error is 0.8 arc min, and the roll error exceeds that specified for HEAO. However, by doubling the feedback gain on the roll axis (axis of minimum inertia), the roll error (not shown) was less than the pointing error. The peak pointing errors are caused by two factors: (1) Just before 4500 seconds, the CMG gimbal positions (Fig. C-37) were very near the gyro hang-up position of $\alpha_1 = -90$, $\alpha_2 = 0$, $\alpha_3 = 90$, and $\alpha_4 = 0$ and (2) The nonlinear terms in the Euler equations added significantly

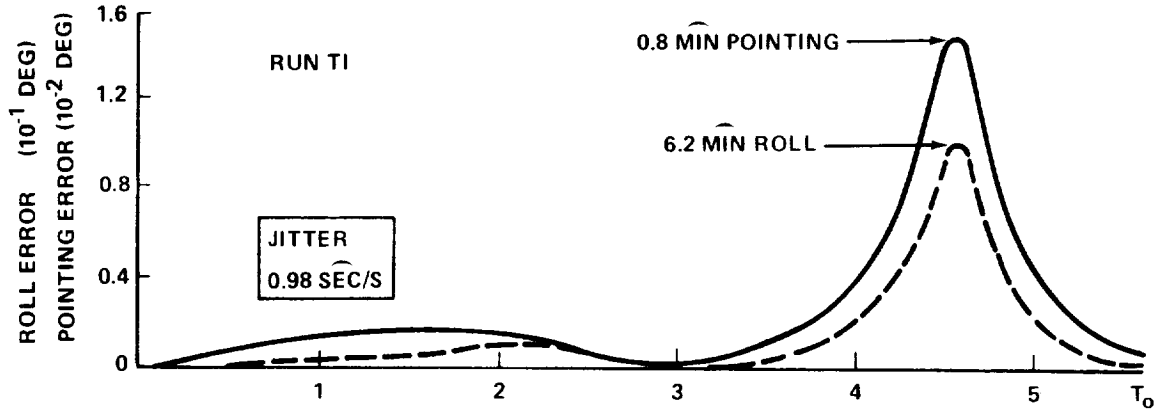

Figure C-36. Performance of the transpose steering law.

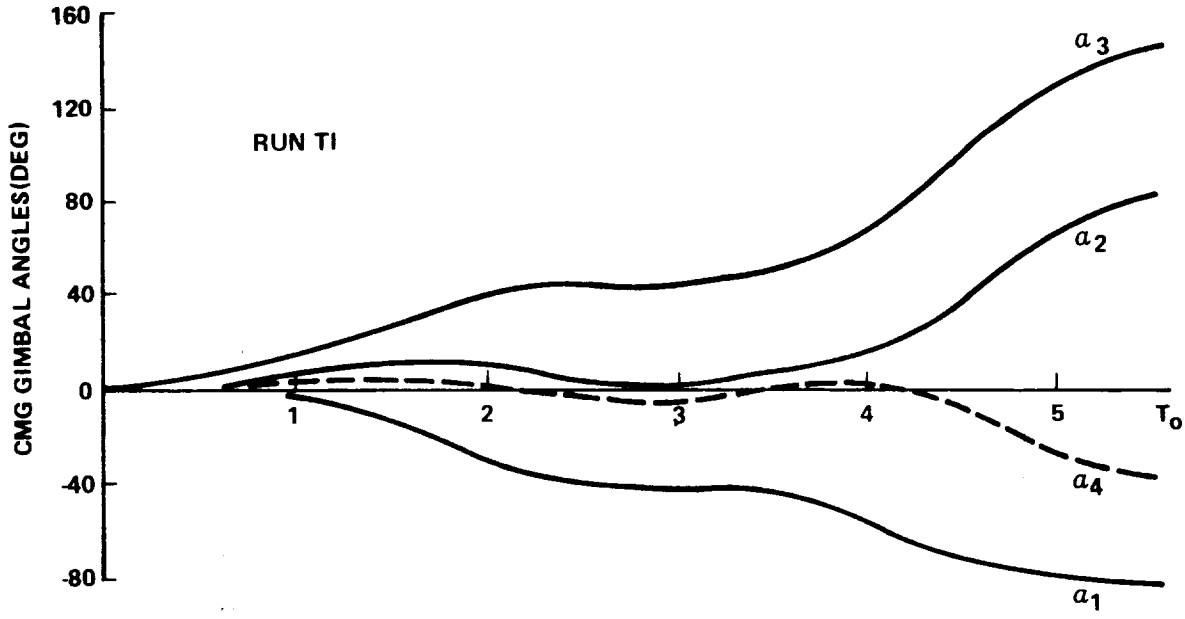

Figure C-37. CMG gimbal angles versus orbit time (10^3 sec) for the transpose steering law.

to the error. These terms are products of the body angular rate multiplied by the accumulated CMG momentum. The body rates (jitter) peaked at about 0.98 arc sec/sec with over 400 ft-lb-sec accumulated in the CMGs which produced errors through their vector cross product terms in the Euler equations.

A magnetic system was added for CMG momentum dump. The performance (Fig. C-38) was about 0.026 arc min pointing and 0.2 arc min roll. The peak jitter (not shown) was 0.27 arc sec/sec. This performance is not quite as good as that obtained with the other steering laws using magnetics, basically because the torque produced per unit torque commanded is not unity. The gimbal angles stay less than 4 degrees when the magnetic system is used for CMG momentum management. During most runs simulating normal pointing modes, the CMG gimbal rate limits are never attained.

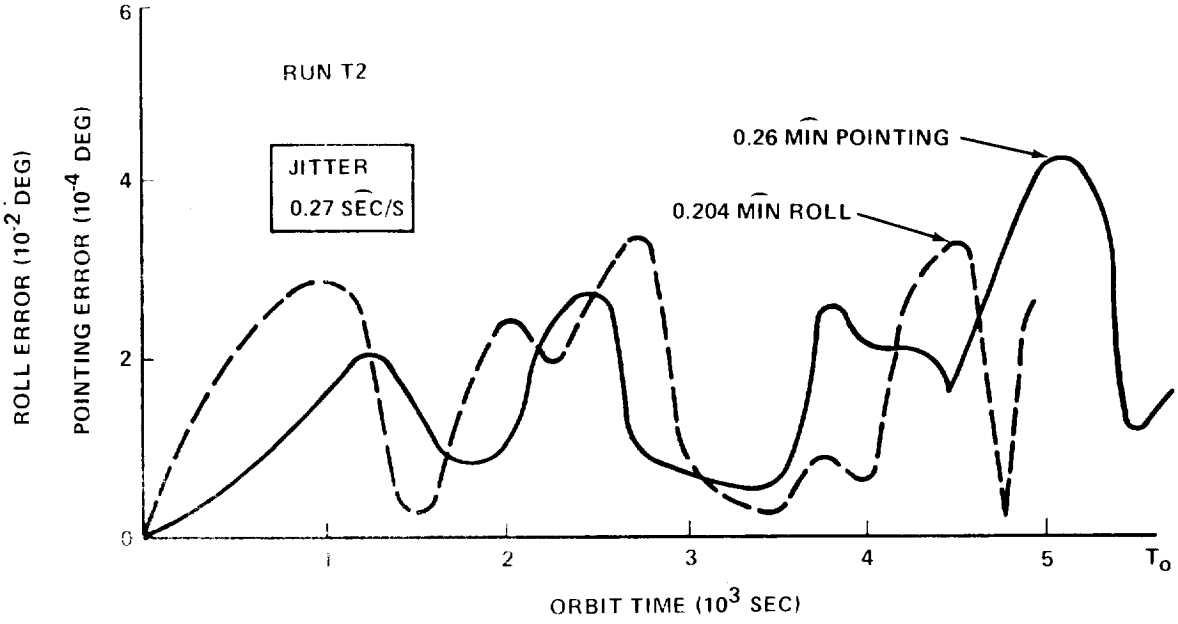

Figure C-38. Transpose performance with magnetics.

The transpose with torque feedback steering law is obtained by feeding back the CMG torque at each instant of time and subtracting it from the torque commanded. The commanded torque in only the gimbal rate equations (steering law) are replaced by

$$T'_{cx} = T_{cx} - \dot{h}_x \quad ,$$

$$T'_{cy} = T_{cy} - \dot{h}_y \quad ,$$

and

$$T'_{cz} = T_{cz} - \dot{h}_z \quad ,$$

where $\dot{h}_{x,y,z}$ is the CMG torque vector components. Figure C-39 shows the pointing performance. The response is oscillatory during the first half-orbit between 0.005 and 0.018 degree. The peak error of 4.7 arc min occurs at 4700 seconds, at which time the roll error is 1.05 degrees and jitter is 0.47 deg/sec. These data are the worst obtained with any steering law. On examination of the gimbal rates they are all chattering between their hard limits of 1 deg/sec. Although it appears that the oscillations have a period of 100 seconds, that could be a false conclusion since the data were hand-plotted from computer printout at each 50 seconds of the orbit. Therefore the gimbal angular rates and pointing errors could be chattering at a higher frequency between the 1000 and 3400 second period. The CMG torque feedback has the effect of greatly increasing the control system gain through the CMG loop, by adding a lead to the system. To properly stabilize the system, tachometer dynamics or a lag filter needs to be inserted in the CMG torque feedback loop. However, this was not done during the simulation, so the results obtained are not representative of a properly operating system. The gimbal angles (not shown) approximately equaled those shown in Figure C-37, but were not as smooth.

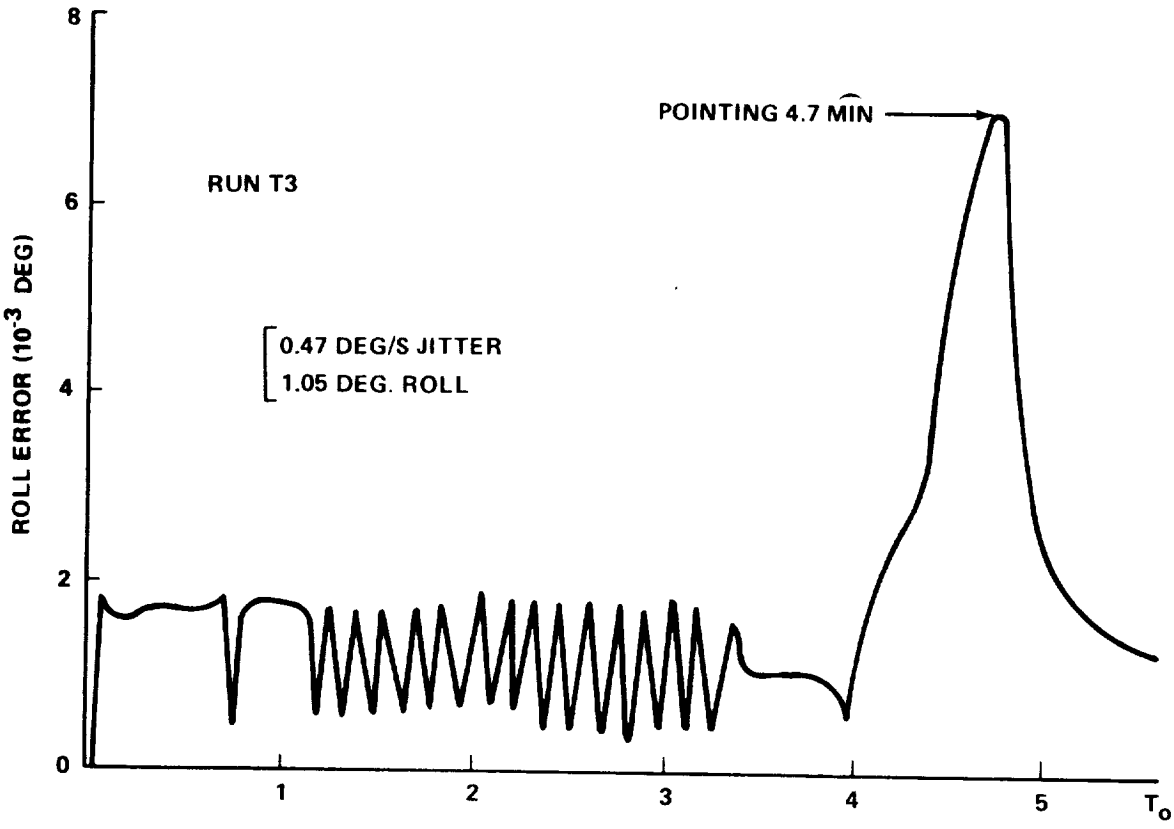

Figure C-39. Transpose with torque feedback performance.

Magnetics were added on the next run. As in the other magnetic runs, the gimbal angles stayed small, less than 4 degrees, over the orbital period. However, the gimbal rates still chattered continuously but the performance was greatly improved. Peak errors were 0.16 arc min in pointing, 1.6 arc min in roll, and 9.3 arc sec/sec in jitter. Data from this run are not shown.

The BECO H-Distribution

Typical performance using the BECO steering law is shown in Figure C-40. The peak pointing error is 0.16 arc min at 4800 seconds and the peak roll error is 0.95 arc min at 1000 seconds. Compared with the pseudo inverse (Figs. C-20 and C-21), the performance is degraded by a factor of 10. However, in additional runs (not shown), the gain factor on the fourth gimbal rate was increased from 0.0006 in run B-10 to 0.001 and the performance was approximately that obtained with the pseudo inverse. In run B-10, the gimbal angles (Fig. C-41) attain slightly larger values than those shown in Figure C-21. At the end of one orbit, $\alpha_1 = -106$, $\alpha_2 = 110$, $\alpha_3 = 166$, and $\alpha_4 = -18$ degrees. As the run continued into the second orbit, a singularity was encountered at 8000 seconds, about one and one-half orbits, at which time control was lost. For this run, pointing control was lost about one-third orbit sooner with the BECO law than with the pseudo inverse.

To test the ability of the BECO steering law for distributing momentum, [illegible] removed from the simulation and a constant torque of 0.2 ft-lb was placed on the Y_v-axis of the vehicle. Since there is a momentum potential of 800 ft-lb-sec on each axis, CMG saturation should occur at 4000 seconds if gyro hang-up is avoided. In this particular situation, the gyro hang-up condition to be avoided is expected to occur at 1500 seconds with $\alpha_1 = 90$, $\alpha_2 = \alpha_3 = 30$, and $\alpha_4 = 0$ degrees. This CMG orientation places all the CMG torque vectors in the X_v Z_v plane. Since the disturbance torque is perpendicular to this plane, the commanded torque will follow the disturbance so that the vector scalar product between the commanded and CMG torque will be zero, hence gyro hang-up. Figure C-42 illustrates the gyro hang-up condition relative to the applied constant torque. With a constant torque input (Fig. C-43), the pointing error is also constant at 0.085 arc min until CMG saturation or gyro hang-up.

With the BECO law, saturation occurred at about 4000 seconds, as predicted, after which control was lost. The gyro hang-up condition was avoided by distributing the momentum between axes, hence, the BECO

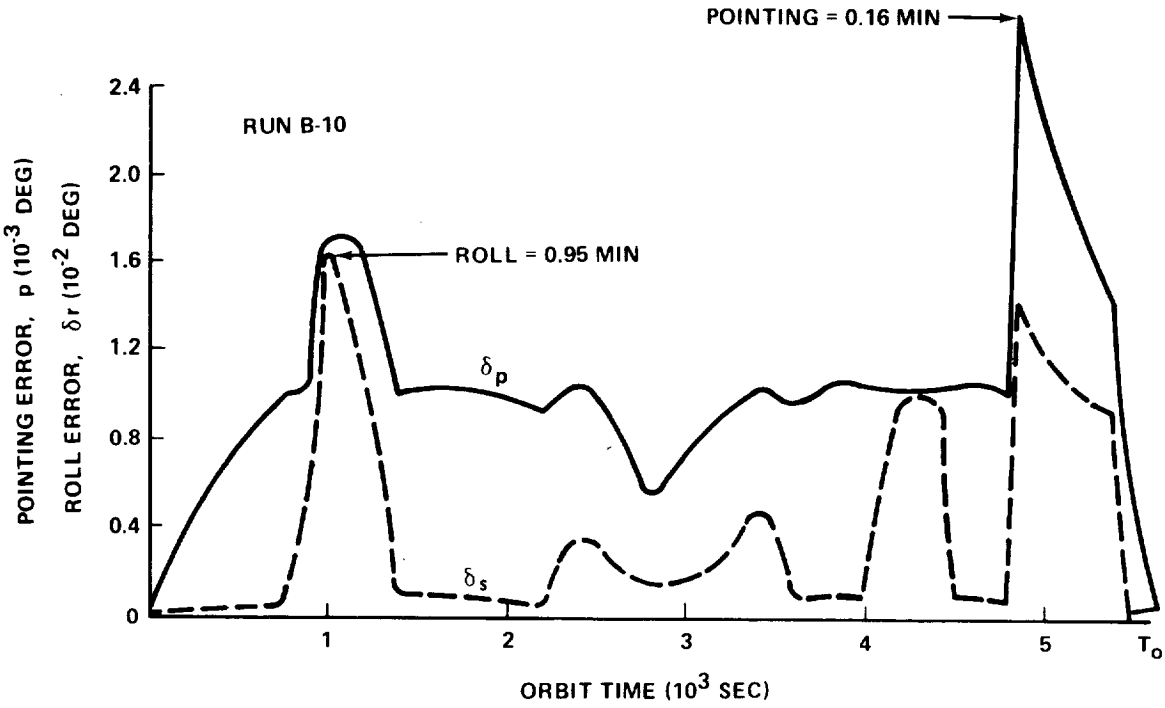

Figure C-40. Performance with the BECO steering law.

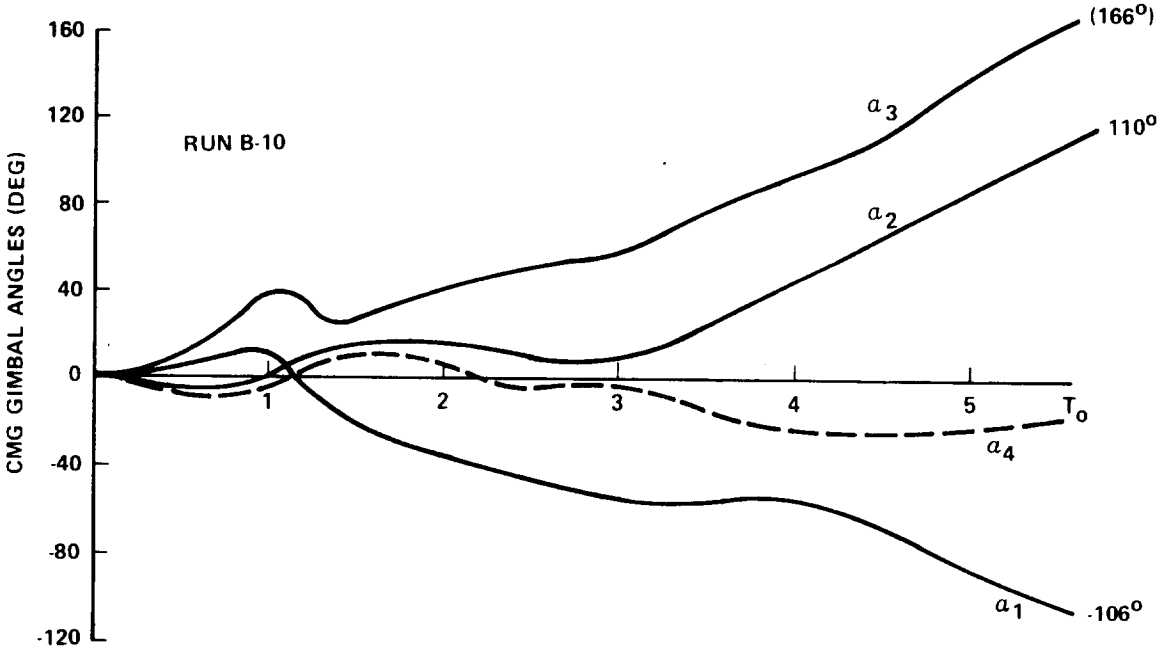

Figure C-41. CMG gimbal angles with the BECO steering law.

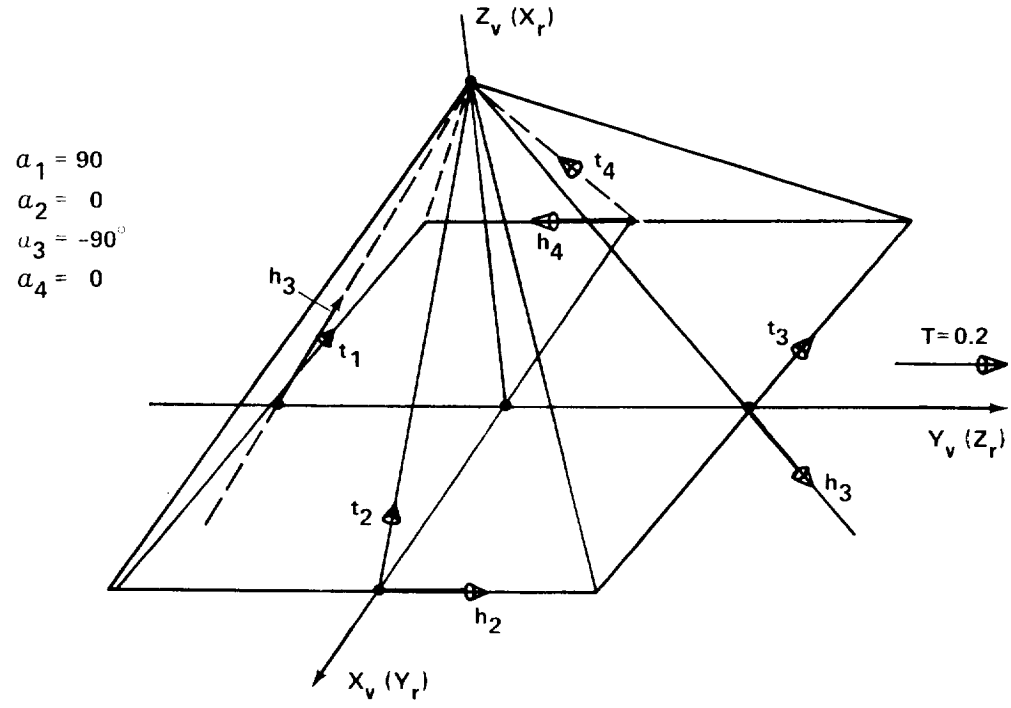

Figure C-42. CMGs in gyro hang-up with torque axes in the X_V-Z_V plane and applied torque along Y_V.

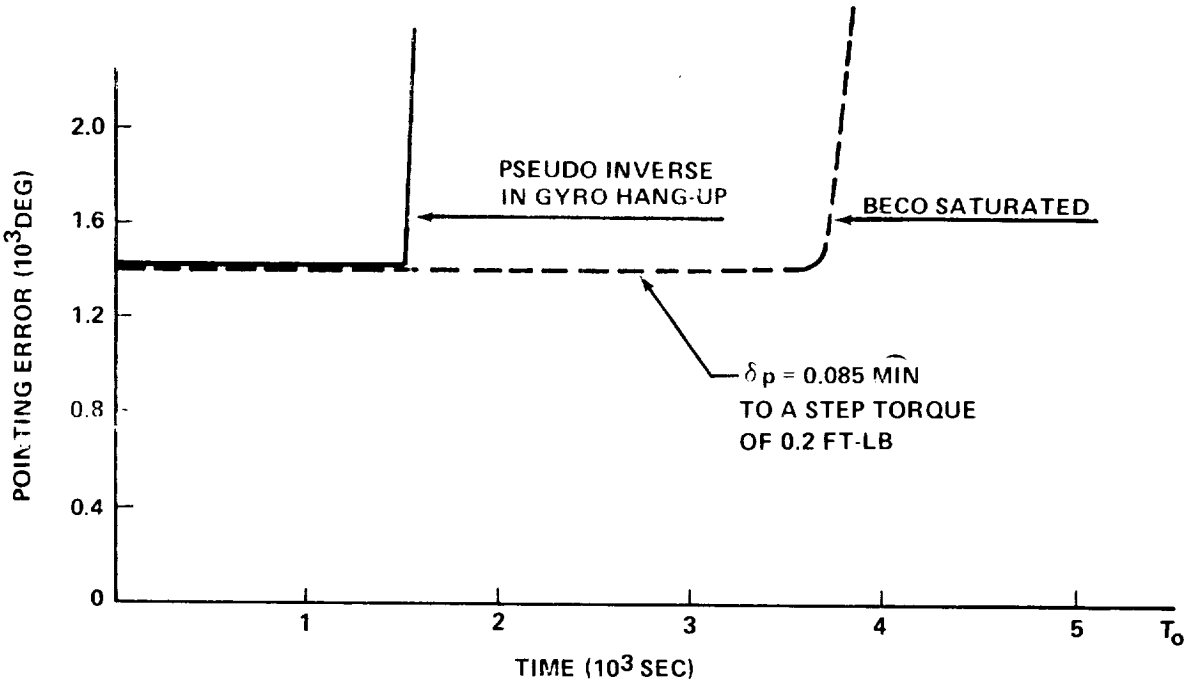

Figure C-43. Pointing error in response to a step torque of 0.2 ft-lb.

H-distribution law performed as advocated. The same conditions were run with the pseudo inverse law but, as shown in Figure C-43, the gyro hang-up condition was encountered at about 1500 seconds and control was lost. The system did not recover but stayed in the hang-up condition. The corresponding gimbal angles are shown in Figure C-44 for the pseudo inverse and in Figure C-45 for the BECO steering laws. The BECO law forced the fourth gimbal angle to move 180 degrees so that the full momentum envelope was utilized. Prior to the gyro hang-up condition, the gimbal angles were the same for either case. However, at 1300 seconds, the BECO law forces gimbals number 4 and number 2 from their null positions to avoid the hang-up condition. In so doing, gimbal number 1 is rapidly forced past the critical 90-degree point, attains a peak of slightly more than 140 degrees, and then decreases to 90 degrees at saturation. The CMGs are saturated in the Y_V-axis at 4000 seconds with $\alpha_1 = 90$, $\alpha_2 = 0$, $\alpha_3 = -90$, and $\alpha_4 = 180$ degrees. As previously defined, saturation represents the ultimate in gyro hang-up but cannot be avoided by any steering law, unless momentum is dumped. Control is always lost at saturation but some cases of gyro hang-up internal to the momentum envelope can be avoided by the steering law. The BECO law may be directional and needs further development to prove its ability in preventing gyro hang-up conditions.

SUMMARY

During the study, several CMG steering laws were evaluated. As long as the gimbal angles stay less than 90 degrees, almost any steering law can meet the HEAO requirements. With 250 ft-lb-sec CMGs, the gimbal angles get large within an orbit, thereby, ruling out the use of a constant gain steering law. When one CMG has failed, the remaining CMGs must work harder. With several of the steering laws (the Bendix three-gimbal inverse, for example) the failure must be identified and corrective changes made. After making any required changes, the resulting steering law must be identical to the exact inverse of the 3 by 3 torque matrix to prevent degradation in pointing performance. Based on both simulation results and mathematical theory, the pseudo inverse steering law reduces to an exact inverse when any CMG is arbitrarily deactivated. With the pseudo inverse, system performance is not degraded by using only three CMGs for control.

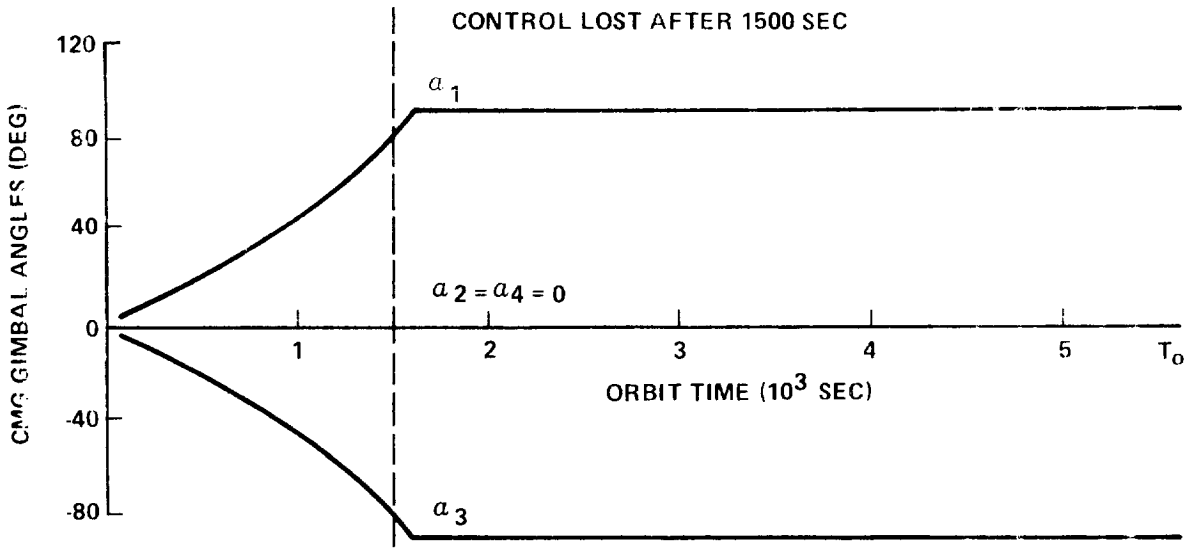

Figure C-44. Gyro hang-up at 1500 sec with pseudo inverse steering law and constant torque.

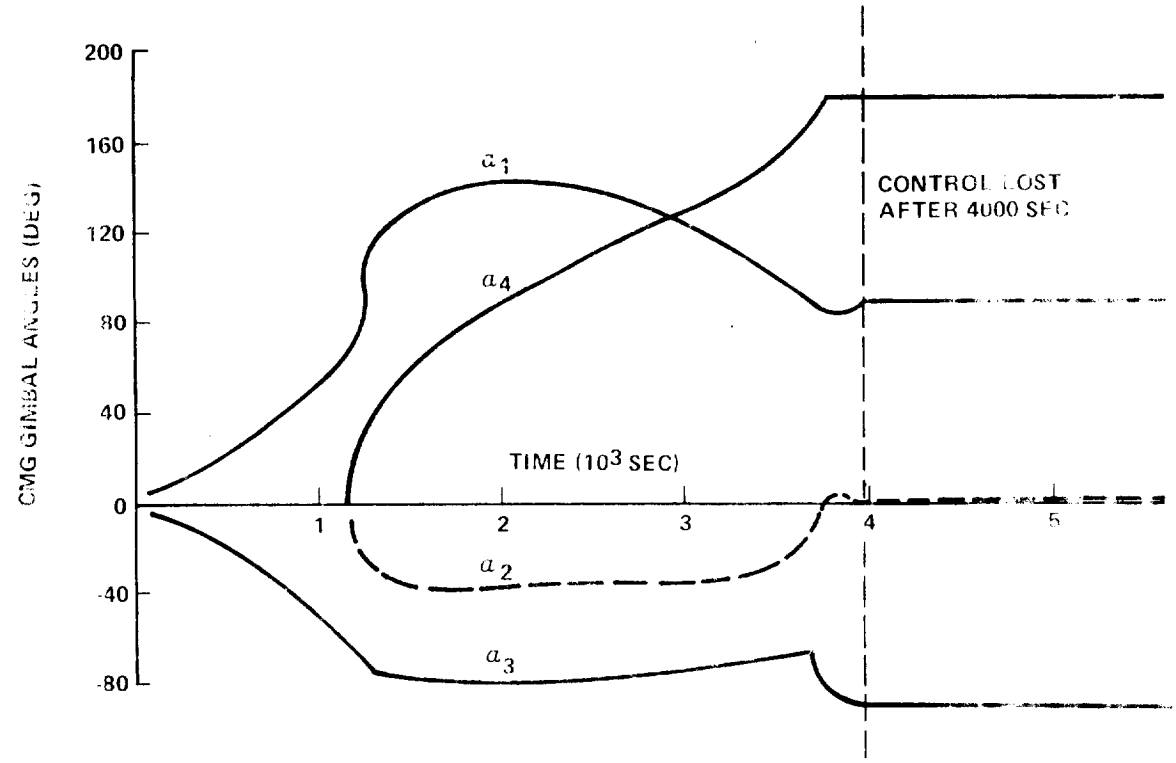

Figure C-45. Saturation at 4000 sec with BECO steering law and constant torque.

To allow more than one CMG failure without affecting performance, consideration should be given to using more CMGs but with each sized to a lower momentum capacity. For the same total momentum capacity, six 125 ft-lb-sec CMGs would permit three failures without degrading performance. However, with three failures, the momentum would have to be dumped about each half-orbit to prevent saturation under worst-case environmental conditions.

Based on estimated impulse requirements for CMG momentum management, the fuel weights for an all-RCS dump could become prohibitive, especially for a growth version of HEAO, for which the inertia distribution becomes less favorable. The alternative system recommended for HEAO utilizes electromagnetic torquers reacting with the earth's magnetic field to dump accumulated momentum. In this case, an RCS is not needed after the OAS burn control period. Tradeoffs show that the magnetic system is better than RCS from both a weight and reliability viewpoint. Moreover, the low torque levels of a magnetic system permits continuous momentum dumping without interfering with experiment pointing. Simulations show and analysis has proven that, as an added bonus, a magnetic CMG desaturation system improves pointing performance by providing integral control of the attitude error signal through the magnetic loop. Since CMG momentum is continuously dumped, the gimbal angles stay small (less than 4 degrees for four 250 ft-lb-sec CMGs) and, typically, the stored momentum is less than 20 ft-lb-sec. Hence, with a magnetic CMG desaturation system, the CMG momentum per wheel could be reduced considerably as compared with the present baseline size. Alternatively, a greater depth of CMG failures could be tolerated without degrading performance.

Magnetic momentum dump always keeps the CMG gimbal angles and momentum small, permitting linear operation of the steering law. The performance of any steering law is enhanced by the magnetic system. With small gimbal angles, the performance obtained by various steering laws was comparable. However, once the gimbal angles get large, the performance is usually degraded by cross coupling and nonlinear effects in the Euler equations. Only the pseudo inverse and H-distribution laws performed without degradation with large gimbal angles. Moreover, maneuvers were commanded with the CMGs near a saturation condition to illustrate the transfer of momentum from one spacecraft axis to another — one of the reasons for selecting a near spherical CMG momentum profile for HEAO-C.

With continuous magnetic dumping, the constant gain steering law meets all HEAO pointing requirements and would be the simplest to implement. The maximum contribution with magnetics offers fail operational capability.

Even with two CMG failures, no program changes are needed. The pseudo inverse must be reprogrammed for two CMG failures. Neither the three-gimbal inverse nor the H-distribution steering laws permit two failures. Although the transpose with torque feedback is similar to the MC, CMG failures were not simulated and additional studies are needed to obtain the proper stabilization networks for optimum performance. For the greatest depth of failures without any program modifications, the maximum contribution steering law could be used for HEAO with a magnetic system utilized for continuous momentum management.

Without magnetics and requiring at least one orbit of CMG control prior to RCS dumping, a sufficiently large momentum envelope must be available for control during attitude hold modes. Over extended periods between dumps, the CMG gimbal angles and stored momentum become large, hence, cross coupling and nonlinear terms in the Euler equations can produce significant pointing errors. Only the pseudo inverse and H-distribution steering laws permitted full utilization of the CMG potential without undesirable side effects. Moreover, either law provides growth potential for greater pointing accuracies than is required for HEAO. But since the pseudo inverse also provides fail operational capability for one CMG out, without reprogramming, it is recommended for use on HEAO with a RCS used for periodic momentum management.

In general with disturbance torques acting on all three axes, gyro hang-up was not encountered using pseudo inverse steering. However, an increase in pointing errors was observed whenever the gimbal angles were near a gyro hang-up or singular condition. With the pseudo inverse steering law as implemented, gyro hang-up also corresponds to singularity. An alternate implementation of the pseudo inverse steering law is possible that will completely remove singularities although internal hang-up conditions can still be encountered. None of the laws simulated were designed to avoid hang-up. However, the BECO law looks promising, although additional work is required to prove its worth. As used in this report, singularities are a mathematical occurrence which is inherent to a specific steering law formulation. Whereas, gyro hang-up is a physical orientation of the gimbal positions which prevents the desired torque from being produced. Currently, it appears that only about 50 to 60 percent of the total momentum envelope of single gimbal CMGs is usable before encountering a possible hang-up position. Much more research is needed to understand and devise ways of avoiding gyro hang-up conditions and is outside the scope of this report.

REFERENCES

1. Conceptual Design of a High Energy Astronomy Observatory. NASA TMX-53976, Marshall Space Flight Center, Ala., Feb. 1971.

2. General Electric Missile and Space Division: Control Laws for CMG Air Bearing Test. General Electric Program Information Release No. PIR-1J71-1332, Valley Forge Space Technology Center, Philadelphia, Penn., Apr. 4, 1971.

3. Teledyne Brown Engineering Company: HEAO-C Baseline Attitude Sensing and Control Systems Description. Report No. SE-PD-1340, NASA Contract No. NAS8-20073, Huntsville, Ala., Jul. 1971.

4. Teledyne Brown Engineering Company: Conceptual Design of a Spacecraft for the High Energy Astronomy Observatory (HEAO) Mission C. Huntsville, Ala., Nov. 1970.

5. Greensite, A. L.: Analysis and Design of Space Vehicle Flight Control Systems. Spartan Books, N.Y., 1970.

6. Bendix Corporation: HEAO Phase B Study Final Report, Volume 1 — System Summary and Description. Teterboro, N.J., Mar. 1971.

7. Sperry Flight Systems Division: Fine Attitude Control System. NASA Contract No. NAS9-10363, Phoenix, Ariz., May 1971.

8. Penrose, R.: On the Generalized Inverse of a Matrix. Proc. Cambr. Phil. Soc., 1955, pp. 406-413.

9. High Energy Astronomy Observatory Attitude Sensing and Control System. Job Number 301200 in support of scientific and engineering operations, Computation Laboratory, Marshall Space Flight Center, May 1971.

10. Davis, Billy G.; A Discussion of Orbital Workshop Orientation and Gravitational Effects. NASA TMX-53829, May 5, 1969.

11. Sperry Rand Corporation: Linear Analysis of Control Systems Applicable to the HEAO-C Satellite. Report No. SP-255-00528, Space Support Division, Huntsville, Ala., Aug. 1971.

12. Greensite, A. L.: Elements of Modern Control Theory. Vol. 1, Spartan Books, N.Y., 1970.

APPROVAL

A COMPARISON OF CMG STEERING LAWS FOR HIGH ENERGY ASTRONOMY OBSERVATORIES (HEAOs)

By Billy G. Davis

The information in this report has been reviewed for security classification. Review of any information concerning Department of Defense or Atomic Energy Commission programs has been made by the MSFC Security Classification Officer. This report, in its entirety, has been determined to be unclassified.

This document has also been reviewed and approved for technical accuracy.

David N. Schultz

DAVID N. SCHULTZ
Chief, Navigation and Control Systems Branch

Fred E. Digesu

FRED E. DIGESU
Chief, Electronics and Controls Division

ERICH E. GOERNER
Director, Preliminary Design Office

James T. Murphy

JAMES T. MURPHY
Acting Director, Program Development

DISTRIBUTION

INTERNAL

DIR
DEP-T
AD-S

SS-H
- Dr. Speer
- Mr. Fichtner
- Mr. Webb
- Mr. Dailey
- Mr. Meyers
- Mr. Shields
- Mr. Wiesenmaier
- Mr. Krome
- Mr. Carlile
- Mr. Owens

S&E-DIR
- Dr. Weidner
- Mr. Richard

S&E-Aero
- Dr. Geissler
- Mr. Dahm
- Mr. Baker
- Mr. Lindberg
- Dr. Lovingood
- Mr. Worley
- Mr. Rheinfurth
- Mr. Buchanan
- Dr. Glaesen
- Dr. Blair
- Mr. Hall
- Mr. Mowery

S&E-ASTR
- Mr. Moore
- Mr. Hosenthien
- Dr. Nurre

S&E-ASTR
- Mr. Kennel
- Mr. Wojtalik
- Mr. Brooks
- Mr. Chubb
- Mr. Rupp
- Mr. Polites
- Mr. Williamson
- Mr. Thompson
- Mr. Davis
- Mr. Fisher
- Mr. Scofield
- Mr. Swearingen
- Mr. Mandel

S&E-ASTN
- Mr. Heimburg

S&E-COMP
- Dr. Hoelzer
- Dr. Polstorff
- Mr. Lawrence

S&E-SSL
- Dr. Haeussermann
- Dr. Naumann

PD-DIR
- Mr. Murphy
- Mr. Jean
- Dr. Mrazek

PD-LST
- Mr. Downey
- Mr. Heyer

PD-MP-DIR
- Mr. Gierow
- Mr. Larson

PD-DO
- Mr. Goerner
- Mr. Marshall
- Mr. Laue
- Mrs. Kozub
- Mr. Darwin
- Mr. Love
- Mr. Butler
- Mr. Digesu
- Mr. Arsement
- Mr. Boehme
- Mr. Rood
- Mr. Schultz
- Mr. Green
- Mr. Davis (40)
- Mr. Nicaise
- Dr. Steincamp
- Mr. Brandon
- Mr. Cole
- Mrs. Reisz
- Mr. Weiler
- Mr. Goldsby
- Mr. Sumrall

A&PS-MS-I
A&PS-MS-IP (2)
A&PS-MS-IL (8)
A&PS-TU-DIR (6)
A&PS-MS-D
A&PS-MS-H
A&PS-PAT
- Mr. Wofford

☆ G.P.O. 1973 – 746-829 / 4787

EXTERNAL

Scientific and Technical
Information Facility (25)
P. O. Box 33
College Park, Maryland 20740
Attn: NASA Rep (S-A)

Dr. W. Trautwein
LMSC, Research Park
Huntsville, Al. 35805

Mr. Marlin Sloan
Northrup Corporation
Research Park
Huntsville, Al. 35805

Mr. K. Bishnoi
BECO, Research Park
Huntsville, Al. 35805

Mr. T. Giesmondi
Sperry-Rand Corporation
717 Arcadia Circle, N.W.
Huntsville, Al. 35801

Mr. Daniel Chirappa
General Dynamics
Box 1128
San Diego, California 92115